TRENDS AND PERIODIC VARIABILITY IN TROPICAL WAVE CLOUDS

by

Lester Charles Burgwardt III
A Dissertation
Submitted to the
Graduate Faculty
of
George Mason University
in Partial Fulfillment of
The Requirements for the Degree
of
Doctor of Philosophy
Earth Systems and Geoinformation Science

Committee:

_____	Dr. Paul Houser, Dissertation Director
_____	Dr. John Qu, Committee Member
_____	Dr. Donglian Sun, Committee Member
_____	Dr. Zafer Boybeyi, Committee Member
_____	Dr. Michael Summers, Committee Member
_____	Dr. Anthony Stefanidis, Department Chairperson
_____	Dr. Donna M. Fox, Associate Dean, Office of Student Affairs & Special Programs, College of Science
_____	Dr. Peggy Agouris, Dean, College of Science
Date: _____	Spring Semester 2017 George Mason University Fairfax, VA

Trends and Periodic Variability in Tropical Wave Clouds

A Dissertation submitted in partial fulfillment of the requirements for the degree of Doctor of Philosophy at George Mason University

by

Lester Charles Burgwardt III
Master of Science
Rochester Institute of Technology, 1999
Bachelor of Science
Rochester Institute of Technology, 1981

Director: Dr. Paul Houser, Professor
Department of Geography and Geoinformation Science

Spring Semester 2017
George Mason University
Fairfax, VA

DEDICATION

To my father Dr. Lester C. Burgwardt Jr.: A man who always steered me in the right direction.

TABLE OF CONTENTS

LIST OF TABLES

LIST OF FIGURES

LIST OF EQUATIONS

LIST OF ABBREVIATIONS AND/OR SYMBOLS

African Easterly Wave ..... AEW
Ambient Geographic Information ..... AGI
Atmospheric Infrared Sounder ..... AIRS
Area of Interest ..... AOI
Cloud Fraction Standard ..... CldFrcStd
Cross Track Infrared Sounder ..... CrIS
El Nino Southern Oscillation ..... ENSO
ECMWF Re-Analysis ..... ERA-Interim
Fast Fourier Transform ..... FFT
Geostationary Operational Environmental Satellite ..... GOES
Hurricane Database ..... HURDAT
Interactive Data Language ..... IDL
Intergovernmental Panel on Climate Change ..... IPCC
IPCC Assessment Report Four ..... IPCC AR4
Laboratory for Atmospheric and Space Physics ..... LASP
Lomb Normalized Periodogram ..... LNP
Multiple Hypothesis Tracker ..... MHT
Madden-Julian Oscillation ..... MJO
North Atlantic Oscillation ..... NAO
National Aeronautics and Space Administration ..... NASA
National Centers for Environmental Prediction ..... NCEP
National Hurricane Center ..... NHC
National Oceanic and Atmospheric Administration ..... NOAA
National Polar-orbiting Partnership ..... NPP
National Weather Service ..... NWS
Oscillation Confluence Factor ..... OCF
Principal Components Analysis ..... PCA
Pre-Depression Investigation of Cloud-Systems in the Tropics ..... PREDICT
Quality Control ..... QC
Solar Radiation and Climate Experiment ..... SORCE
Total Irradiance Monitor ..... TIM
Top of Atmosphere ..... TOA
Total Solar Irradiance ..... TSI
Tropical Weather Discussion ..... TWD

ABSTRACT

TRENDS AND PERIODIC VARIABILITY IN TROPICAL WAVE CLOUDS

Lester Charles Burgwardt III, Ph.D.

George Mason University, 2017

Dissertation Director: Dr. Paul Houser

This dissertation describes the acquisition and analysis of tropical wave cloudiness. Tropical wave positions for the years 2003 through 2013 were extracted, via text mining, from the National Hurricane Center's Tropical Weather Discussion, a bulletin released every six hours, and published on-line. Tropical wave tracks were developed from these positions using the Multiple Hypothesis Tracking algorithm. Satellite data from the Atmospheric Infrared Sounder (AIRS) was downloaded from the NASA Mirador web site based on time and position of tracked tropical waves. The AIRS data was mosaicked to provide complete coverage between satellite swaths. The AIRS Level 2 Cloud Fraction Standard product was used exclusively in the analysis. Cloud fraction data was divided into upper and lower levels as provided in the AIRS product. A cloud fraction ratio was also developed to provide some indication of the insulating quality of clouds. The analysis discovered secular trends of varying degrees and direction depending on location of tropical waves. The analysis also found significant periodic variability within cloud

fraction values, much of which correlated to known global oscillations such as El Nino and the Madden-Julian Oscillation. However a number of periodic signals found within tropical wave cloudiness could not be correlated with any of the known global and non-earth oscillations tested against. Future research ideas in the conclusions include an examination of those un-correlated periodic signals. Also included in the conclusions are theories about differences in correlations to periodic signals within a tropical wave core versus correlations that are seen in surrounding cloud patterns.

INTRODUCTION AND LITERATURE REVIEW

Introduction

This dissertation begins by discussing the motivation for this research, the research objective and hypothesis. Included is a literature survey that covers previous research related to locating and tracking of tropical waves, and research related to the life cycle of a tropical wave. The dependency of this research on observations made by the National Hurricane Center and the creation of a tropical wave database are discussed. In determining which atmospheric parameters to use when monitoring tropical waves several articles on tropical wave life cycle were reviewed. Most of these articles discuss tropical wave life cycle in terms of tropical cyclone genesis while the weak yet observable tropical waves were of less interest. The section on the research approach and methodology discusses methods used by the author to automate tracking of tropical waves based on archived observations and automated selection of Atmospheric Infrared Sounder (AIRS) data based on the tracking results. Detailed explanation is given about the software that was written to data mine archived tropical wave observations, the tracking algorithm to connect individual observations into tracks, automated selection of AIRS data files, and analysis methods. The measured parameters provided by AIRS are listed along with the techniques for analyzing the data.

Motivation

Tropical waves remain an enigma. After decades of study much is still unknown about them. Tropical waves are often precursors to large destructive Hurricanes such as Sandy in 2012. In addition, cloudiness associated with tropical waves has the potential to impact the climate. So any investigation that can reveal new information about tropical waves is warranted.

In his explanation of tropical waves on a National Oceanic and Atmospheric Administration (NOAA) web page Chris Landsea (Landsea 2014) states "It is currently completely unknown how easterly waves change from year to year in both intensity and location and how these might relate to the activity in the Atlantic (and East Pacific)."

Many of the articles in the literature survey provided evidence of the connection between tropical waves and hurricanes.

Another motivating factor for this research is that our understanding of the importance of tropical waves with regard to global climate systems has been increasing in recent years. Khouider et al. (Khouider et al. 2013) reviewed the interaction between cloudiness in the tropics and its impact on climate projections. The authors showed that there is a connection between the cloudiness associated with tropical waves and global climate variability. In addition Majda (Majda 2000) has established that tropical systems have global influence on climate.

The motivation for this research can be summarized in these three statements:

a) Much is still unknown about the year to year changes in tropical waves
b) Tropical waves are often precursors to hurricanes
c) There is a connection between tropical waves and climate variability

Research objective and hypothesis

The objective of this research was to detect previously unknown multiyear trends and periodic variability in the attributes of tropical waves. To support this objective this research tested the hypothesis that attributes of a typical tropical wave life cycle have changed from 2003 to 2014. This hypothesis was tested by examining how tropical wave cloudiness evolves during a tropical wave life cycle. These observations were expanded over an eleven year period to determine if cloud attributes of a tropical wave life cycle are trending.

Background (Literature Review)

A literature review was performed to investigate two background areas. The first area is the location, tracking, and geographic extent of tropical waves. The second is the measurement of physical parameters of the atmosphere within a tropical wave.

For topics associated with location, tracking, and geographic extent of tropical waves, data mining the Tropical Weather Discussion (TWD) issued by the National Hurricane Center (NHC) appears to be novel. There are reports of data mining other types of weather reports but not the TWD. The literature review revealed many instances of tracking weather systems with the Multiple Hypothesis Tracking (MHT) algorithm and this provided a basis for how this research established tracks for the weather system of interest here: tropical waves.

A gap was identified as most reports discussing tropical wave life cycles were focused on tropical cyclone genesis and not a general overview of tropical wave life cycles. In the literature reviewed, many of the parameters measured in these reports are available from AIRS. However the literature also included measurements of wind or

vorticity which are not part of the AIRS set of products. Since the scope of this research only includes AIRS data, measurements of wind and vorticity were not used.

Locating tropical waves

Early observation techniques of tropical waves using satellite imagery were described by Neil Frank (Frank 1969). Frank's technique was based on recognizing an inverted Vee pattern in clouds. By the year 2000 tropical wave observations using analysis of satellite imagery became standard practice as part of NOAA's TWD (Holweg and Center 2000) and continue to this day.

The TWD is a bulletin issued every six hours in a text format. The bulletin is based on surface analysis and satellite imagery. When tropical waves are observed, the TWD provides geographic coordinates of the location of the tropical wave. Multiyear information on locations of tropical waves was a crucial part of this research. In the process of developing these data requirements, NOAA's archive of TWDs going back to 2003 was accessed and a review found the needed geographic coordinates in all years of the archive. However, the geographic coordinates were embedded in natural language text; what was needed was a database or spreadsheet with each tropical wave identified and tracked over its lifetime using geographic coordinates and times of observations.

A tropical wave database

In correspondence with NOAA it was determined that the agency does not have a tropical wave data base. In searching for such a database a few possibilities emerged. The Automated Tropical Cyclone Forecasting System described by Miller et al. (Miller et al. 1990) (Sampson and Schrader 2000) and the associated Real-Time Tropical Cyclone

Products web site do not include tropical waves in their database or forecasting software. The HURDAT2 database (Landsea and Franklin 2013) includes entries for tropical waves associated with named storms but those are incomplete. For example, the best track report for hurricane Sandy (Blake et al. 2013) discusses a tropical wave associated with the hurricane. However in the HURDAT2 data base only two instances of a low (LO) are shown, the first of which is dated 21 October 2012, while the best track report first mentions the associated tropical wave being observed much earlier on 11 October 2012. The NHC TWD reported its first observation of the tropical wave only one day later on 12 October 2012 (FORMOSA 2012). Another example is hurricane Raphael which also occurred in 2012. GOES imagery shows a tropical wave moving across the Atlantic, growing, and developing rotation and becoming Raphael. However, the HURDAT2 data base indicates a Tropical Storm (TS) as the first entry for Raphael on 12 October 2012.

Tropical waves are not easy to distinguish (Krishnamurti et al. 2013). They are not merely low pressure systems nor cloud formations. Reliable automated recognition of tropical waves does not match that of skilled human observation of the various factors that indicate the existence of a tropical wave. Tropical storms and hurricanes are much easier to distinguish with automation and there is an immediate societal need to identify and track these weather systems. So it follows logically that the HURDAT2 database would emphasize named storms for operational use rather than tropical waves.

To build a tropical wave database for operational use may not make sense, but for this research one needed to be created.

Data mining archived Tropical Weather Discussions

Four TWD bulletins are issued by NOAA every day. With archived bulletins dating back to 2003, over 14,000 bulletins had to be searched for tropical wave coordinates. Therefore, an automated method was needed to parse through the text based bulletins and extract geographic coordinates and times for tropical wave observations. To do this, data mining software was written to search for tropical wave coordinates in the TWD bulletins. This is not a new idea; data mining in support of weather forecasting and climate studies is reported in a number of articles. A system to acquire data from a number of sources is described by Yang (Yang et al. 2010). Olaiya and Adeyemo (Olaiya and Adeyemo 2012) use neural network and decision tree algorithms to analyze an archive of local Nigerian weather reports and build a weather prediction model. Data mining of Doppler radar and tip bucket data was used by Kusiak (Kusiak et al. 2013) to predict rainfall. Compared to some of the massive datasets described by Fayyad and Smyth (Fayyad and Smyth 1999) the data mining problem in this research was quite small, and because standardized phrases were usually used to report tropical waves in the TWD bulletins, the data mining requirement became a relatively simple text parsing exercise. In their book on data science, Provost and Fawcett (Provost and Fawcett 2013) discuss text mining methods including a decision tree format for data mining models which was followed for this research.

For this research the TWD was the authoritative source for identifying and locating tropical waves. It is currently described as an operational maritime text product that gives an official National Weather Service (NWS) (National Weather Service)

description of the current state of the atmosphere. Methods used by the NWS to detect and track tropical waves are described by Pasch and Avila (Pasch and Avila 1994).

During the more active season the TWD will have multiple tropical waves identified in each bulletin and there is often no attempt to link a particular tropical wave in one bulletin with tropical wave observations in any other bulletin. However, because time, date, and geographic coordinates for each tropical wave observation are known, a tracking algorithm was successfully applied to link tropical waves from one observation to the next.

Building tropical wave tracks

Tracking of moving objects was widely discussed in technical literature. Of interest here was the tracking of multiple tropical waves from a series of comingled single point observations. In his survey of object tracking methods Yilmaz (Yilmaz et al. 2006) identified the MHT algorithm as the best choice for the frame to frame point tracking used to join multiple observations of the same moving object. The MHT algorithm has evolved over time. In an important breakthrough that enabled practical implementation of the algorithm Cox and Hingorani (Cox and Hingorani 1996) were able to limit track option growth without impacting accuracy in their implementation of the MHT algorithm. Blackman (Blackman 2004) dives deeper into the implementation of the MHT algorithm and in a valuable paper teaches its principles. Hodges (Hodges et al. 2003) provided climatology examples by using the MHT to build tracks in the validation of reanalysis projects that focus on Atlantic tropical waves. Root (Root et al. 2011) provided more examples of using MHT in weather related applications. Cloudiness was

an important part of this research and Sieglaff (Sieglaff et al. 2013) provide an example of MHT usage in the creation of a tool to identify developing convection. Further examples of MHT usage in weather and climate related research was given by Miller (Miller et al. 2013). Here, a real time application was discussed which demonstrated that a fast analysis could be provided by the use of MHT algorithms. In their paper Lakshmanan and Smith (Lakshmanan and Smith 2010) discussed details of a weather related implementation of a tracking algorithm. For example, they showed how to use the search radius for the next point and the length of time to "coast" a point before it is discarded as not being associated with any track. Antunes (Antunes et al. 2011a) (Antunes et al. 2011b) developed an implementation of the MHT algorithm which was released as an open source Java library and was used in this research.

Tropical wave life cycle

The life cycle of tropical waves has been studied in the past. Typically these studies have been in regard to the tropical cyclogenesis of named storms. However in 1969 Frank (FRANK 1970) did an early study in the life cycle of tropical waves observed from three surface locations: Dakar, Barbados, and San Andres Island. Frank's interest was in the less intense tropical systems, such as tropical waves, as opposed to named storms. Later, in 1979, Murakami (Murakami 1979) documented periodicities in Atlantic tropical waves. The first was a 4 to 5 day mode in which enhanced convection moved westward from Africa through the tropical Atlantic. Murakami also notes a diurnal mode. During the life of typical tropical waves observed by Murakami, convection is enhanced along with moistening in the cloud layer and drying in the sub-cloud layer. In work

related to the Fourth Assessment Report of the Intergovernmental Panel on Climate Change (IPCC AR4), a study evaluating tropical intraseasonal variability in climate models is presented by Lin (Lin et al. 2006). In this study Lin found that climate models, as of 2006, had difficulty simulating tropical intraseasonal variability. The validation datasets came from 8 years of GOES Precipitation Index (1997-2004) and from 8 years (1997-2004) of the daily Global Precipitation Climatology Project (GPCP) 1 degree precipitation product. Some clues regarding the life cycle of tropical waves may be embedded in Lin's validation datasets but they were not brought to light in the report. The Lin validation datasets provided insight into the various global oscillations that impact formation of tropical waves as reported by Straub and Kiladis (Straub and Kiladis 2003), however no specific mention of tropical waves appears in the report by Lin et al.

Dunkerton (Dunkerton et al. 2009) describes a number of features within a tropical wave life cycle that lead to formation of tropical depressions and tropical cyclones. The initial study, based on the 4 year period 1998-2001, covers tropical cyclogenesis from tropical waves in the Atlantic and eastern Pacific. Increasing moisture, convection, and vorticity are among the factors that this study uses to describe a tropical wave life cycle leading to tropical cyclone formation. The authors also presented the "Marsupial Paradigm" in which rotation in a tropical wave forms a pouch in which the beginnings of a tropical cyclone can form.

A later single season (2010) study by Montgomery (Montgomery et al. 2012), that included Dunkerton on the team, focused on the life of cloud systems before a tropical depression forms. Their campaign was labeled the Pre-Depression Investigation of

Cloud-Systems in the Tropics (PREDICT). In their article they referred to the fact that very few in situ observations of tropical wave life cycles exist due to a lack of knowledge of where to sample these disturbances. This is a problem my research solved by locating tropical waves based on skilled interpretation by the NHC of both surface and satellite data and by using automation to select AIRS granules that cover tracked tropical waves. The primary measurement platform for the PREDICT campaign was an aircraft equipped with dropsondes and onboard sensors.

Most of the parameters measured by the PREDICT campaign can be taken directly from the AIRS version 6 products. One exception is the 3-D wind parameter set. Wind and vorticity are not included in the AIRS product set. However, using the tropical wave location data, future research could acquire other remotely sensed data that provide wind information. While it is valuable to learn of a parameter set such as this, the PREDICT campaign was limited in its geographic coverage. With its primary base of operations in St. Croix, the aircraft could only cover eastward out to about 37 degrees west longitude leaving out the portion of tropical wave life cycle that occurs between the African coast and the 37 degree eastern limit. Complete coverage of the Atlantic was not a goal of PREDICT as tropical depression formation typically occurred within the covered area.

A number of other articles published by this group from the Naval Postgraduate School in Monterey CA covered the involvement of tropical waves in tropical cyclogenesis with the most recent from Lussier et al. (Lussier et al. 2015) examining the role of a tropical wave in the formation of hurricane Sandy. A similar study was

presented as a class paper by the author (Burgwardt et al. 2013) which demonstrated the ability to track moisture growth in a tropical wave from satellite sounder data. Doyle (Doyle et al. 2012) examined the sensitivity of tropical disturbances such as tropical waves to triggers that cause intensification leading to a tropical cyclone. Increasing moisture and temperature throughout the life of tropical waves are important considerations in their findings. Most notable was the rate the moisture and temperature increase. Faster increases allow more opportunity for perturbations to trigger intensification leading to cyclonic vorticity. Zhuo Wang (Wang 2012) focused on the thermal dynamic aspects of the pouch that forms in tropical waves as a precursor to tropical cyclone formation. In the article Wang emphasized the importance of deep convection in the pouch area. Cecelshi and Zhang (Cecelski and Zhang 2013) provided another example of exploring the tropical wave life cycle with regard to tropical cyclogenesis. In their work the focus is on hurricane Julia (2010). Again, pronounced upper tropospheric warming and deep convection are highlighted. In this work and others that follow the work by Dunkerton and Montgomery, a critical latitude is discussed as part of each tropical cyclogenesis model.

Diaz and Aiyyer (Diaz and Aiyyer 2013) explore the current notion that African easterly wave formation takes place upstream from earlier African easterly waves. Here a residual eddy remains and when combined with diabatic heating in the Darfur region of east Africa, convection and a resulting African easterly wave can develop. Downstream, as the disturbance moves over the Atlantic Ocean, the life cycle of a tropical wave begins. The growth of an African easterly wave into hurricane Alberto (2000) is covered

in detail by Diaz and Aiyyer. They used the gridded Interim European Centre for Medium-Range Weather Forecasts (ECMWF) Re-Analysis (ERA-Interim) for their analysis.

Latent heating and cooling rates in tropical waves were discussed by Park et al. (Park et al. 2013) in their analysis of two developing and two non-developing tropical disturbances. Although their observations were made in the western Pacific the principles apply to Atlantic disturbances as they cited Neil Frank's (FRANK 1970) study of Atlantic tropical systems. Their observations of convection were done using airborne Doppler radar. They also mentioned that as important as latent heating and cooling is in tropical disturbances, numerical simulations have rarely been compared with retrievals from observations.

Ventrice and Thorncroft (Ventrice and Thorncroft 2013) used a wide range of data sources to show that convectively coupled Kelvin waves modulate African easterly wave activity. Their subject example was the pre-Alberto (2000) African easterly wave which had been studied by others. The primary attribute the authors measured was convection, although wind played an important part as well. As with many of the other studies, Ventrice and Thorncroft concentrated on formation of African easterly waves and their life cycle over land rather than the ocean.

Klotzbach and Oliver (Klotzbach and Oliver 2015) provided a long term study of tropical cyclone activity over the Atlantic from 1905 to 2011. Their paper documented impacts of the Madden-Julian Oscillation (MJO) on Atlantic basin tropical cyclone

activity over a multi decade time scale. In my research the influence of the MJO and other oscillations on the life cycle of tropical waves was studied in detail.

This literature survey on work done by others to describe tropical wave life cycles was unable to find a study of tropical waves that was not associated with tropical cyclogenesis. In the spirit of Neil Frank (FRANK 1970) in his article in 1970 my focus was on all tropical waves including the less intense tropical systems during the 2003 to 2013 time frame. To the best of my knowledge there was not a study with this focus in the literature.

Numerical models

Numerical models of tropical cyclogenesis are well covered in the literature. Most tropical cyclones originate from tropical waves, but not all tropical waves evolve into tropical cyclones. As a result, numerical models of tropical waves typically exist in the context of cyclogenesis. An exception to this is work done by Mapes (Mapes 2000) who explores deep convection in a vertical model of a tropical wave. In this model Mapes can adjust Convective Available Potential energy (CAPE) and Convective Inhibition (CIN) and uses a triggering energy K to represent small scale fluctuations.

Using a numerical model Kiladis (Kiladis et al. 2009) identifies a variety of equatorial waves leading me to expect my study would find periodic variability in tropical wave cloudiness. The paper gives a historical overview of equatorial waves. One of the historically early waves defined were labeled “easterly waves” due to their propagation from out of the east, today we refer to them as tropical waves. Kiladis refers to a classic paper by Matsuno (MATSUNO 1966) who created a basis for numerical

models of equatorial waves known as the "shallow water (SW) equations on an equatorial beta plane." As Kiladis points out; the results of this work correlates with the now well-known Kelvin, equatorial Rossby, westward and eastward inertia-gravity, and mixed Rossby gravity waves. The historical overview goes on to mention work done by Takayabu (Takayabu 1994) who found spectral peaks in satellite imagery correlating with a number of equatorial waves including Kelvin waves.

In a two part series Kiladis (Kiladis et al. 2006) and Hall (Hall et al. 2006) develop tropical wave models and run them using reanalysis data. The results show a 5.5 day period of tropical wave occurrence and a wavelength of 3500 km. They also note that the tropical wave core is stable and resistant to external influences. Their work focused on African Easterly Waves over the Sahel region and just off the west coast of Africa. They conclude that as these waves move out over water the structure and dynamics become more complex.

Reanalysis data

Cloud layers found in reanalysis data provide a longer term simulated record of tropical wave clouds. In order to locate tropical waves beyond the scope of this eleven year study, additional reanalysis variables would be needed to locate the vorticity and diffusion found in a tropical wave trough. Hodges (Hodges et al. 2003) demonstrated success in tracking of tropical waves in an ensemble of reanalysis projects. However the spatial distribution of the systems tracked varied among the reanalysis projects suggesting significant uncertainty in simulated cloudiness. Dee (Dee et al. 2011) reports on status of the ERA-Interim reanalysis. Among the challenges listed in this report is

representation of the hydrological cycle. Indeed, this supports the notion that clouds remain the source of most uncertainty in a climate model. Future work on ERA-Interim will include a focus on assimilation of in-situ accumulated rainfall, soil hydrology, snow, and better use of satellite observations over land, all leading to more accurate representations of clouds and precipitation. The National Centers for Environmental Prediction (NCEP) Climate Forecast System Reanalysis (Saha et al. 2010) was used by Brammer and Thorncroft (Brammer and Thorncroft 2015) to track African Easterly Waves (AEW) from West Africa into the tropical Atlantic. The focus of this study was to understand predictors in an AEW that lead to tropical cyclogenesis. The outcome showed that waves that ingest moist air into the lower levels of the system as it moves off the African coast are favorable for cyclogenesis. An important concept presented in this paper is the method used to identify and track tropical waves. Agudelo (Agudelo et al. 2011) and Bain (Bain et al. 2014) use Hovmoller plots to provide a longitudinal track of tropical waves, while the method described by Berry (Berry et al. 2007) locates the tropical wave trough. These methods, or ones like them, would be needed to automate tropical wave identification and location in a multi-decade study of trends and periodic variability in tropical wave cloudiness based on reanalysis data.

Frank and Roundy (Frank and Roundy 2006) use 29 years of reanalysis data to study the relationship between tropical waves and tropical cyclogenesis. The scope of their study was worldwide and in it they found mixed Rossby-gravity waves, easterly waves, equatorial Rossby waves, Kelvin waves, and the Madden-Julian oscillation. They concluded that equatorial Kelvin waves do not play a major role in tropical cyclogenesis,

while other wave types do. A wave centered sampling approach was applied in their study which was also used in this study to analyze clouds belonging only to tropical waves.

Literature review summary

The literature review explored both the earth systems and geo-information science aspects of this dissertation. The literature review also established the importance of gaining further knowledge on the year to year changes in tropical waves.

The lack of a tropical wave data base as identified in the literature review revealed a fundamental gap in enabling researchers to explore tropical waves. The articles reviewed made evident the novelty of constructing a tropical wave data base by data mining the Tropical Weather Discussion for observation coordinates and then using the Multiple Hypothesis Tracking Algorithm to tie observations of individual tropical waves together. The format of NOAA's hurricane database, HURDAT2, is based on numbered cyclones. The format allows the inclusion of tropical waves of any intensity but unless a tropical wave is associated with a numbered cyclone the structure of HURDAT2 does not allow for its inclusion.

The literature review revealed that a long term, multiyear collection of AIRS data specifically targeted on known locations of tropical waves over the Atlantic Ocean appears to be novel. The assessments made in this research have a wider scope than previous research in that they cover all tropical waves within the time frame and geographic region of this research without regard to intensity of the tropical wave or its association with a named storm.

DATA

Acquiring tropical wave observation coordinates and times

Automatic generation of tropical wave tracks consists of two steps: 1) acquire observation coordinates and times through text mining; 2) use of a tracking algorithm to extract individual tropical wave tracks from the time and location information acquired in step 1. These steps will be described in the following sections. The extracted tracks can be used to describe trends in tropical wave locations, speed, seasonality, year to year changes in these parameters, and as a guide to acquiring archived satellite data for further research.

The tropical wave positions are manually derived by experts using satellite imagery and derived wind patterns. When tropical waves are observed their positions are published every six hours in the NHC TWD. In this research I used text mining to extract observation coordinates and times from archived TWDs for the years 2003 through 2013.

The text mining software was written using the Visual Basic language included with Microsoft Excel. The software was divided into four sub procedures each performing a step in the text mining process. The text mining process began with acquiring a list of files from the NHC archive. This was followed by a procedure that downloaded each of the TWD text files from the file list created in the previous step. An initial text mining step searches the downloaded TWD text files looking for phrases that may have information about the existence and location of tropical waves. The final text

mining step analyzes each of the phrases looking for text strings that conform to certain patterns used by the TWD authors when tropical waves are reported. Included in these strings are the geographic coordinates of the observed tropical wave. These coordinates were indexed in the tropical wave database along with the date and time of the observation. A total of 19,668 observations were recorded in the tropical wave database for all years from 2003 through 2013.

Text mining results

The text mining software was initially developed based on TWDs issued in 2012. The software was then used to text mine TWD files for all available years: 2003 to 2013. It was quickly observed that there is a decrease in tropical wave detections for the years prior to 2010. Minor differences in prior year format or wording impacted the ability of the software to identify geographic coordinates. One example is the use of the forward slash "/" to indicate a range of coordinate values as demonstrated in the phrase "A TROPICAL WAVE IS ALONG 40W/41W S OF 8N MOVING W NEAR 15 KT." from the June 18, 2009 TWD. This was not successfully parsed with the first version of software, so earlier TWD styles had to be included in the text mining software to generate a complete database. However, overall it appears that consistent reporting styles do exist within a year or few years' worth of TWDs so that an impractically large range of style options did not need to be included in the text mining software.

Compared to data from more recent years, the ability to identify tropical wave phrases did not decrease in the text mining of TWDs for years prior to 2010. The

identification of a tropical wave section has been historically the "…TROPICAL WAVES…" text string.

A metric was used to determine the success of finding geographic coordinates within a tropical wave phrase by calculating the ratio of coordinates found to tropical wave phrases found. Note that this metric was influenced by how many tropical waves are mentioned in a phrase, multiple tropical waves will bias this metric higher. But in general there was a ratio of greater than 1.0 for all years. Another way of looking at this metric is as an indicator of how many tropical waves are observed within a single TWD bulletin. These values are an average for the entire season so one could say, as shown in Table 1, that years 2005 and 2006 had a higher concentration of tropical waves than the years 2004 and 2012.

Table 1 provides a detailed analysis of the text mining results. Results for each year are shown. The number of active days is the number of days from the first report of a tropical wave, usually in May, to the last report of a tropical wave, typically in October or November. As can be seen in the table the number of active days for tropical waves over the Atlantic ranges from 164 to 206.

Table 1: Analysis of text mining TWD text for geographic coordinates of tropical waves for the years 2003 through 2013.

Year	Active Days	Phrases	Obv With Coord Pairs	Ratio Pairs to Phrases	GetTW LatLon Attempts	No points returned	GetTW LatLon failure rate
2003	174	900	1859	2.07	1944	85	4%
2004	184	1336	1937	1.45	2010	73	4%
2005	197	932	2308	2.48	2435	127	5%
2006	193	870	2138	2.46	2268	130	6%
2007	183	825	1907	2.31	2109	202	10%
2008	206	910	2183	2.40	2307	136	6%
2009	180	808	1680	2.08	1735	60	3%
2010	188	784	1695	2.16	1754	59	3%
2011	187	665	1193	1.79	1218	28	2%
2012	164	781	1309	1.68	1327	18	1%
2013	170	767	1459	1.90	1467	8	1%

The column labeled “Phrases” in Table 1 shows the number of tropical wave phrases extracted from the TWD. The number of phrases ranges between 665 and 1336. Note that the number of phrases appears to correlate with the number of active days. Also, a single phrase may contain multiple observations.

The number of observations with at least one set of coordinate pairs extracted from the TWDs for each year is shown in the fourth column of Table 1. A typical tropical wave observation will include two pairs of coordinates, one pair indicating the location of the north end of the wave axis and the second pair indicating the location of the southern end of the axis. However some TWD observations include extra points within the axis indicating the axis is curved. In other cases a single coordinate pair is given in the TWD, always indicating the northern end of the axis. For the purposes of this study only a single

pair of coordinates (latitude and longitude) was needed. Any occurrence of at least a single pair of coordinates being extracted was counted in the fourth column of Table 1.

The ratio of coordinate pairs to tropical wave phrases is shown in Table 1 to indicate the efficiency of the text mining software to produce coordinate pairs from each tropical wave phrase. As discussed above this is dependent on the number of tropical waves mentioned in a single phrase.

The column in Table 1 labeled “GetTW_LatLon Attempts” shows the number of times a sentence or string was found that starts with "TROPICAL WAVE." The text mining procedure then went on to attempt to extract the geographic coordinates that typically followed these words. The success of these attempts is indicated in the next two columns of Table 1. The column labeled “No Points Returned” shows how many times an attempt was made to extract coordinates but no coordinates were found. This failure rate shown in the next column ranges from 1% to 10%. This indicates that a tropical wave phrase was found but between 1% and 10% of the time the software was unable to extract a coordinate pair. This metric may have been confounded by the software erroneously finding a phrase that was not a tropical wave phrase and therefore did not include tropical wave coordinates.

The most significant adjustment that was made during development of the text mining software was to accept the fact that in the years preceding 2010 TWD bulletins typically did not report both the north and south vertices of a tropical wave axis. The tracking software worked on just the northern set of axis coordinates as long as they are consistently reported in the TWD. My experience was that when only one set of

coordinates is reported a phrase similar to “a tropical wave is south of _____ “ (coordinates given) was used. Later, by using statistics of tropical wave axis length and bearing, I was not only able to estimate the southern vertex of the axis but also estimate the center of the tropical wave axis. Overall the number of coordinate pairs extracted from TWD bulletins was over 1000 for each year.

Extraction of tropical wave tracks

The MHT algorithm was employed to tie together the individual observations of each tropical wave from its beginning, typically off the coast of West Africa, to its end, often in the Caribbean region. This allowed data collection software to automatically select appropriate files from NASA and NOAA websites to drive research. Selection of the MHT algorithm for tracking tropical waves was made after a literature review (Yilmaz et al. 2006),(Cox and Hingorani 1996),(Hodges et al. 2003),(Blackman 2004),(Root et al. 2011),(Sieglaff et al. 2013),(Miller et al. 2013),(Lakshmanan and Smith 2010) showed this to be the preferred method used for tracking a variety of other weather patterns. An open source implementation of the MHT algorithm created by David Antunes (Antunes et al. 2011a),(Antunes et al. 2011b) was downloaded and modified for use in this project. Details on the algorithm are beyond the scope of this paper, but much of that information is covered in the references.

As discussed in the previous section, text mining was applied to the TWD bulletins produced by the NHC every six hours. When tropical waves were observed over the Atlantic, they were reported in the TWD along with geographic coordinates.

Coordinates for the northern end of the tropical wave axis were always given so these were used for tracking purposes.

The tracking software was written in Java and was primarily a library of calls to perform various tasks in the tracking algorithm. The software also included some examples that were modified to suit the tracking of tropical waves. The software came with default settings which were initially used, but later, experiments were run to determine the best settings to use. Eventually, a number of parameters were added to the software to further optimize the tracker for the tropical wave application.

Tropical wave tracking results

Figure 1 shows examples of tracks automatically generated from the TWD text mined observations. Table 2 shows parameters for the tracks in Figure 1. The tracks were named using the format TWTyyyy_nnn where TWT stands for Tropical Wave Track, yyyy is the year of the track, and nnn is the number of the track incremented chronologically from the first tropical wave of the year to the last. The MHTID is the identification number of the track assigned by the tracking software.

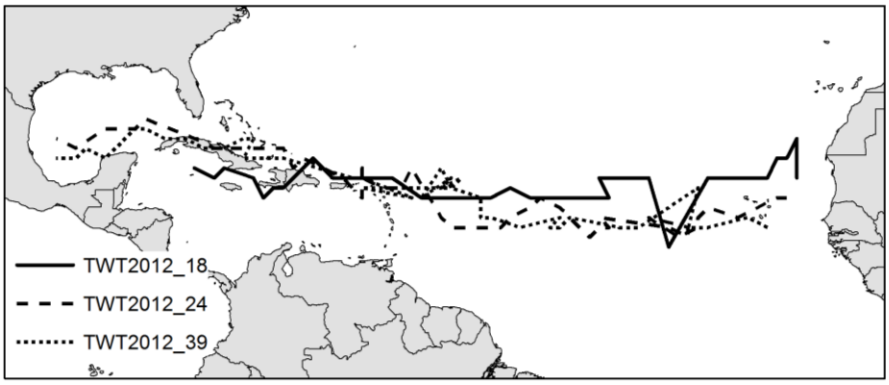

Figure 1: Examples of tropical wave tracks

The time and date for each track beginning and end are taken from the time the TWD bulletins associated with the first and last observations were released. Times are in GMT. The geographic coordinates for the first and last point in the track are shown. These coordinates are always given in whole degrees revealing the relatively coarse resolution these observations were made by the NHC. In the last column of Table 2 is the number of vertices or observations within each track.

Table 2: Parameters of tropical wave tracks

Name	MHTID	Begin Date	Begin Time	End Date	End Time	Duration (Days)	Begin Lon	Begin Lat	End Lon	End Lat	Vertices
TWT2012_18	2414	7/16/2012	23:50	7/25/2012	11:45	8.50	-20	19	-81	20	37
TWT2012_24	3354	7/31/2012	23:36	8/11/2012	23:44	11.01	-21	17	-95	23	49
TWT2012_39	4978	9/11/2012	17:48	9/24/2012	00:01	12.26	-23	14	-95	21	53

For initial runs, only modifications that allowed the MHT software to work with the text mined data were made. Using original settings, the MHT tracking software was run on year 2012 tropical wave observations. For that year's dataset, 1200 observations of tropical waves were detected through text mining. Of those, only 1133 observations passed a quality assurance test that included checking for one complete set of coordinate pairs. Out of the 1133 coordinate pairs processed by the MHT tracking software, 806 where assigned to 78 tracks. This leaves 327 (29%) good observations not assigned to a track. Out of the 78 tracks generated not all were of useful quality.

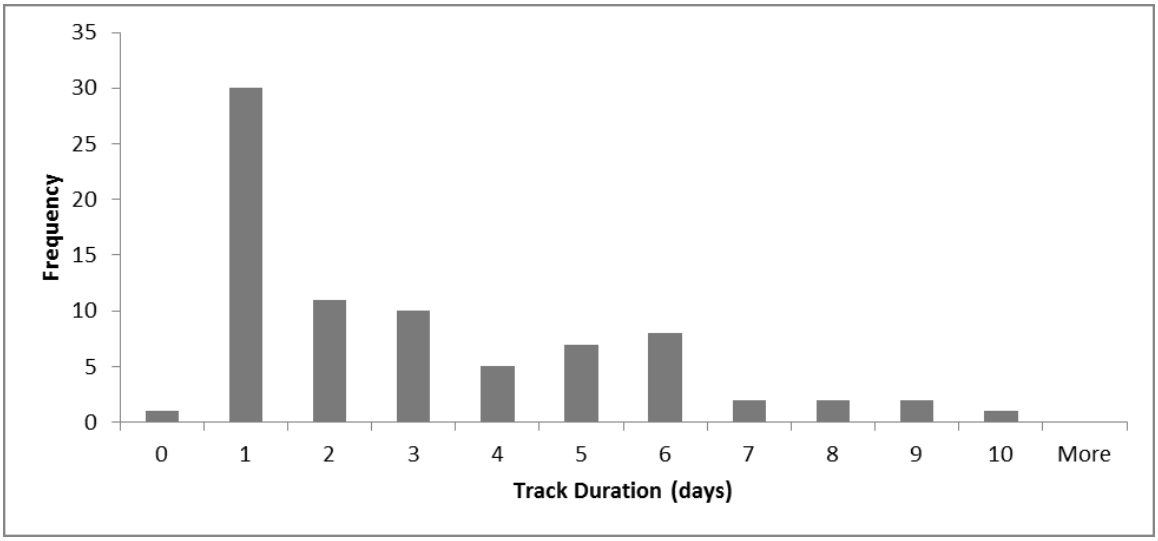

Figure 2: Histogram showing distribution of track duration

To the best of my knowledge, a fully automated approach to track quality assurance has not been created, but a look at the distribution of track length and duration provided some insight. Figure 2 is a histogram showing the duration in days for the tracks. The most frequent occurrence was 30 tracks having duration of between 0 and 1

day. These are very short tracks, but include at least 2 observations. The next two bins have a combined total of 21 tracks with durations of 2 to 3 days. These are also short lived tracks, but some include as many as 12 observations. There is a histogram mode for track durations of between 4 and 7 days with a peak in the 5 to 6 day region. These four histogram bins account for 20 tracks. Because their durations are approaching the average lifespan of a tropical wave, it is likely that many high quality tracks fall into this range. The longest duration tracks are those lasting 7 days or more. Again, these are likely to be high quality tracks successfully generated by the tracking software using "out of the box" settings.

In addition to track duration, the analysis took a look at the number of observations per track. Because NHC TWD bulletins are released on a regular 6 hour cycle, there should be some degree of correlation between observations per track and track duration. Figure 3 is a histogram showing the distribution of observations per track. The second bin in Figure 2 corresponds with the second bin in Figure 3. In Figure 3 there are 32 tracks with 1 to 4 observations compared to 30 tracks with durations of 1 day or less. The next two bins show the number of tracks with between 8 and 12 observations. This totals 22 tracks and is in close agreement with the 20 tracks that have durations of 2 to 3 days as shown in Figure 2.

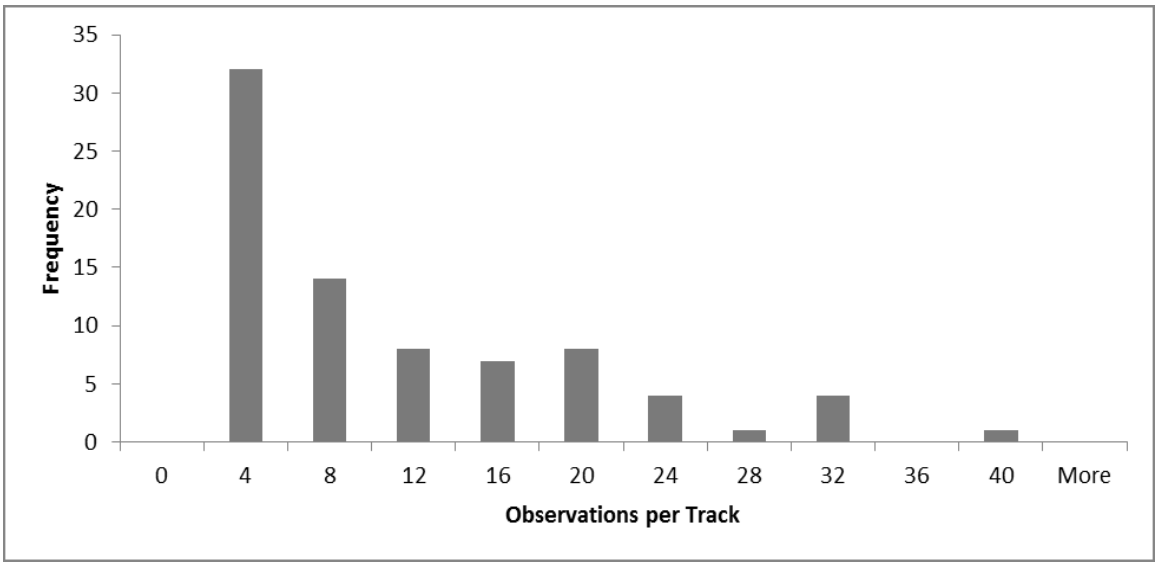

Figure 3: Histogram showing distribution of observations per track

A local minimum is barely apparent in the 16 observations per track bin and begins a mode similar to the one discussed in Figure 2. The three bins ranging from 16 to 24 observations per track include a total of 19 tracks. As in the mode observed in Figure 2, these are likely to be high quality tracks because a relatively large number of observations were assigned to each track by the MHT tracking software. The remaining bins in Figure 3 account for a total of 6 tracks, each containing more than 24 observations.

These initial results showed that improvements in track generation needed to be made. A set of experiments were designed to determine the optimal settings for the generation of tropical wave tracks. Additionally, it was apparent that additional parameters would be needed to optimize tropical wave tracking. The original software settings were designed to work with objects moving in any direction. But, in the case of

tropical waves, objects moving in a west to east direction were less likely to be a tropical wave than objects moving east to west – the prevailing direction of tropical wave motion.

A series of sensitivity experiments were run to determine which of the existing settings had a significant impact on track generation. The track quality assessment parameters at this point consisted of number of tracks, average track length, track length standard deviation, average number of points per track, number of points per track standard deviation, average track duration, and standard deviation of track duration. The sensitivity experiments revealed that probability of a new target and probability of a false alarm had the greatest effect on the quality assessment parameters.

After running some experiments that adjusted settings for the original set of parameters, new parameters were developed and included in the MHT software. The parameters added were:

- Prevailing direction – The dominant direction of tropical wave motion
- Probability direction minimum – This is the minimum probability to use. It is approximately equal to the probability that motion is opposite the prevailing direction that tropical waves travel.
- Distance gain – A value greater than 1.0 amplifies the effect of distance on the probability that the observed object belongs to the track currently being constructed.
- Distance limit – This is the threshold used by InGate. Distance measurements between two observations greater than this are disregarded. The observed object does not belong to the track currently being constructed.

In addition to adding parameters to the MHT software, a better quality assessment method was developed. These new quality parameters were included with the parameters mentioned earlier:

- Percentage of points used
- Maximum eastward movement
- Maximum north-south movement

The quality parameters were weighted so that a single number could be generated stating the quality of the tracks produced using a particular set of MHT settings. Although a broad range of carefully weighted quality parameters were used, the ability to pick up tracker errors was limited. Several full factorial experiments were run while adjusting the MHT settings with each run. The biggest problem with the tracker at that point was "back scans." This is when the tracker searches for the next point in a westward moving track and selects a point far to the east. To better understand this issue, track results were transformed into ESRI shapefiles and displayed on ArcGIS. The back scan problem was readily apparent when visually reviewing the tracks. I then realized that the quality metric had a maximum east value which only picked out one eastward moving segment of a track. Reviewing the tracks showed that a single track can have many segments moving to the east. Maximum east was replaced by a ratio of west to east where the higher the ratio, the more likely the track is correct. There was also a number of interacting quality parameters: number of tracks, average track length, and average track duration. With a set number of points, less tracks automatically results in longer track duration and length. Only one of the three interacting parameters needed to be

chosen for the quality metric. Since track duration is the main goal of building tropical wave tracks it was chosen as the parameter to use. This led to a reduced set of parameters to make up the track quality metric:

- Ratio of west to east – This is the total westward movement of all segments in a track divided by the total eastward movement of all segments in the track. The larger this ratio is the more correct the track is.
- Average track duration – This is the average duration of all tracks in an experiment run. Longer duration is associated with better track quality.
- Fraction of points used – This is the number of points assigned to tracks divided by the number of points available to the tracker. The more points used the more likely higher quality tracks will result.

As before, these three parameters were weighted so that a single quality number could be generated. Table 3 illustrates the procedure and decisions made in weighting the three quality parameters. Comparison among the three parameters as to which was more important than the other was based on looking at many tracks, in other words, experience. To illustrate, the quality parameter effort was preceded by several weeks of manually constructing and reviewing tracks. These manual reviews consisted of looking at points in sequential TWD bulletins and determining if they were correctly assigned to a track and if not, why not. By the time only three quality parameters remained for consideration, quite a bit of expertise had been developed in determining what constitutes a good track. However, two other parameters are used in the tracking discipline.

Table 3: Matrix used to determine weighting of parameters based on importance

	Avg track duration	% of points used	Ratio W to E	Total	Fraction of Grand Total
Avg track duration		2	2	4	0.571
% of points used	0.5		1	1.5	0.214
Ratio W to E	0.5	1		1.5	0.214
				7	
Criteria	Avg track duration	% of points used	Ratio W to E		Total Weight
Weight	0.571	0.214	0.214		1

The first is percent of auto track that covers a manually derived track. This parameter is difficult to automate, and automation is required here because of the large number of data points involved. But this parameter was actually used in the manual review just discussed. By looking at a long series of points and manually determining their status as a member of a particular track, I effectively used the method of comparing an auto track to a manually derived track.

The second parameter asks the question: how well does the tracker replicate end points? Again this requires a manual comparison of auto-generated tracks to points. The experience in this project was that the final point of a tropical wave as reported in a TWD was to a great extent included in a track. However, the first point of a track was often not included in a track. For tropical waves, many of the unused points are located just off the coast of Africa, where tropical waves are usually first observed. In conversations with other users of the MHT algorithm, this is a common problem. Manually attaching the

unassigned points to existing tracks was only considered and not done since the time spent doing it would not have added significant value, plus, since it was done manually, it was prone to human error.

The quality parameters were used to pick the optimal combination of settings in the MHT software. Earlier experiments, including sensitivity experiments, showed that the two dominant factors are time undetected, and the distance limit. Time undetected is one of the original MHT settings and is in units of minutes. The MHT uses this parameter as a way to terminate a track. If a viable point has not been detected within the allotted time, the code terminates that track. For the final experiment the settings were 1 day (1440 minutes) 2 days (2880 minutes), and 3 days (4320 minutes). Distance limit was added as an adjustable parameter replacing the original MHT "measurement InGate" value that was hard coded. (Points beyond this threshold were not added as a new point to the current track.) The distance limit was set to three levels: 10, 14, and 18 degrees longitude. Table 4 shows how all the settings were used in the final experiment. The table shows nine runs with all but time undetected and distance limit held constant for the entire experiment. Values that were held constant were determined by previous experiments, including sensitivity experiments.

Table 4: Settings used for each run of final experiment to optimize track quality

Run	1	2	3	4	5	6	7	8	9
maxNumLeaves	6	6	6	6	6	6	6	6	6
maxDepth	6	6	6	6	6	6	6	6	6
timeUndetected (minutes)	1440	2880	4320	1440	2880	4320	1440	2880	4320
bestK	10	10	10	10	10	10	10	10	10
probUndetected	0.01	0.01	0.01	0.01	0.01	0.01	0.01	0.01	0.01
probNewTarget	0.0001	0.0001	0.0001	0.0001	0.0001	0.0001	0.0001	0.0001	0.0001
probFalseAlarm	0.001	0.001	0.001	0.001	0.001	0.001	0.001	0.001	0.001
prevailingDir (radians)	3.14	3.14	3.14	3.14	3.14	3.14	3.14	3.14	3.14
probDirMin	0.01	0.01	0.01	0.01	0.01	0.01	0.01	0.01	0.01
distGain	1	1	1	1	1	1	1	1	1
distanceLimit (deg)	10	10	10	14	14	14	18	18	18

Table 5 shows the results of the final experiment. Using the weighted quality parameters, run number 2 produced the highest quality score of 0.897. The final scores for each of the runs varied over a narrow range of 0.08 indicating that the changes in parameter settings had subtle effects on the score. The settings used for run 2 were held steady for the remainder of the study.

Table 5: Results from final track quality experiment

	Run	1	2	3	4	5	6	7	8	9
Avg track duration	Raw	6.234	6.393	6.585	6.684	7.098	7.230	7.014	7.469	7.771
	Norm	0.802	0.823	0.847	0.860	0.913	0.930	0.903	0.961	1.000
	Wtd	0.458	0.470	0.484	0.492	0.522	0.532	0.516	0.549	0.571
Fraction of points used	Raw	0.936	0.936	0.937	0.941	0.942	0.942	0.942	0.944	0.945
	Norm	0.991	0.991	0.991	0.996	0.998	0.997	0.997	0.999	1.000
	Wtd	0.212	0.212	0.212	0.213	0.214	0.214	0.214	0.214	0.214
Ratio West to East	Raw	16.09	16.14	14.32	9.168	8.909	8.820	6.601	6.257	5.967
	Norm	0.997	1.000	0.887	0.568	0.552	0.546	0.409	0.388	0.370
	Wtd	0.214	0.214	0.190	0.122	0.118	0.117	0.088	0.083	0.079
	Score	0.884	0.897	0.887	0.827	0.854	0.862	0.817	0.846	0.865

The tracks generated for run 2 were put into shape files. Two sets of shape files were made for each year, one shape file holds the point data for a year, and the other shape file holds the tracks for the year. The tracks were then reviewed visually using ArcGIS. Although the experiments produced the best achievable quality metric, many of the tracks still did not look right. They looked incomplete, either ending too early or starting too late. A Quality Control (QC) column was added to each track shape file attribute table and the following process was used to inspect the tracks:

- Using ArcGIS for each year
    - Open the shape file attribute table
    - Sort ascending on the Duration column
    - Start editing
    - Select the first track in the attribute table to highlight the track in the map
    - Inspect the track and add P (pass) or F (fail) or leave blank if undecided

- Go to next track

This final QC step established the set of tropical wave tracks used for this research. The eventual selection of satellite data was based on first selecting tracks that have a "P" in the QC column, and then going on to select satellite data for each point within the track based on time and location.

Table 6 shows how the final QC process eliminated about half of the tracks generated by the MHT tracker. The tracks that were eliminated were incomplete tracks, tracks that were broken up into segments or tracks that started too far to the west. It is possible that tropical wave life times and therefore the duration of a track can be short, however the result of this process produced 345 tracks (on average 31 tracks per year) of good quality and were judged to be of sufficient number to study trends in tropical wave behavior over the study period.

Table 6: Final results of track generation

Year	Number of tracks	Number of QC passed tracks	Percent of tracks passed
2003	63	37	59%
2004	70	32	46%
2005	84	36	43%
2006	68	37	54%
2007	69	30	43%
2008	69	44	64%
2009	59	30	51%
2010	64	28	44%
2011	47	24	51%
2012	53	25	47%
2013	60	22	37%
Total	706	345	49%
Average	64	31	49%

Validation

To confirm the approach used in this research, comparison was made of the tropical wave locations derived from the TWD to the locations of tropical waves derived from other sources. A range of reference sources were explored in an attempt to match those used by the NHC TWD authors in locating tropical waves. Among those sources were imagery from GOES and Meteosat, NECP Reanalysis data, and NECP charts. In communication with NOAA it was learned that the agency considers their methods to locate tropical waves to be subjective, but the agency intends to eventually use a more objective approach similar to that described by Berry (Berry et al. 2007).

Since it would be impossible to duplicate the expertise, judgement, and resulting subjectivity intrinsic to the TWD, the objective approach sought by NOAA was used to validate the tropical wave locations acquired from the TWD. Data from the NECP reanalysis was used to create streamline graphics from 700mb u and v wind data using the Interactive Data Language (IDL) streamline function. Tropical wave locations from the TWD text mining were superimposed onto the streamline graphics, approximating the location of tropical wave axes. This was done for a sample of the tropical wave tracks data set. Data was selected at 1800Z, mid-month, for July, August, and September of each year in the study period. Each of the graphics was visually examined to see if the axes drawn on the streamlines were placed with respect to trough positions in a manner described by Berry. In general the axis was positioned to the right or left of the center of a trough. (A trough in this case being a northward diversion of the jet stream followed by a southern diversion.) Air to the right (or East) of the trough is forced upward, resulting in precipitation and clouds. This was a satisfactory alignment of tropical wave axes in many cases. Axes that were located to the left of the trough did not correspond to the normal definition of tropical waves, however they do correspond to the Berry method. Alignment of tropical wave locations to troughs was most successful in the eastern most and central Atlantic regions. Alignment degraded in the western region due to diminishing strength of the troughs. Examples from the validation effort are given in the Appendix. Although this was intended to be an objective method of locating tropical waves, the visual interpretation of the streamline graphics had significant uncertainty and required more subjective analysis than was initially hoped for.

However, the research was able to show objectively that the points identified in the TWD were propagating in a westward motion across the Atlantic. In addition, tropical wave positions reported in the TWD aligned well with synoptic cloud patterns observed in GOES and Meteosat imagery. Mosaics of AIRS percent cloud product were also used to verify TWD observations on a sample of the data set. Using this more objective information a modified version of criteria set forth by Berry was applied with positive results to the sample of the tracked weather systems assumed to be tropical waves:

1. The weather system was first observed moving off of the African coast near 15 deg N.
2. The system was observable for at least 24 hours.
3. The system was at least 500 km in meridional extent over the Atlantic Ocean at some point during its life cycle.
4. The weather system intersected with the African Easterly Jet at some point during its life cycle.
5. The system was tracked as a westward moving feature.

To summarize this validation, note that the TWD bulletins report on many types of weather features in the tropical Atlantic and the positions are given with the interests of mariners in mind and with apparently less priority given to the atmospheric scientist. Thus we see a more subjective reporting of tropical waves than might otherwise be given if the objective process described by Berry was followed. However, the analysis of streamlines proved to be subjective as well. Visual interpretation of the streamlines not only required locating points where turns exist, but also which set of streamlines to

follow. The streamline method could be automated but it may turn out to be a much more complex problem than it appears at first. Finally, given the synoptic extent of weather systems associated with tropical waves it is likely that the accuracy and resolution of the coordinates based on TWD bulletins provided sufficient positional guidance for selection of the satellite data sets used in this research.

Collection, Organization and Assembly of Data

Atmospheric measurements within an individual tropical wave were centered on the mid-point of the tropical wave axis. Figure 4 and Figure 5 show where the axis of a tropical wave is in relation to the wave itself and the weather conditions influenced by the tropical wave. Axis parameters are shown in Figure 6. If coordinates for both the northern and southern ends of the tropical wave axis are known, axis length and azimuth can be calculated. However both northern and southern coordinates were not always reported in the Tropical Weather Discussion. As mentioned earlier, bulletins issued before 2010 typically only contained coordinates for the northern extent. However, there were some bulletins issued in each of the earlier years that provided coordinates for both the northern and southern extent of tropical waves, making it possible to calculate mean values for axis azimuth and axis length for all years. To check on the feasibility of using data for years that primarily reported only the northern coordinates, mean axis azimuth was calculated for tropical waves in 2006, the year with the lowest number of two sets of coordinates reported, and 2013, the year with the highest number of two sets of coordinates. The results are shown in Figure 7 and Figure 8. In both cases the average axis azimuth was 185 degrees. Other analysis showed that 1000 km is a good estimate for

tropical wave axis length. Using these ideas, coordinates for tropical wave centers were estimated for all tropical wave observations that only included the northern set of coordinates. The next step was to select the AIRS data that is centered on each observation of the tracked tropical waves.

Figure 4: Atmospheric measurements within an individual tropical wave were centered on the mid-point of the tropical wave axis. This illustration shows where the axis of a tropical wave is in relation to the wave itself. Illustration from http://www.meteoweb.eu/wp-content/uploads/2013/06/Easterly_Waves_fig01-300x149.jpg

Data from the AIRS instrument aboard the Aqua satellite was used to analyze the atmospheric characteristics of tropical waves. Aqua is part of NASA's A-Train satellite family. Aqua is in a 705 km sun synchronous polar orbit and crosses the equator in the afternoon at 1:30 pm local time on the ascending node and again at night local time on the descending node. Measurements for this research centered around 14 degrees north latitude so collections were made slightly ahead or behind the equator crossing time

depending on the orbital node. AIRS combines optical and passive microwave measurements to produce atmospheric profiles of temperature, moisture and pressure. The microwave frequencies are measured with the Advanced Microwave Sensor Unit (AMSU).

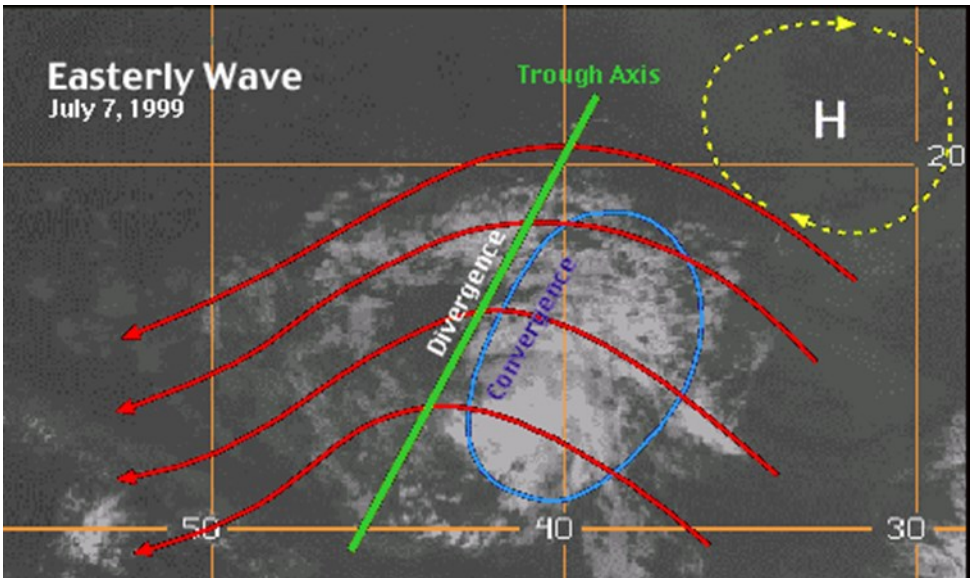

Figure 5: This more detailed illustration shows where the axis of a tropical wave is in relation to the wave but also to the weather conditions influenced by the tropical wave. Illustration from http://people.cas.sc.edu/carbone/modules/mods4car/tropcycl/pages/easterlywave.html

Data was downloaded for this research project from NASA's Mirador web site in the summer of 2014. The region covered was from the equator to 45 degrees north latitude and from 0 degrees longitude west to 100 degrees west longitude. The time span for this data down load covered all of 2003 through 2013 which includes the first full year of AIRS operation and the full year preceding 2014 when the download occurred.

The dataset includes all of the AIRX2RET AIRS level 2 version 6 products and consists of 126,944 HDF-4 files totaling 450.5 GB.

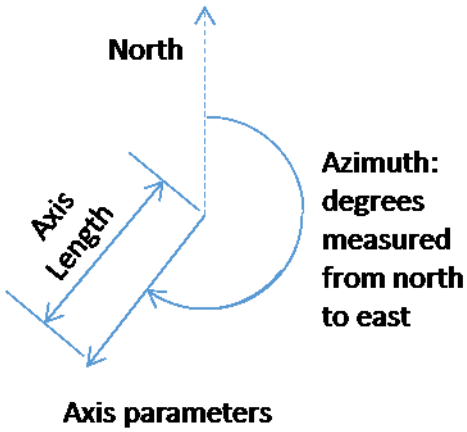

Figure 6: Axis parameters are shown here. The tropical weather discussions that document tropical wave locations typically specify coordinates for the northern and southern extent of the tropical wave. Axis length and azimuth can be calculated from these coordinates.

AIRS makes a collection every six minutes. All collections are at nadir. The optical component of an AIRS collection has a square pixel size of 15 km while the passive microwave produces a 45 km square pixel. Most of the AIRS products which use a combination of optical and microwave measurements have a 45 km pixel size. However, some products do have a 15 km pixel size. One example of this is the version 6 cloud products used in this research. The area of Earth's surface covered in a single collect is represented in a rectangle 90 pixels wide by 135 pixels high. Based on the 15 km per optical pixel this translates to an area 1350 km wide by 2025 km high.

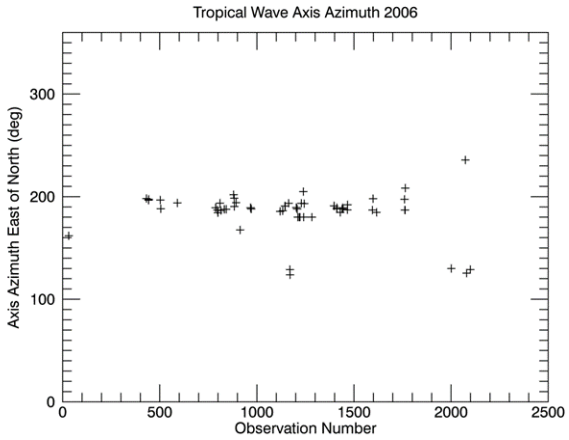

Figure 7: Azimuth chart for 2006

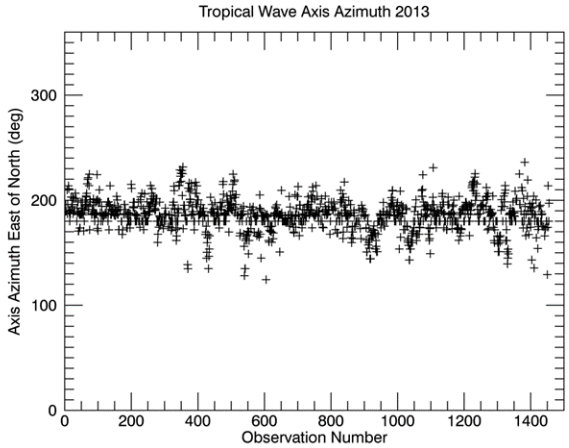

Figure 8: Azimuth chart for 2013

Each swath covered by AIRS consists of nominal 2025 km long sections that are generally adjacent to each other with little overlap or gaps in between. However, swaths from successive orbits do have substantial gaps between them. To compensate for gaps in data collected during one node, data was also collected from opposite nodes preceding or

following the primary node by approximately 12 hours. Mosaics for each point in a tropical wave track were assembled beginning with a central AIRS image, then the preceding and following images in the same swath were added, followed by three images each from adjacent swaths. This results in a three by three mosaic of nine images with the central image containing the center of the tropical wave. Another nine images from the opposite node, closest in time to the primary node, were inserted beneath the primary images in the mosaic. This layered arrangement filled gaps between swaths almost completely. Areas in each mosaic that were not filled with valid data were assigned a value of Not-A-Number (NAN) and were treated as missing data during analysis. These large mosaics ensured that tropical waves could be analyzed with extents as large as 2000 km square. The mosaics contained as many layers, or bands, as the data product they were created from.

ANALYSIS

Tropical Wave Extent

Although the center point of each tracked tropical wave was either known or estimated, measurements needed to be made on larger areas representing a reasonable sampling of the tropical wave. To establish a sampling area, an image processing method of determining the extent of a tropical wave was tried. This method used temperature, moisture, and pressure profiles to create a mask that identified pixels in a sounder image where measurements are to be made. The technique was initially demonstrated on sounder data provided by the Cross Track Infrared Sounder (CrIS) aboard the Suomi National Polar-orbiting Partnership (NPP) satellite. However, as with image processing algorithms in general, thresholds determining where the sampling should be placed could not be automatically determined reliably.

Rather than use an image processing technique to establish measurement areas a much simpler approach was used. This approach established three different sized Area Of Interest (AOI) centered on the tropical wave center point. The sizes were 500 km, 1000 km, and 2000 km squares. These sizes were chosen based on a typical north to south axis length of 1000 km as reported by the National Hurricane Center in their Tropical Weather Discussion bulletin. However, it is likely that non-tropical wave clouds would be included in the larger 1000 km and 2000 km AOIs. For this reason analysis was done separately for each of the AOIs. Ultimately, the three sizes proved to be appropriate as

characteristics close to the center of a tropical were often different compared to characteristics further out. This phenomenon was observed in the analysis of periodic variability of tropical wave cloudiness and provided the basis for a theory regarding stability in the core of a tropical wave when compared to the surrounding area.

Tropical Wave Age

In this research tropical wave life cycle was defined in terms of position rather than time. Time might be preferred, and is probably the first parameter that enters one's mind when thinking about life cycle. But, in the case of tropical waves it was difficult if not impossible to determine the date of birth of a tropical wave. The first observation of a tropical wave could have been recorded as its birth, but is this really the birth of a tropical wave? Additionally, the multiple hypothesis tracking algorithm that was used had the characteristic of not reliably including the first observation of a tropical wave in its track. So for these reasons tropical wave life cycle was defined in terms of position. Because tropical waves moved reliably from east to west, position was defined primarily in degrees longitude. Of course there were north and south components of tropical wave motion but the primary movement was in the east to west direction. Tropical wave life cycle was standardized by defining a set of regions as shown in Figure 9. As a tropical wave moves through these regions it enters into a series of stages within its life cycle. The early stage occurs in Region 1 with the more mature and final stages occurring in the more western regions. The regions are 15 degrees wide in longitude, and extend from the equator to 45 degrees north latitude. The eastern edge of Region 1 is at 15 degrees west longitude and the western edge of Region 6 as at 105 degrees west longitude. At 15

degrees north latitude, the nominal centerline for tropical wave tracks, the width of each region is 1613 km.

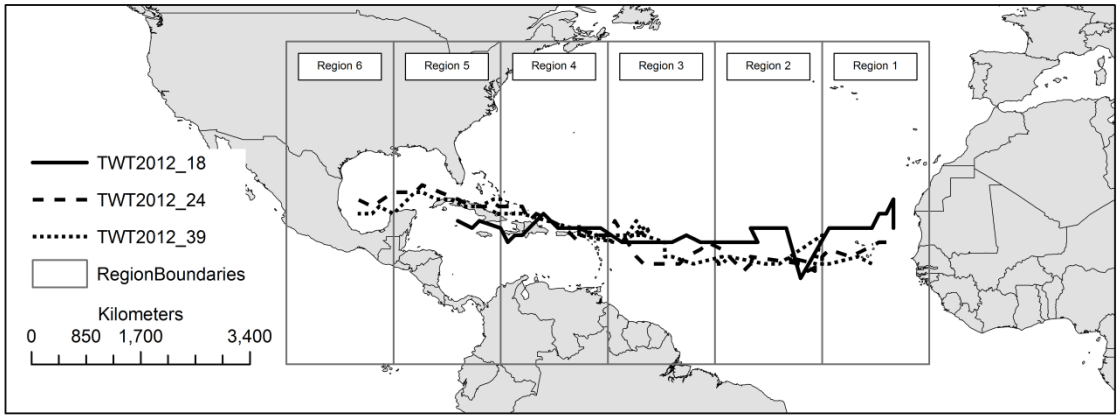

Figure 9: Tropical wave regions

Selection of Data Products

NASA produces a variety of products based on the AIRS instrument. These products include atmospheric profiles of temperature, moisture and pressure. Included in the version 6, level 2 product collection, are cloud products. The product labeled Cloud Fraction Standard (CldFrcStd) provides percent cloud per pixel for both an upper and lower cloud layer. The AIRS sounder captures radiance values in spectral channels sensitive to cloud fraction and height, and from this the two layer CldFrcStd product is derived (Kahn et al, 2013).

Clouds are a significant component of tropical waves, and the vast quantities of clouds produced by tropical waves may have a global impact on climate. The Fifth Assessment Report (AR5) report on climate change (Boucher et al. 2013) discusses the

concept of cloud feedback, and the potential it has on the Earth's radiation budget. Clouds reflect radiation from the sun back into space no matter what altitude they are at. The bottoms of clouds also reflect long wavelength heat from the atmosphere downward. This is the insulating effect that clouds have. Note that the more of the atmosphere there is radiating heat, the more heat will be reflected downward. With this in mind, the amount of heat reflected back is a function of cloud height. The higher the cloud layer, the more heat there is to reflect back to the surface. So the two factors that are at work are the tops of the clouds reflecting radiation back into space, and the bottoms of the clouds reflecting radiation back into the atmosphere and the surface. From this one can imagine a ratio of high clouds to low clouds being a measure of how cloud layers will function in a cloud feedback system. In the measurements made in this research a high altitude to low altitude cloud fraction ratio was derived from the AIRS cloud fraction standard product and included as a parameter of tropical wave cloudiness.

Time Series Analysis of Tropical Wave Cloudiness

The primary goal of this research was to gain some understanding of year to year changes in the life cycle of tropical waves. For this study a tropical wave life cycle was defined in terms of region, but since the interest was in how tropical wave life cycles have changed year to year, the focus was transposed to study trends within each region over a span of years. Once the year to year variability within each region was understood, this knowledge was transposed back to a year-to-year life cycle frame of reference.

To study year to year trends a time series was created across the years for each region. Figure 10 shows a time series for Region 3. In this case the AIRS CldFrcStd

product, Layer 0, is shown. The pronounced clumping of points is due to the seasonality of tropical waves, which only appear from May through November of each year. In addition, changes in the distribution of the cloud fraction from year to year can be seen. For example the range of cloud fraction values for 2006 is smaller than for any other year. The variations in the distributions suggest trends and other patterns that can be examined analytically. Since there may be a secular trend in this data an investigation for detecting such a trend was undertaken.

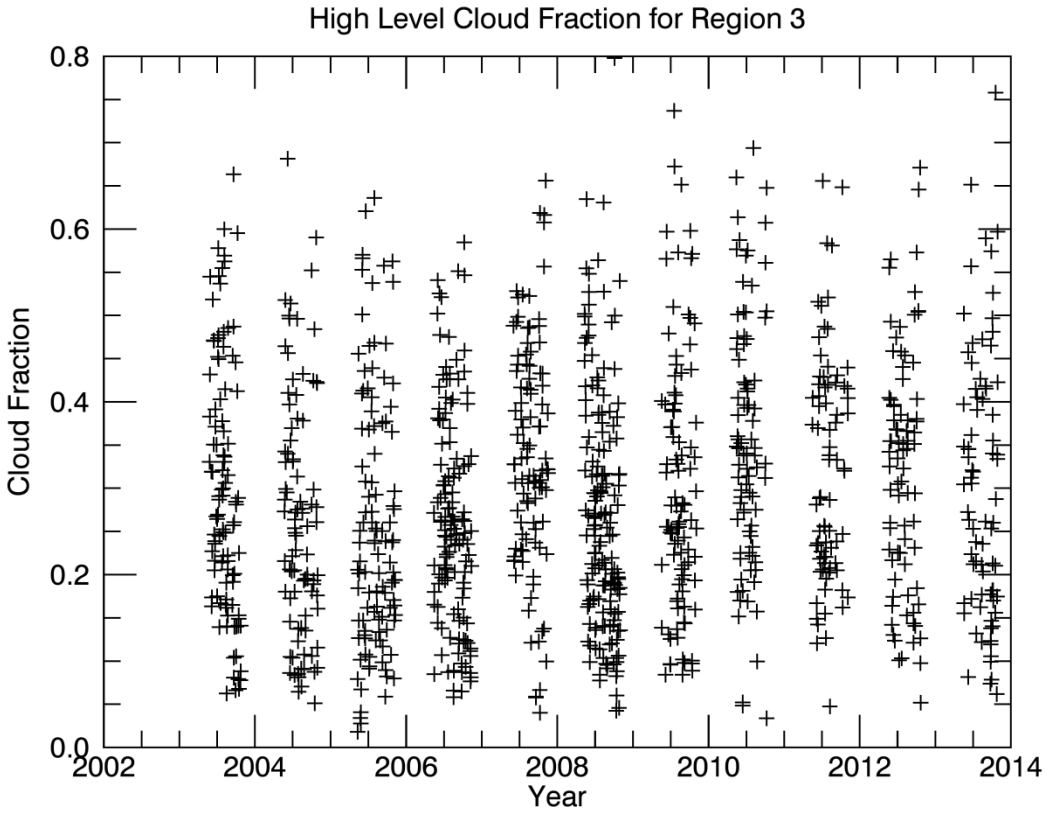

Figure 10: High level cloud fraction for Region 3

Two tests for trend were explored: Kendall's tau and Spearman's rho. These tests are based on rank correlation. If there is no correlation between time and the parameter being tested, in this case cloud fraction, then the variables are independent and there is no trend. On the other hand, if some degree of correlation is found, then, depending on the level of confidence assumed, the notion that there is no trend is rejected.

Both Kendall's tau and Spearman's rho are non-parametric tests for a linear trend. Hirsch (Hirsch and Slack, 1984) lists reasons for choosing a non-parametric test that matched up with my data. The first reason is non-parametric tests do not require that the data have a normal distribution. Secondly, non-parametric tests are insensitive to missing data. This last statement is important. As shown in Figure 10 there is no tropical wave data between the months of December and April. Finally, a non-parametric test does not need to have uniform sampling. Although the TWD bulletins were issued every 6 hours, that schedule only guided the selection of satellite data within a 6 hour window. Actual data collection time can be anywhere within that window.

The question of seasonality was explored. As can be seen in Figure 10 a strong seasonal pattern is apparent. This led to considering the trend test for seasonal data described by Hirsch (Hirsch et al. 1982) (Hirsch and Slack 1984) which is based on month by month sampling over a multi-year dataset. But in the examples given in their articles the patterns were not the simple on/off patterns seen in the tropical wave data, which is essentially a case of missing data. Therefore the month by month sampling over the multi-year dataset was not used here. However Kendall's tau (Kendall 1938), which

is the basis for the seasonal tests described by Hirsch, still appeared to be a good choice to detect the presence of a monotonic trend in the tropical wave data.

To calculate tau, the IDL function R_CORRELATE with the option /KENDALL was used. This function reports tau and also copes with ties, that is, x or y values that are the same and result in a delta of zero between two subsequent, ranked values. However, this IDL function does not report a test statistic. To add a test statistic, the IDL R_CORRELATE function was modified so that a Z score was included in the output. From this, following the method described by Helsel and Hirsch (Helsel and Hirsch 2002), the Z score was used to test the significance of tau. To select the null hypothesis, H0 : tau = 0 or the alternative hypothesis H1 : tau $\neq$ 0, Z was used in a two tailed test at a significance level of 0.05 to yield the results shown in Table 7. In this table, results are given for layers 0 (high altitude cloud fraction) and 1 (low altitude cloud fraction) at three sampling AOI. Under regions 1 through 6, tau, number of tropical wave observations (N), and results of the hypothesis test are listed. A failure to reject H0 indicates that tau is within the .05 confidence limit of being zero and thus we can assume there is no trend. In other cases where H0 is rejected there is enough of a signal to indicate a trend is likely. In Table 7, trends are detected (Reject H0) in all of the regions but are most numerous in the higher altitude cloud layer of regions 2 and region 3. These trends were confirmed by looking at the Spearman's rho results.

Table 7: Results of hypothesis testing for trend in individual cloud layers using Kendall's tau

			Region 1			Region 2			Region 3		
Parameter	Layer	AOI (km)	tau	N	Reject H0?	tau	N	Reject H0?	tau	N	Reject H0?
CldFrcStd	0	500	0.034	562	Fail to Reject H0	0.051	1062	Reject H0	0.068	1112	Reject H0
CldFrcStd	1	500	0.016	562	Fail to Reject H0	-0.009	1062	Fail to Reject H0	0.008	1112	Fail to Reject H0
CldFrcStd	0	1000	0.047	562	Fail to Reject H0	0.089	1062	Reject H0	0.073	1112	Reject H0
CldFrcStd	1	1000	0.002	562	Fail to Reject H0	-0.002	1062	Fail to Reject H0	0.004	1112	Fail to Reject H0
CldFrcStd	0	2000	0.104	562	Reject H0	0.124	1062	Reject H0	0.064	1112	Reject H0
CldFrcStd	1	2000	0.017	562	Fail to Reject H0	-0.008	1062	Fail to Reject H0	-0.022	1112	Fail to Reject H0

			Region 4			Region 5			Region 6		
Parameter	Layer	AOI (km)	tau	N	Reject H0?	tau	N	Reject H0?	tau	N	Reject H0?
CldFrcStd	0	500	0.052	985	Reject H0	0.067	840	Reject H0	-0.050	188	Fail to Reject H0
CldFrcStd	1	500	-0.017	985	Fail to Reject H0	-0.023	840	Fail to Reject H0	0.116	188	Reject H0
CldFrcStd	0	1000	0.039	985	Fail to Reject H0	0.042	840	Fail to Reject H0	-0.014	188	Fail to Reject H0
CldFrcStd	1	1000	-0.039	985	Fail to Reject H0	-0.021	840	Fail to Reject H0	0.112	188	Reject H0
CldFrcStd	0	2000	-0.011	985	Fail to Reject H0	0.008	840	Fail to Reject H0	0.013	188	Fail to Reject H0
CldFrcStd	1	2000	-0.070	985	Reject H0	-0.068	840	Reject H0	0.004	188	Fail to Reject H0

The use of Spearman's rho is well covered in Iman (Iman 1994) where the test statistic T_R is presented in Iman's equation 11.8:

Equation 1: Test statistic for Spearman's rho

$$T_R = r_R \sqrt{\frac{n-2}{1-r_R^2}}$$

where r_R is Spearman's rho and n is the number of samples. Calculation of rho was provided by the R_CORRELATE function in the IDL programming language. Using the test statistic T_R, the null hypothesis, H0 : rho = 0 and alternative hypothesis H1 : rho ≠ 0 were tested in a two tailed test at a significance level of 0.05 to yield the results shown

in Table 8. As described regarding Table 7, results were generated for the AIRS product CldFrcStd, layers 0 and 1 at three sample areas for each region. The decision to reject H0 in each case agreed with the decisions made using Kendall's tau. Again there were indications of trends in all of the regions but were most numerous in the higher altitude cloud layer of region 2 and region 3.

Table 8: Results of hypothesis testing for trend in individual cloud layers using Spearman's rho

			Region 1			Region 2			Region 3		
Parameter	Layer	AOI (km)	rho	N	Reject H0?	rho	N	Reject H0?	rho	N	Reject H0?
CldFrcStd	0	500	0.052	562	Fail to Reject H0	0.077	1062	Reject H0	0.100	1112	Reject H0
CldFrcStd	1	500	0.026	562	Fail to Reject H0	-0.013	1062	Fail to Reject H0	0.013	1112	Fail to Reject H0
CldFrcStd	0	1000	0.072	562	Fail to Reject H0	0.132	1062	Reject H0	0.109	1112	Reject H0
CldFrcStd	1	1000	0.004	562	Fail to Reject H0	-0.002	1062	Fail to Reject H0	0.006	1112	Fail to Reject H0
CldFrcStd	0	2000	0.156	562	Reject H0	0.183	1062	Reject H0	0.097	1112	Reject H0
CldFrcStd	1	2000	0.026	562	Fail to Reject H0	-0.011	1062	Fail to Reject H0	-0.035	1112	Fail to Reject H0

			Region 4			Region 5			Region 6		
Parameter	Layer	AOI (km)	rho	N	Reject H0?	rho	N	Reject H0?	rho	N	Reject H0?
CldFrcStd	0	500	0.079	985	Reject H0	0.101	840	Reject H0	-0.077	188	Fail to Reject H0
CldFrcStd	1	500	-0.022	985	Fail to Reject H0	-0.031	840	Fail to Reject H0	0.181	188	Reject H0
CldFrcStd	0	1000	0.058	985	Fail to Reject H0	0.063	840	Fail to Reject H0	-0.020	188	Fail to Reject H0
CldFrcStd	1	1000	-0.058	985	Fail to Reject H0	-0.028	840	Fail to Reject H0	0.171	188	Reject H0
CldFrcStd	0	2000	-0.019	985	Fail to Reject H0	0.012	840	Fail to Reject H0	0.014	188	Fail to Reject H0
CldFrcStd	1	2000	-0.105	985	Reject H0	-0.103	840	Reject H0	-0.001	188	Fail to Reject H0

For lower altitude cloud layers (Layer 1) and the 2000 km extent, regions 4 and 5 indicate a negative trend, while all other trends are positive and appear in higher altitude cloud layers. Regions 4 and 5 encompass the entire Caribbean Sea, the eastern half of the Gulf of Mexico, and all of the West Indie Islands including Puerto Rico and Cuba. As land forms, these features are unique in the tropical wave life cycle, and along with the advanced age of tropical waves entering these areas, present an opportunity for further

research into why this reversed trend exists and what impact it has on weather and climate.

Cloud fraction ratio is the ratio of higher altitude cloud fraction to lower altitude cloud fraction. To calculate the cloud fraction ratio, I simply divided the Layer 0 higher altitude cloud fraction by the Layer 1 lower altitude cloud fraction:

Equation 2: Cloud fraction ratio

$$Cloud\ fraction\ ratio = \frac{Layer\ 0\ cloud\ fraction}{Layer\ 1\ cloud\ fraction}$$

Region 4 cloud fraction ratio is shown in Figure 11 as an example. Very large and non-finite ratios resulting from division by very small and zero value cloud fractions were eliminated using the IDL FINITE function and clipping any ratio over 100. Cleaning the data in this way retained 99.4% of the original samples and maintained a large enough sample set to test for trending of the cloud fraction ratio.

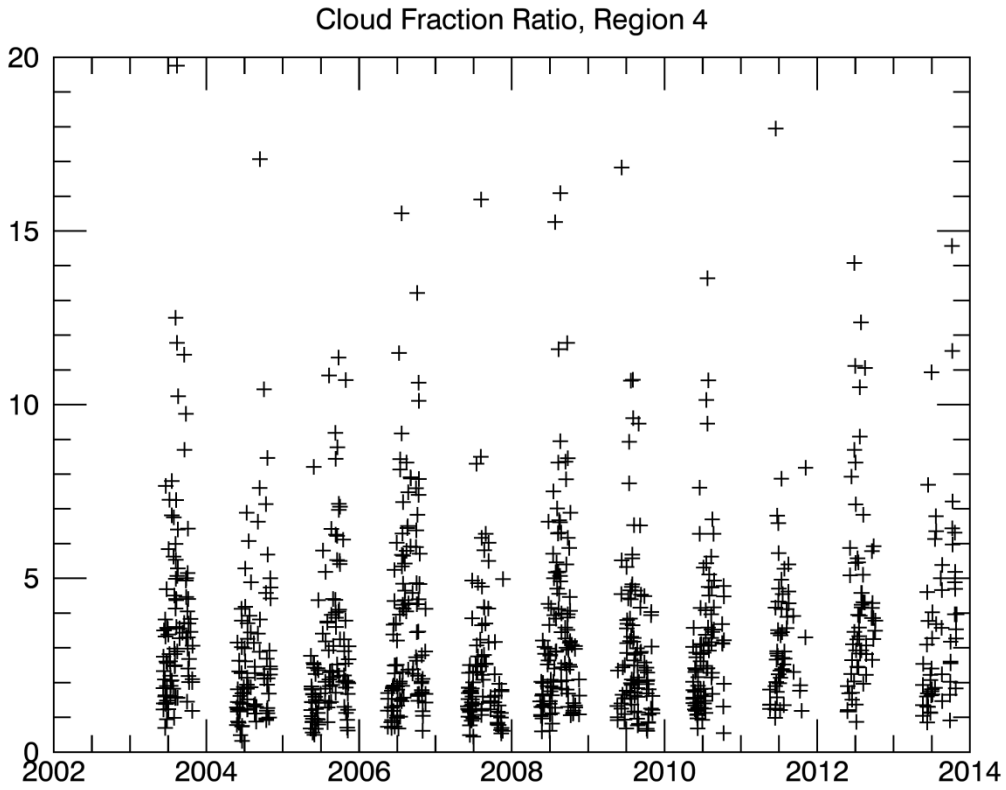

Figure 11: Cloud fraction ratio for Region 4

Trend analysis for cloud fraction ratio was performed using the same methods as was done with the individual cloud layers. Results are shown in Table 9 and Table 10. Results for Kendall's tau and Spearman's rho agreed across all combinations of region and AOI size. The null hypothesis that there is no trend was rejected in regions 2, 3, 4, and 5 for all area extents (AOI). In region 1, only the 2,000 km extent showed a trend. In region 6, a negative trend is indicated for the 500 and 1000 km extents. This was the only occurrence of a negative trend in the analysis of cloud fraction ratio.

Table 9: Results of hypothesis testing for trend in cloud fraction using Kendall's tau

		Region 1			Region 2			Region 3		
Parameter	AOI (km)	tau	N	Reject H0?	tau	N	Reject H0?	tau	N	Reject H0?
CldFrcRatio	500	0.012	560	Fail to Reject H0	0.042	1060	Reject H0	0.047	1110	Reject H0
CldFrcRatio	1000	0.035	562	Fail to Reject H0	0.058	1061	Reject H0	0.048	1112	Reject H0
CldFrcRatio	2000	0.057	562	Reject H0	0.090	1062	Reject H0	0.066	1112	Reject H0

		Region 4			Region 5			Region 6		
Parameter	AOI (km)	tau	N	Reject H0?	tau	N	Reject H0?	tau	N	Reject H0?
CldFrcRatio	500	0.053	984	Reject H0	0.075	839	Reject H0	-0.149	188	Reject H0
CldFrcRatio	1000	0.077	985	Reject H0	0.058	839	Reject H0	-0.142	188	Reject H0
CldFrcRatio	2000	0.092	985	Reject H0	0.107	840	Reject H0	0.008	188	Fail to Reject H0

Table 10: Results of hypothesis testing for trend in cloud fraction using Spearman's rho

		Region 1			Region 2			Region 3		
Parameter	AOI (km)	rho	N	Reject H0?	rho	N	Reject H0?	rho	N	Reject H0?
CldFrcRatio	500	0.013	560	Fail to Reject H0	0.064	1060	Reject H0	0.072	1110	Reject H0
CldFrcRatio	1000	0.052	562	Fail to Reject H0	0.089	1061	Reject H0	0.073	1112	Reject H0
CldFrcRatio	2000	0.083	562	Reject H0	0.137	1062	Reject H0	0.101	1112	Reject H0

		Region 4			Region 5			Region 6		
Parameter	AOI (km)	rho	N	Reject H0?	rho	N	Reject H0?	rho	N	Reject H0?
CldFrcRatio	500	0.078	984	Reject H0	0.109	839	Reject H0	-0.219	188	Reject H0
CldFrcRatio	1000	0.115	985	Reject H0	0.087	839	Reject H0	-0.216	188	Reject H0
CldFrcRatio	2000	0.137	985	Reject H0	0.159	840	Reject H0	0.015	188	Fail to Reject H0

A negative trend in cloud fraction ratio suggests that increases in high altitude cloud layers are occurring at a slower rate than increases in the low altitude clouds. Since higher clouds have a greater insulating effect than lower clouds, a negative trend in cloud fraction suggested a decreasing insulating effect over time and the potential for increasing negative cloud feedback in the Earth's radiative balance. The magnitude of these effects was found by measuring the slope of the trends using regression.

The tau and rho correlation values for region 5 cloud fraction ratio was quite strong, so a more detailed look at the trends for this region, beginning with the individual cloud layers, was informative. The plots in Figure 12 were created using the IDL LINFIT function to perform a regression on cloud fraction values for region 5 at each of the measurement extents.

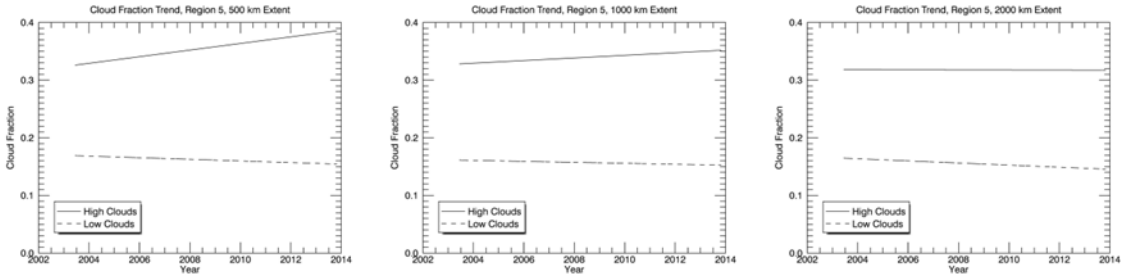

Figure 12: Regression of cloud fraction ratio at various measurement extents

Although cloud fraction ratio trends were detected for all cases in region 5, trends were not always detected in the individual cloud fraction data sets. The only trends detected were a positive trend in high clouds for the 500 km extent and a negative trend for low clouds in the 2000 km extent. These trends can be seen in Figure 12. Other trends are also perceptible in Figure 12, but were not inside the confidence limits of the tau and rho rank correlation hypothesis tests.

Calculating the ratio of high altitude cloud fraction to low altitude cloud fraction appeared to amplify the impact insignificant trends have when compared in this way. As shown in Figure 13 not only do the tau and rho tests indicate trends in cloud fraction ratios, but they are also readily seen in trend plots. Figure 13 shows the change in cloud

fraction ratio for region 5 over the course of the study period. The rate of change, or slope, is greater for areas close to the center of tropical waves.

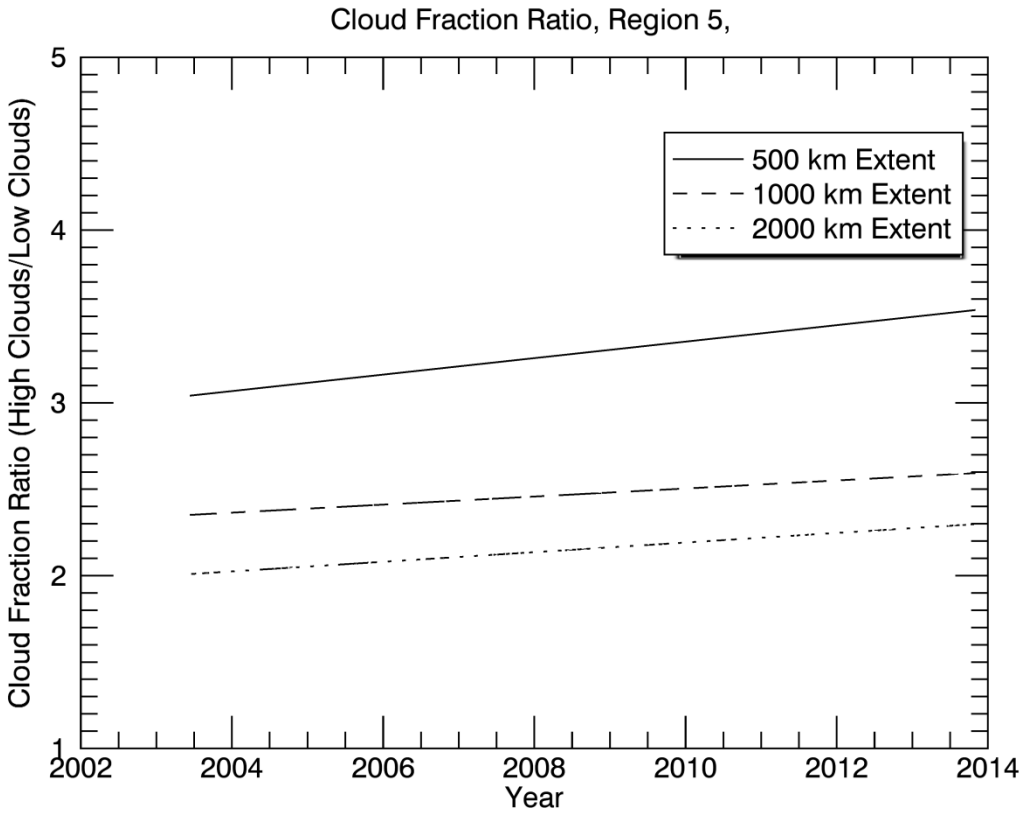

Figure 13: Cloud fraction ratio in Region 5 at various measurement extents

Close inspection of the cloud fraction ratio time series revealed a suggestion of intra-year seasonality. Figure 14 shows cloud fraction ratio associated with tropical waves in Region 4. There is a distinct arc up and then down for the minimal cloud fractions during 2006. There was evidence of cloud fraction ratio intra-year seasonality in

other years but not all. This is one of the most pronounced. Because any indication of seasonality was intermittent, this research concentrated on year to year trends and did not consider monthly year to year trends. That could be a topic of future research.

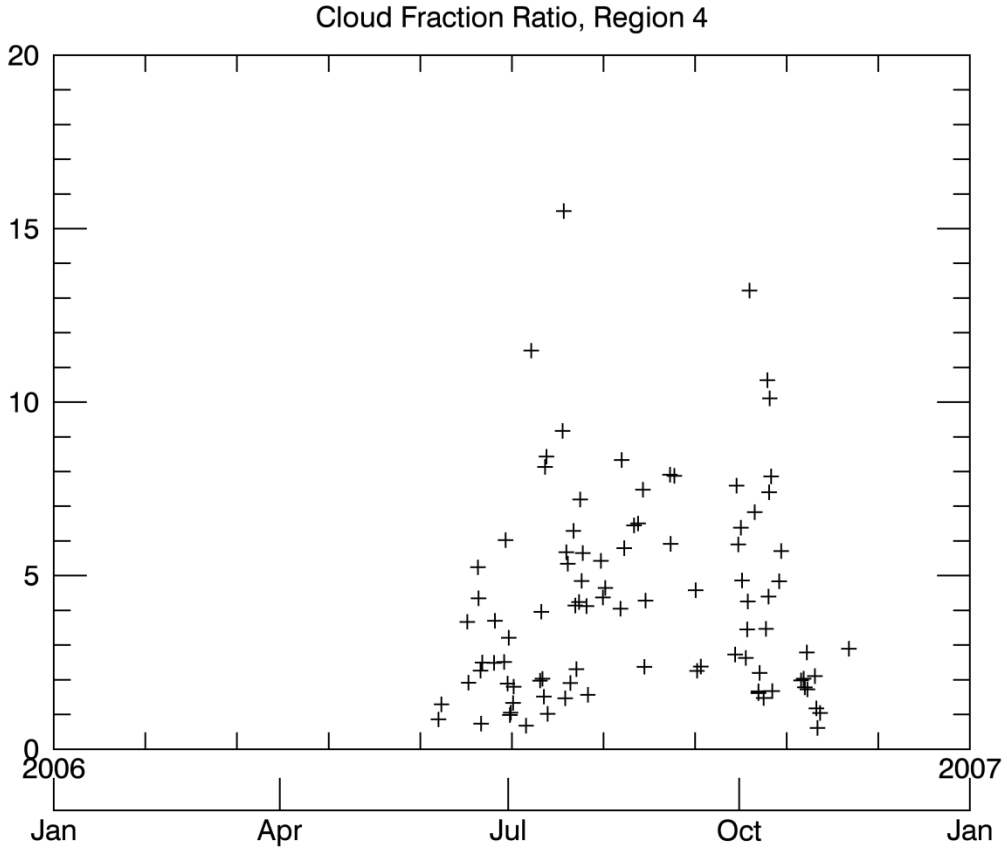

Figure 14: Cloud fraction ratio in Region 4 for 2006

An additional analysis of tropical wave cloudiness was applied which found the average cloud fraction for each season of the study period. This resulted in a plot of cloud fraction for each year. By transposing these plots, cloud fraction within a tropical wave

life cycle for each year was displayed. Figure 15 shows how high altitude cloud fraction changed over the life cycle of a tropical wave as it moved through each region. High altitude cloud fraction typically reached a minimum midway through a tropical wave life cycle. In some years the minimum was well pronounced as in 2013. In other years it may have been non-existent as in 2010. Figure 16 shows results for low altitude cloud fraction. In a fashion similar to high altitude cloud fraction, the low altitude cloud fraction throughout the life cycle of a tropical wave often experienced a minimum midway. There are years however when a well pronounced dip was not evident. Note how the years 2010 and 2013 show about the same amount of dip as the high altitude cloud fraction did in Figure 15. In Figure 17 the cloud fraction ratio finds a maximum midway through the life of a tropical wave. The location of the peak varied from year to year. There was always a return to a low value as the tropical wave entered the Caribbean region, region 6, as low clouds increased in relation to high clouds causing the high to low cloud ratio to decrease.

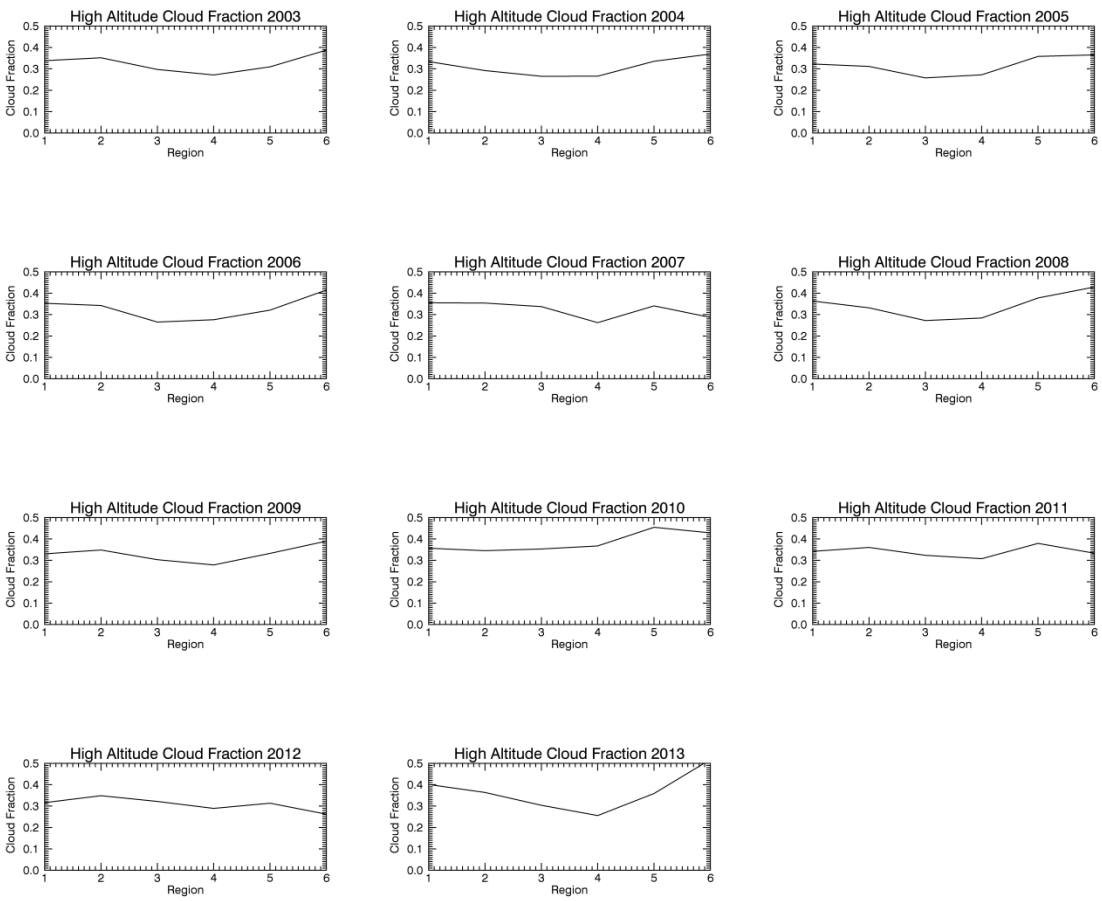

Figure 15: Tropical wave life cycle of high altitude clouds for all years, 500 km AOI

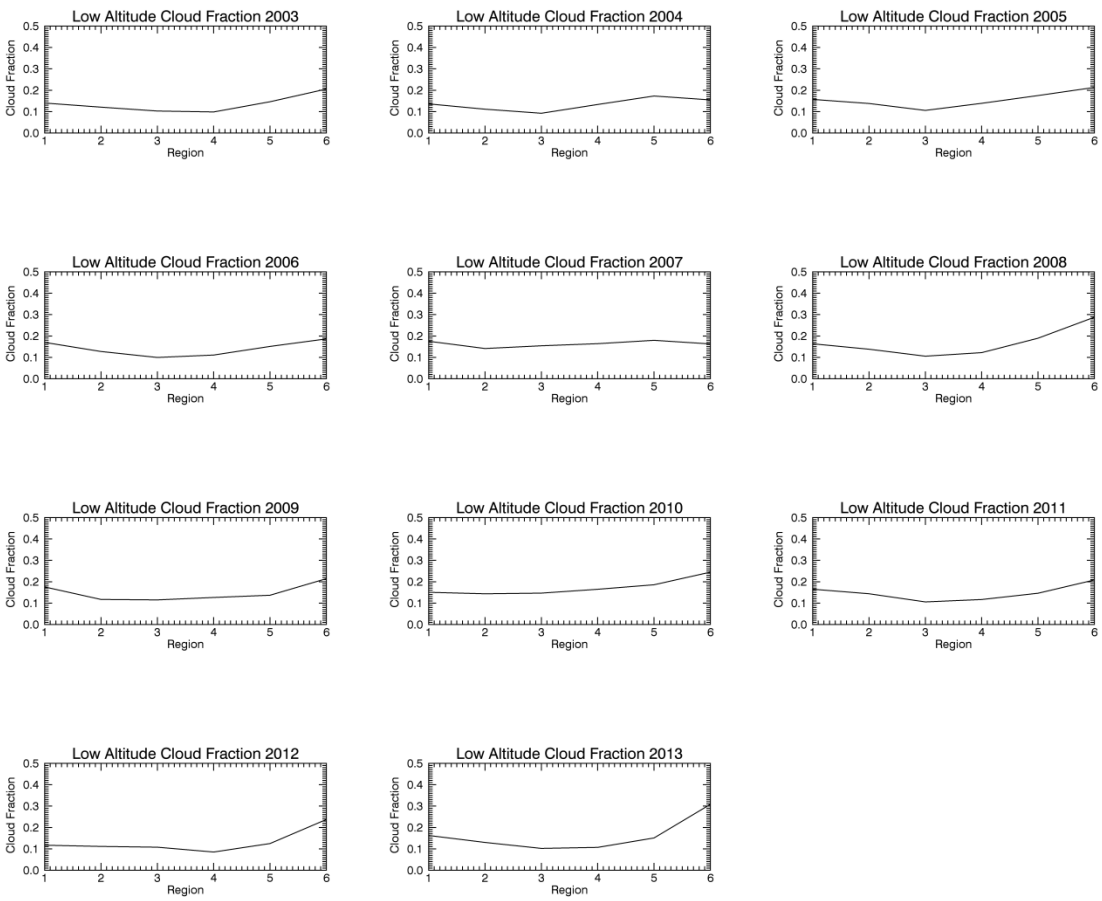

Figure 16: Tropical wave life cycle of low altitude clouds for all years, 500km AOI

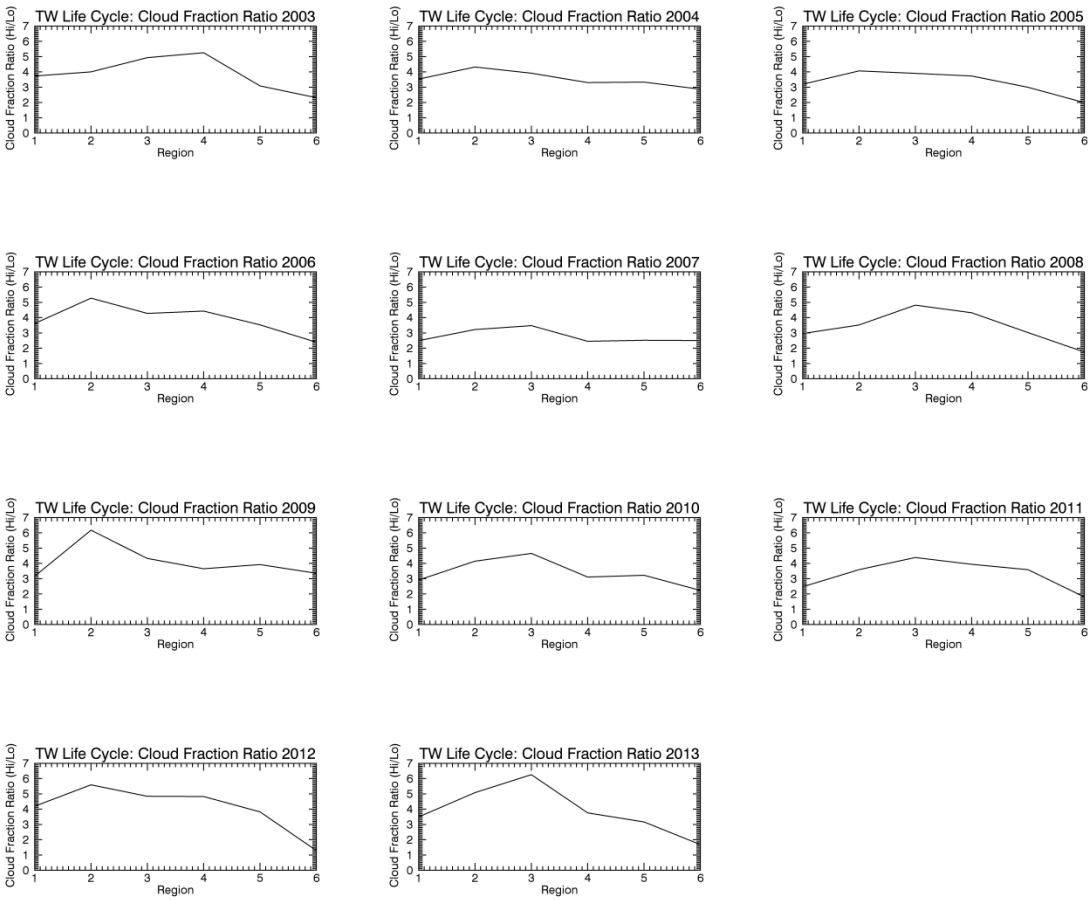

Figure 17: Tropical wave life cycle of cloud fraction ratio for all years, 500km AOI

Seasonal time series within each of the 6 geographic regions can be used to help explain multi-year variability of cloudiness. The year to year changes seen in tropical wave life cycles may be due to random processes or they may be due to known, or unknown, systematic processes in the atmosphere. By analyzing each region independently it may be possible to construct a model of year to year variability of tropical wave cloudiness.

Peaks and valleys of seasonal time series for each region corresponded to changes in the tropical wave life cycle plots shown in the previous figures. The seasonal time series, and the life cycle plots, are averages of cloud fraction measured over each season.

To perform a more detailed analysis a higher sampling rate needed to be used. Higher sampling rates were created using the raw data points.

Uneven sampling and missing data

Depending on the analysis method used, samples regularly spaced in time may be required. However tropical wave data was not collected at regular time intervals. For this research, tropical wave location was more important than collection time, therefore the samples were taken at the time Tropical Weather Discussion bulletins are issued. In these cases sample intervals tended to fall on a 6 hour cycle. However, the timing was not perfect as the bulletin release times varied by several minutes around the scheduled release time. More importantly, there are gaps in the data since there was not always a tropical wave for a bulletin to report on.

For situations where collection time is more important than tropical wave location actual AIRS collection time can be used. In these cases the data tends to fall on 12 hour intervals with the alternating ascending and descending nodes. Variations in the 12 hour cycle is due to the location of the Aqua satellite when the collection is made. Since six minutes is the AIRS collection cycle time, this would vary in 6 minute increments over the approximately 18 minute window during which the AOI is in the field of view. That variation impacts sample interval, but as with bulletin based sample intervals there will be missing data. Missing data may occur because there are no tropical waves being

reported or an AIRS collection cannot be found that aligns with a tropical wave position reported in the bulletin. The inability to provide regularly sampled data had a significant impact on analyzing periodic variability of tropical waves.

Periodic Variability of Tropical Wave Cloudiness

Time domain and spatial domain analyses are enhanced by observing data in the frequency domain. Beyond the secular and cyclical trends previously discussed, true periodic functions are likely to be found in the tropical wave cloud data. The tropical wave data has both time and space components which can be transformed into *temporal-frequency* and *spatial-frequency domains*.(Gaskill 1978). The method used here is temporal-frequency analysis applied over a series of spatial regions, the six regions previously discussed that define a tropical wave life cycle.

The goal of frequency analysis is to understand the components that make up a complicated, apparently non-periodic time series. The Fast Fourier Transform (FFT) segregates a time series into its cosine basis functions, with each cosine basis function being a periodic function with a known frequency and phase. Recombining these cosine basis functions using the Inverse FFT (IFFT) will result in the original time series minus any computational clipping or rounding that might have occurred in the process.

The assumption was made that the tropical wave time series is a linear combination of periodic functions plus non-periodic variability. From a frequency analysis standpoint, the non-periodic variability is noise. Within the periodic portion of the tropical wave time series, the dominant component was seasonality since the tropical wave data used in this research only exists during the northern summer season varying in

range from April to October. The off season portions of the time series were treated as missing data within the Kendall's tau and Spearman's rho analysis. The FFT however requires not only a regular sampling rate, but also values across the off season portions of the time series – missing data is not allowed. This was resolved by first interpolating the in season data to a regular sampling time line, and setting all the off season data points to zero. This appeared in the time domain as a series of rectangular clusters of data. A model for this seasonal effect is the RECT function which has the SINC function as its Fourier transform (Gaskill 1978).

Attempts were made to find periodic components in the tropical wave data using the FFT. Low frequencies, such as those with a period of greater than one were hard to resolve, but there was a low frequency peak that may have been related to El Nino. A higher frequency with a period of 68 days was also visible that might have been related to the MJO which has a typical period documented at 30 to 60 days. In the end however, poor low frequency resolution, noise, and aliasing prevented a satisfactory analysis of periodic variability using FFT. Another frequency analysis method needed to be used.

Just as trends in noisy data can be detected using the Kendall and Spearman analyses, periodic components in a time series can be identified using the Lomb Normalized Periodogram (LNP). The LNP and rank correlation methods are similar in that they work with unevenly sampled data, tolerate missing data, and provide a test statistic against noise so that hypothesis testing can be applied. The implementation of the LNP used in this research was the IDL function LNP_TEST which is based on the *fasper* routine described in Numerical Recipes (Press 2007). A limitation of LNP_TEST was

that it provided the probability that the peak frequency is not noise, but no probability or test statistic for other frequencies. To create a test statistic for all frequencies an exponential distribution was created based on the Lomb values and used to assign a probability to each frequency that it is noise. Using a 0.05 confidence limit, frequencies falling below that level were determined to not be noise and used in further processing.

The Lomb periodogram provided a noise free spectrum without aliasing and high resolution into the low frequencies that have multi-year periods. This worked with irregularly sampled data, missing data and provided a test statistic to segregate periodic signals from noise. No preprocessing of the time series was needed and in particular no requirement to fill in missing off season periods with zeros. However, with no adjustment to the off season characteristic of the time series the Lomb periodogram returned a strong 180 day period due to the seasonality of the data.

The 180 day period was the dominant frequency component in the Lomb periodogram output and needed to be removed so that other periodic components could be more accurately assessed. To accomplish this, frequency subtraction of the 180 day period and its harmonics was applied to the Lomb periodogram output as follows. The seasonal spectrum was modeled by first creating a rectangular waveform with the same duty cycle as the tropical wave season. The Lomb periodogram was applied to the rectangular waveform creating a seasonality spectrum. The seasonality spectrum was subtracted from the tropical wave spectrum, negative values set to zero, and magnitude of the 180 day period in the difference spectrum was tested. If the 180 day period had a magnitude of zero, or was no longer the dominant period, or if its probability of being

noise is greater than the 0.05 confidence limit, the difference spectrum was accepted. However, if none of the test conditions were met, an increased gain factor was applied to the seasonality spectrum and subtraction and testing of results was performed again. This process continued until the one of the test conditions was satisfied. The result was a clean spectrum for each of the AIRS cloud products with the frequency components due to seasonality attenuated or eliminated altogether. This process is illustrated in the Appendix, Figure 37.

A final adjustment to all periodogram results was to ensure that periods are not extrapolated beyond the duration of the study period. The eleven year study period consists of 4,015 days. Any periodogram results that were longer than 4,015 days were dropped from analysis. As it turns out, there were few instances of periods greater than 4,015 days.

High Altitude Cloud Fraction Periodograms

Figure 18, Figure 19, and Figure 20 show the high altitude cloud fraction spectrum viewed at three different AOIs centered on tropical waves in each region. Each of the regions appears to be rich in spectral components. However, there is a lower density of spectral components in the 500 km AOI than in the two larger AOIs. Increased spectral content with larger AOI was a continuing theme through the analysis results.

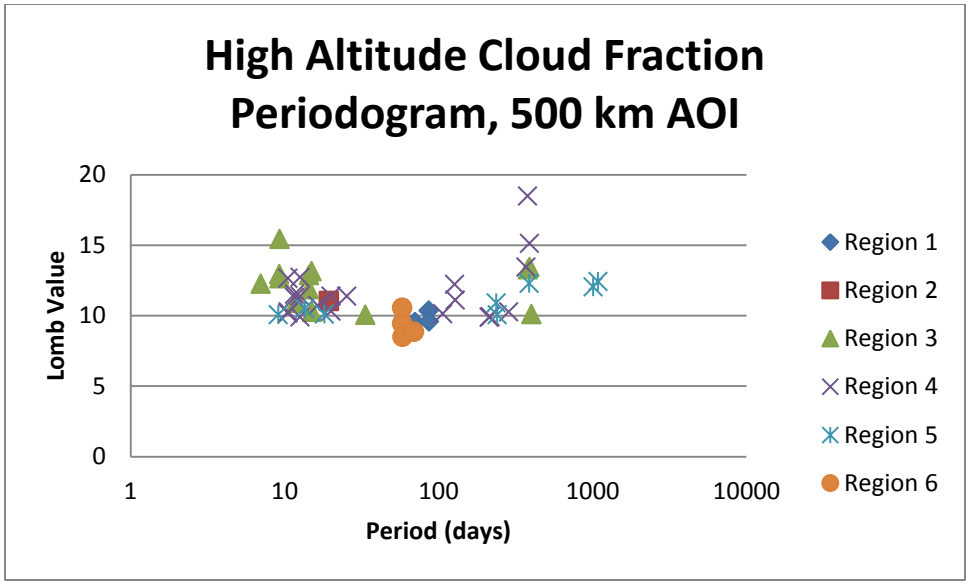

Figure 18: High altitude cloud fraction periodogram for 500 km AOI

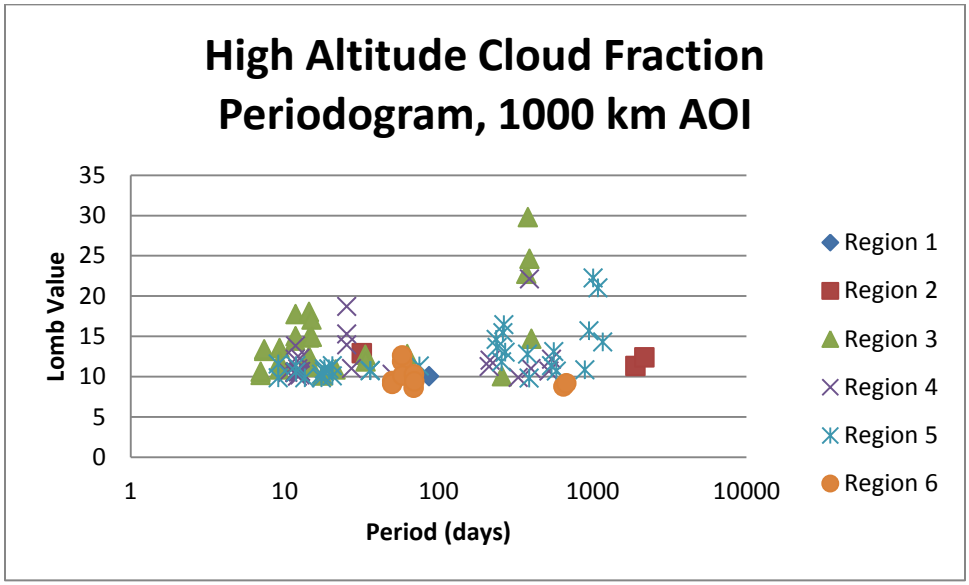

Figure 19: High Altitude cloud fraction periodogram for 1000 km AOI

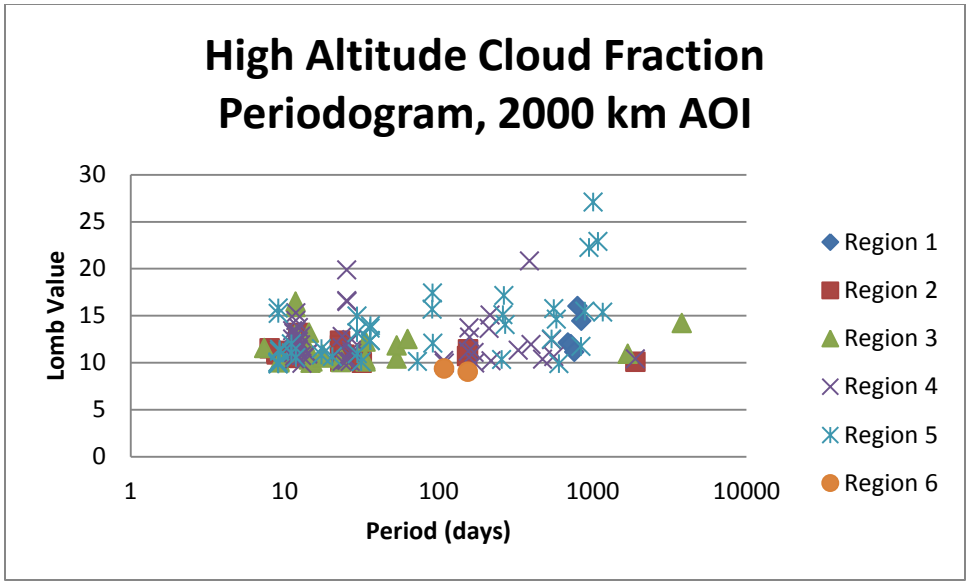

Figure 20: High Altitude cloud fraction periodogram for 2000 km AOI

Low Altitude Cloud Fraction Periodograms

The low altitude cloud fraction spectrums shown in Figure 21, Figure 22, and Figure 23 have distinctly different patterns from what was seen in the high altitude cloud fraction spectrum results. The 500 km AOI, although similar to the high altitude results in that it shows the lowest density of the three AOIs, was unique in that there is a significant gap in spectral components in the 100 to 1000 day region. The high altitude spectrums had relatively consistent spectral coverage across their entire ranges.

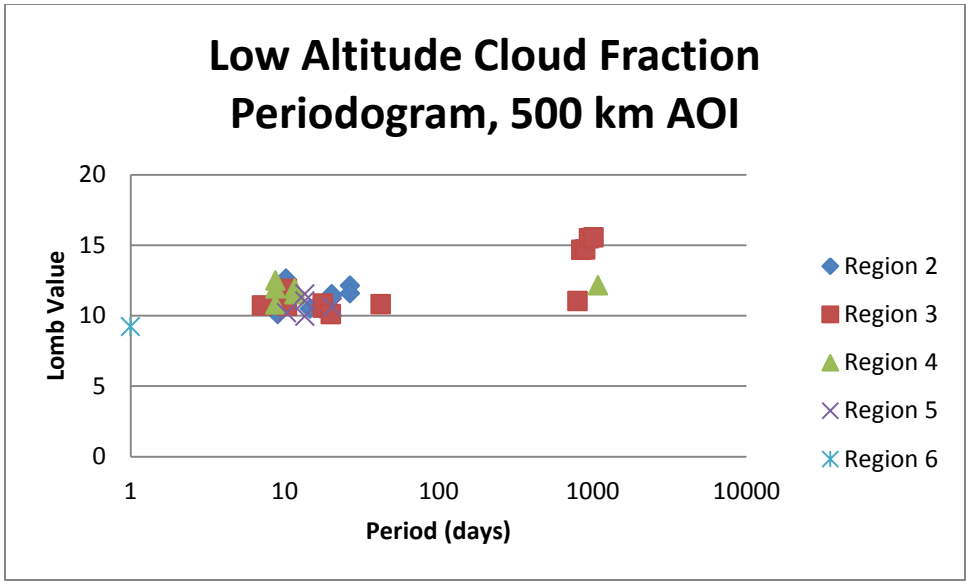

Figure 21: Low altitude cloud fraction periodogram for 500 km AOI

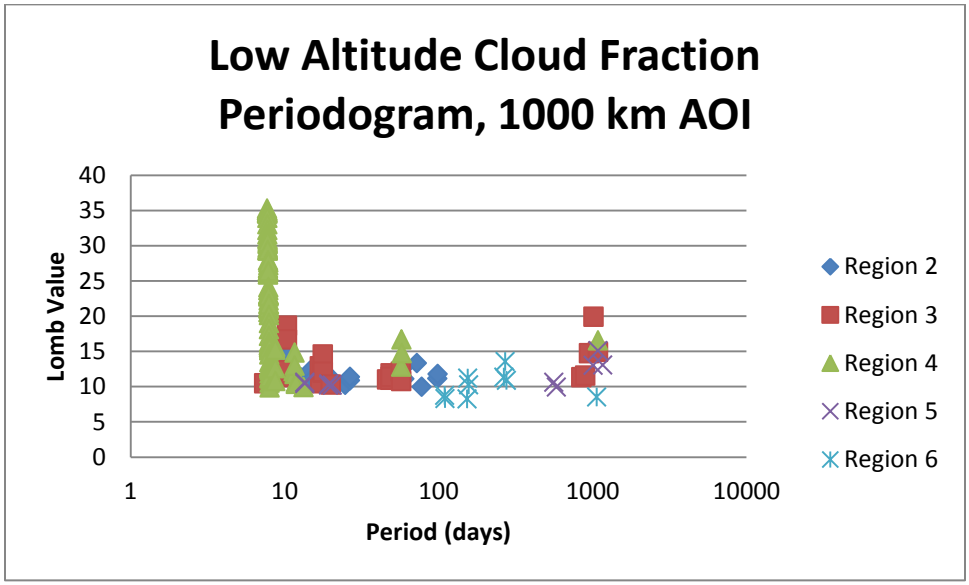

Figure 22: Low altitude cloud fraction periodogram for 1000 km AOI

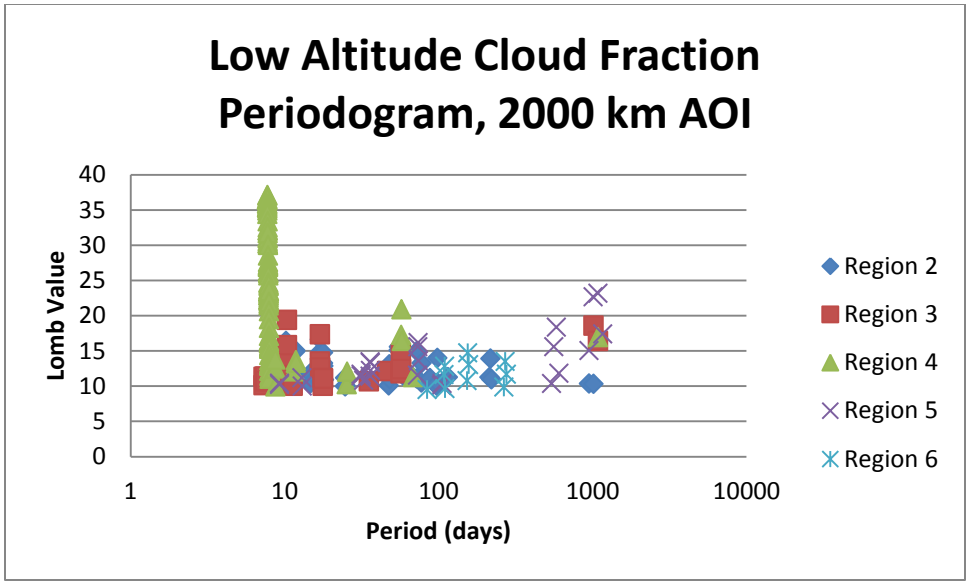

Figure 23: Low altitude cloud fraction periodogram for 2000 km AOI

It is also apparent in the low altitude cloud fraction spectral results that no periodic components were found in region 1 for all three AOIs. This indicates that although there was variability in the low altitude cloud fraction in Region 1, there is no periodic variability. This could be due to tropical waves in Region 1 being in the infant stage of development, having just moved off the coast of Africa. They had not yet come under the influence of the harmonic stimulation that is more apparent in later stages of development mid-ocean. In addition, these are low altitude clouds and are more subject to friction with the surface causing a dampening effect that reduces the ability of the air to sustain a cyclical characteristic.

Another characteristic in the low altitude cloud fraction periodograms is the tall spike of periodic components in Region 4 for the 1000 km and 2000 km AOIs. Here, the low clouds were in the western Caribbean, relatively close to the surface, and beginning

to engage some resistance with the Earth's surface as the tropical waves engage the Lesser Antilles, Puerto Rico, and Hispaniola. Alternatively, the tall spike of periodic components may be associated with Convectively Coupled Kelvin waves, an equatorial wave that spans the 7.7 to 8.0 day periods embedded in the region 4 spike.

Increasing spectral components with increasing AOI was a repeating characteristic as mentioned before. In the case of low altitude cloud fraction it is possible that clouds farther away from the tropical wave core were influenced more by external oscillatory influences than clouds closer to the tropical wave core. This effect is especially apparent in Regions 5 and 6 where a tropical wave would be in the final stages of its life entering the Caribbean Sea and Gulf of Mexico. Low frequency components tended to increase more in these regions than components with higher frequencies and shorter periods. Because tropical waves at these later stages in their life cycle were getting closer to land, they were becoming more influenced by atmospheric activity associated with land. In addition, some of these long term components were likely associated with the El Nino Southern Oscillation (ENSO) and as a tropical wave approaches the western Atlantic and Eastern Pacific, the impact of ENSO was intensified.

Cloud Fraction Ratio Periodograms

The cloud fraction ratio, a ratio of high altitude cloud fraction to low altitude cloud fraction, is a secondary derived product that not only has the potential to tell us something about the insulating quality of clouds, but combines the periodic variability of the low and high altitude layers in unique ways. Periodograms for cloud fraction ratio are shown in Figure 24, Figure 25, and Figure 26. Of particular note is the extremely sparse

periodic variability of the cloud fraction ratio within a 500 km AOI centered on tropical waves. The only detection of periodicity in this parameter was when tropical waves are in Region 2, an early intermediate stage of the tropical wave life cycle. The period as seen in Figure 24 was 98 days, well within a single season of tropical wave activity. Two factors may be at work here. First, as discussed earlier, the 500 km AOI holds a higher percentage of the tropical wave core than the larger AOIs. This leads to the belief that the resiliency and robustness of the tropical wave structure resists the tendency to respond to the global oscillations that impact the larger AOIs to a greater extent. And secondly, there may be a destructive combination of the periodic components in all frequency bands except the bands with periods around 100 days. In comparing the 500 km AOI periodograms for the high and low altitude cloud fractions, periodic components exist in both layers at all periods except for the periods around 100 days. Here only the high altitude cloud fraction periodogram has signals as can be seen on Figure 18, but none of these signals are at the 98 day period. Although there appears to be evidence of time domain signal cancellation in the cloud fraction ratio periodic spectrum, further review showed that the single 98 day period that exists in the cloud fraction ratio is not found in the underlying low and high cloud fraction spectrums.

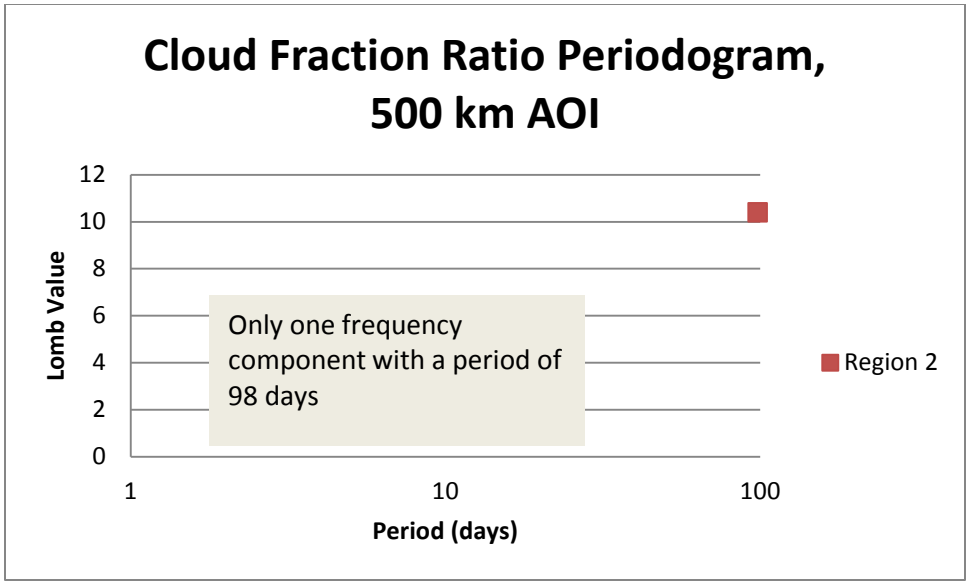

Figure 24: Cloud fraction ratio periodogram for 500 km AOI

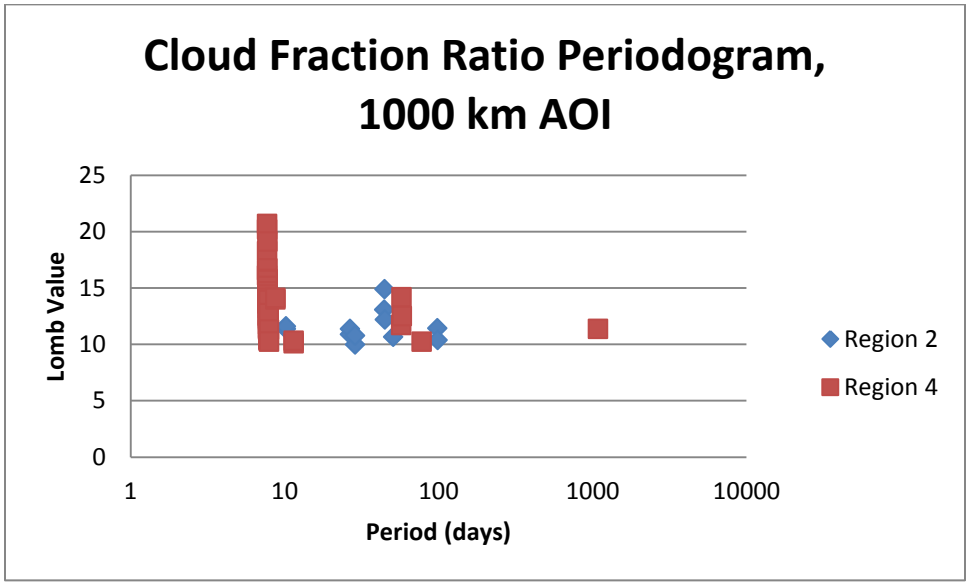

Figure 25: Cloud fraction ratio periodogram for 1000 km AOI

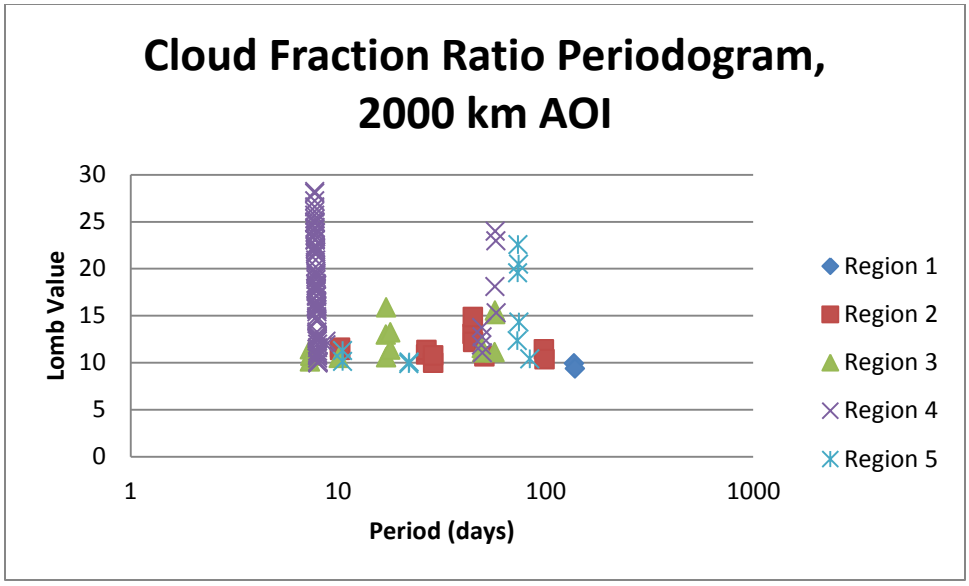

Figure 26: Cloud fraction ratio periodogram for 2000 km AOI

The cloud fraction ratio periodograms for the 1000 and 2000 AOIs had many more components than the periodogram for the 500 km AOI. Again we note the strong signal seen in the 7 day period region in both the 1000 and 2000 km periodograms. Another cluster of periodic signals can be seen in the two larger AOI periodograms between 10 and 100 days. Region 2 is significant in both of these AOIs indicating that oscillatory behavior starts appearing as the tropical wave moves further into the open ocean. Region 4, where tropical waves have just entered the Caribbean Sea, contains not only the strong 7 day period but also periods in the 100 day region.

Global Oscillations

The question of where does periodic variability within tropical wave cloudiness come from has two possible answers. They may emerge from oscillatory instabilities within the tropical wave itself or the atmospheric mechanism that forms a tropical wave, or periodic variability may result from global oscillations that impact tropical waves

during their life cycles. To determine which source periodic variability comes from known global oscillation data were collected followed by a search for evidence of their influence on tropical wave cloudiness. Any periodic variability within tropical waves that cannot be assigned to global oscillations would be candidates for oscillations originating from within tropical waves or from unknown outside influences.

Several global oscillations are recorded by NOAA and available on NOAA websites. ENSO and MJO are two that appear to be independent signals. This is compared to the teleconnections that NOAA records. The only teleconnection used in this analysis is the North Atlantic Oscillation (NAO) because it is the dominant teleconnection recorded by NOAA and its geographic impact coincides with the tropical wave zone being studied. Two non-earth cycles were considered, the 28 day lunar cycle and Total Solar Irradiance (TSI).

El Nino Southern Oscillation

ENSO had a strong influence on tropical wave cloudiness. Cross correlation of the AIRS low altitude cloud fraction product with ENSO, shown in Figure 27, showed a negative correlation with a five to seven month lag. These results were based on the entire eleven year data set. The negative correlation was as expected since El Nino events tend to lead to reduced weather activity in the Atlantic. A small difference in positive lag can be seen with region 3 having a lag of five months and Region 4 having a lag of seven months. These are peak negative correlation values and the influence is actually over a broader time frame. This is more apparent in the Region 4 correlation since the correlation curve has a flatter bottom. This indicates somewhat of a smearing effect of

ENSO on cloudiness in Region 4, in other words, the duration of the ENSO impact is longer in Region 4 than in Region 3. As seen in an earlier discussion, Region 4 tended to be more active when it comes to periodic variability than the other regions. Also of interest is the fact that 500 km AOI observations are showing such a strong correlation when up to this point periodic variability tended to be moderated closer to the tropical wave core.

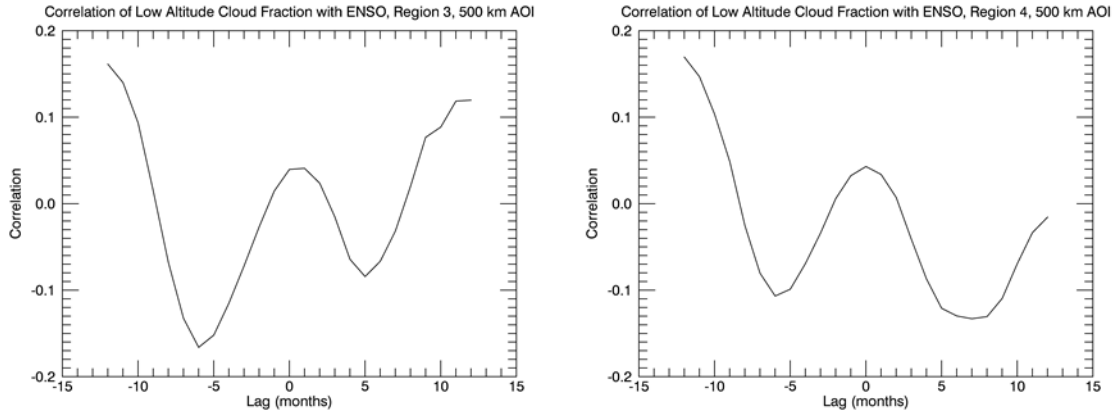

Figure 27: Correlation and lag for ENSO impact on tropical wave cloudiness

Madden-Julian Oscillation

The periodogram for the MJO is shown in Figure 28. Periodic components are tightly grouped around the dominant period of 44 days. There is however a 373 day period that the Lomb analysis assigns a probability of noise of 0.046, just under the 0.05 confidence limit. The next period in the Lomb series is at 382 days with a probability of being noise of 0.057, over the confidence limit for noise. There are a few other periodic components reported by the Lomb analysis in the mid 300 day region but at much higher

probabilities of being noise. The 373 day outlier period will continue to be included in the analysis.

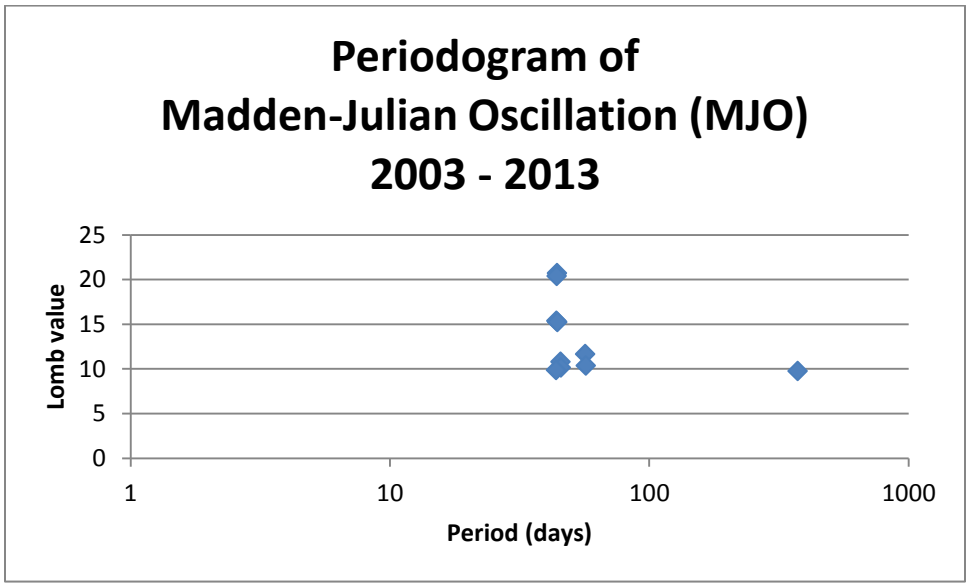

Figure 28: Periodogram of the Madden-Julian Oscillation for years 2003 to 2013

North Atlantic Oscillation

The periodogram for the NAO is shown in Figure 29. Contained in the NAO spectrum are a number of frequency components that correspond to the ENSO and MJO. Figure 30 shows these components in more detail. This is an example of interaction among atmospheric oscillations. To further analyze the impact of the NAO on tropical wave cloudiness the ENSO and MJO frequency components need to be removed. Fortunately the spectral components for ENSO and MJO are easily distinguished from the NAO. The dominant period in the NAO spectrum is 292 days while the dominant period for MJO is 44 days with a maximum of 56.9 days (excluding a single 373 day

period) and frequency components in the ENSO spectrum range upward from 569 days. For analysis, only periods between 56.9 and 569 days in the NAO spectrum were used.

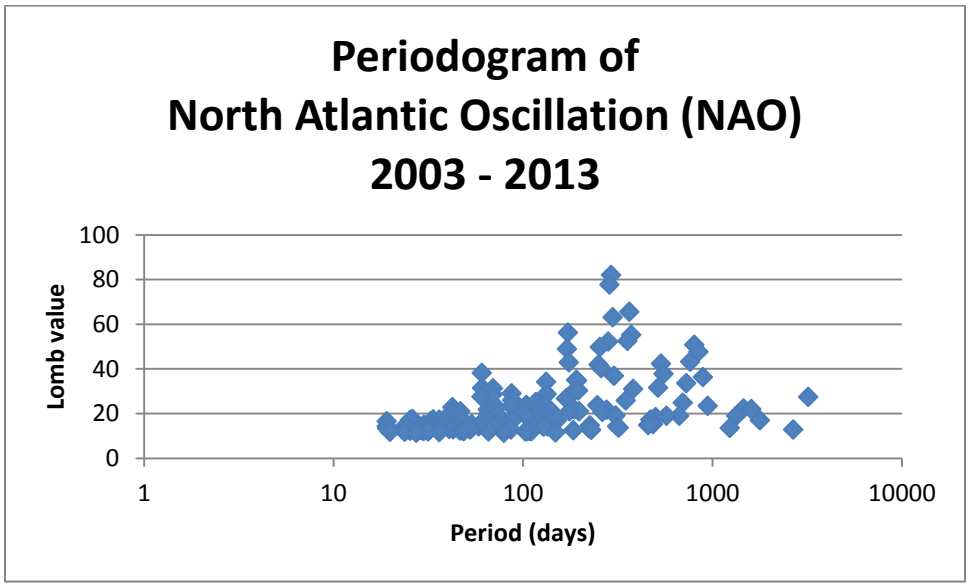

Figure 29: Periodogram of the North Atlantic Oscillation for years 2003 to 2013

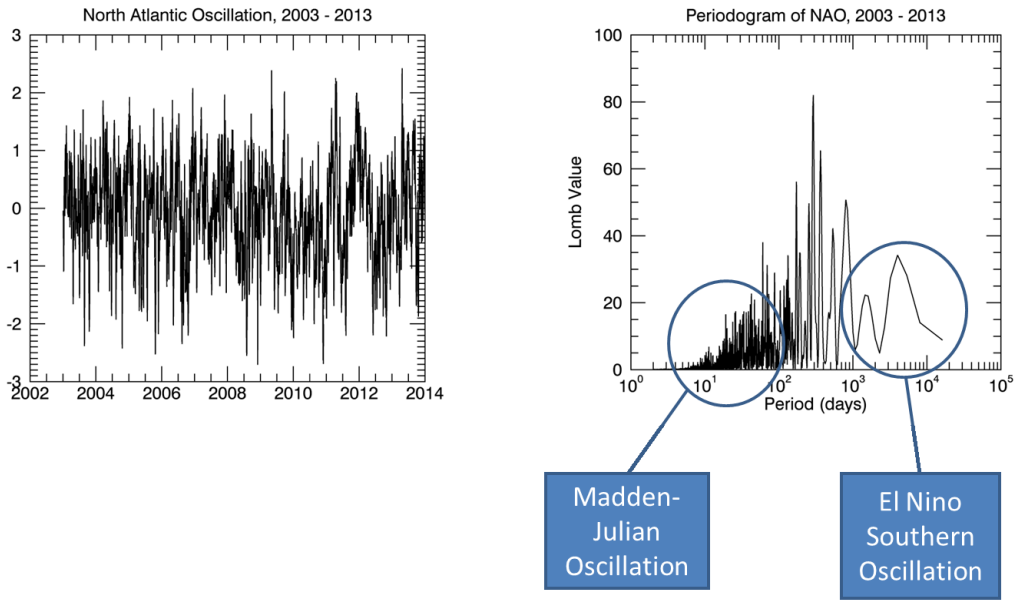

Figure 30: Interaction among atmospheric oscillations

Teleconnections

The only teleconnection tracked by NOAA that was assessed here is the NAO. Other teleconnections exist and may or may not be good candidates for analysis with regard to tropical wave cloudiness. For one thing, these teleconnections are all based on measurements made north of 20 degrees latitude, above the center line for the tropical wave zones. Table 11 provides an indication of the likelihood each of the 10 major teleconnections may have an impact on tropical wave activity based on teleconnection location and season. Teleconnection maps only go as far south as 20 degrees north latitude so the ability to see if they will be strong in the tropical wave zone is somewhat of an extrapolation. If a region of teleconnection strength is cut off by the 20 degree parallel, then there is a possibility that the teleconnection extends below the 20 degree line.

Table 11: Possible impact of teleconnections on tropical waves

Teleconnection pattern name	Season	TW Region?
North Atlantic Oscillation	All	Yes
East Atlantic	All	Marginal
West Pacific	All	Marginal
East Pacific North Pacific	All	Marginal
Pacific/North American	All	Yes
East Atlantic Western Russia	All	Yes
Scandinavia	All	Marginal
Tropical Northern Hemisphere	Winter	Yes
Polar-Eurasian	All	Yes
Pacific Transition	Late Summer	Yes

Non-Earth Cycles

Two non-Earth cycles were considered in this research. First, the 28 day lunar cycle that may have an impact on tropical wave cloudiness via tides. However, no 28 day periods were seen in the tropical wave spectrums.

The second non-Earth cycle explored was the eleven year sun spot cycle. It was expected that solar output would have an impact on tropical wave cloudiness. If there was a periodic component attributable to cyclical behavior of solar irradiance perhaps it can

be recognized in the tropical wave data. It was an unfortunate coincidence that the range of collected tropical wave data was eleven years. Since both the sampling duration and the eleven year period being sought were the same, the Lomb periodogram (or FFT) would only see a single cycle. The ability to distinguish an eleven year periodic signal from periodic artifacts due to the eleven year sampling aperture contained enough uncertainty to exclude comparisons of spectral components of tropical wave cloudiness to the sun spot cycle. However, a number of data sources were reviewed looking for solar cycles with a shorter period. The NASA Heliophysics web site was explored but it proved to be too detailed and not relevant for a general overview of solar activity. Working through NOAA information led to data posted by the Laboratory for Atmospheric and Space Physics (LASP) at the University of Colorado from the Solar Radiation and Climate Experiment (SORCE) Total Irradiance Monitor (TIM).

SORCE is a NASA satellite mission launched in early 2003 with the first TIM data available on February 25, 2003. Unfortunately, TIM experienced technical difficulties starting in November of 2012 and ceased operations on July 30, 2013. However, for this research there was enough overlap in the data to demonstrate any correlation between TSI and tropical wave cloudiness. All that was being missed is the last half of the tropical wave season in 2013.

TIM recorded TSI with an ambient temperature active cavity radiometer, essentially a bolometer. This gave an extremely broad spectral response to any energy that would warm the Earth since the energy would also warm the temperature sensor in the instrument. Daily data was downloaded from the LASP website and read using the

IDL code also posted on the LASP website. TSI was presented in two ways, first as a "true Earth" and secondly as a "one astronomical unit" reading. The true Earth seemed like the most accurate choice, but as can be seen in Figure 31 an annual cycle exists as the Earth's distance from the sun varies over a year. The original intention was to look at the relationship between tropical wave cloudiness and the sun spot cycle. This is more accurately depicted in Figure 32 which shows the TSI at 1 Astronomical Unit (AU) from the sun. However, since the eleven year sun spot cycle is being excluded from this analysis, the true Earth or Top of Atmosphere (TOA) was analyzed instead.

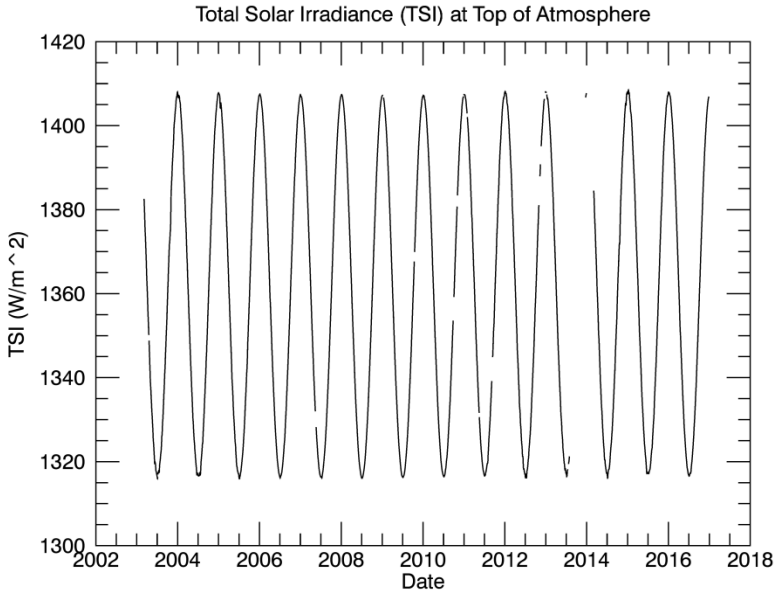

Figure 31: Total solar irradiance at top of atmosphere

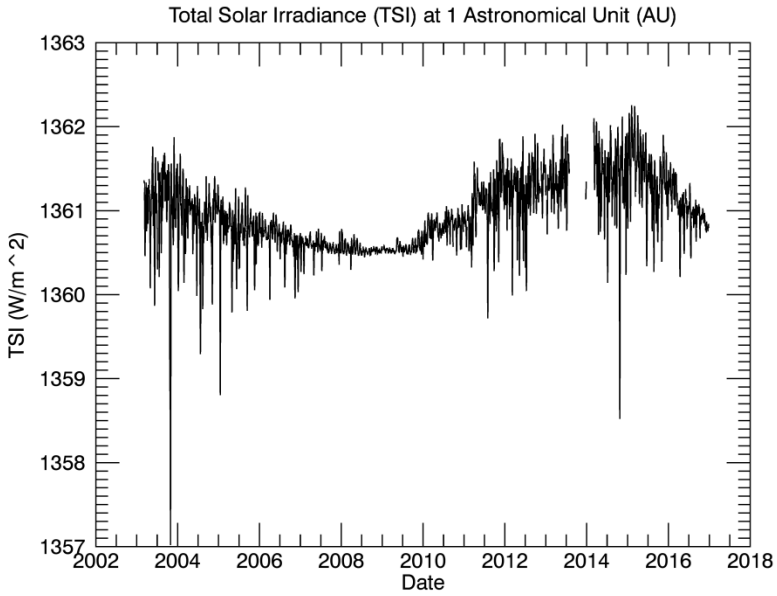

Figure 32: Total solar irradiance at 1 astronomical unit

The TOA TSI was analyzed using cross correlation at a range of lag values. TOA TSI is primarily dependent on the distance of the Earth from the Sun, which varies with a 365 day period due to Earth's moderately elliptical orbit. Based on measurements at TOA the TSI minimum occurred within the tropical wave season, the northern hemisphere summer. Variations of TSI at TOA during the tropical wave season were analyzed and found peak correlation values between 20 to 40 days of lag. This suggests that any impact on cloudiness within a tropical wave region lags behind any shift in TSI by a 20 to 40 day amount.

Subtraction of known oscillations from tropical wave spectrums

Finding common frequencies in two time series is informative, but beyond that I wanted to remove known frequency components from a tropical wave time series so that

the result is a more “pure” form of periodic variability within a tropical wave life cycle. Describing that systematic variability became a key finding in this dissertation.

Periods associated with known global oscillations can be subtracted from the full tropical wave spectrum to determine periods that are not associated with global oscillations. In the process of removing seasonality from tropical data, as discussed earlier, a frame work was developed for frequency subtraction. The process illustrated in the Appendix, Figure 37, shows how seasonality was subtracted from the tropical wave spectrum. However, the process did not produce satisfactory results when attempting to subtract global oscillations from a tropical wave spectrum. If the periods in the spectrums did not match perfectly they were not subtracted. This was not a problem when removing seasonality because there were relatively few frequency components that needed to be matched and subtracted. But with the more complex time series, such as El Nino, narrow band frequencies that should have been matched weren’t.

Manual matching of frequency components found in tropical wave cloudiness with frequency components found in ENSO, MJO, and the North Atlantic Oscillation was tried, but this turned out to be a subjective and tedious time consuming effort. I furthered my search for a more formal and analytical way to correlate harmonic elements in one waveform with another.

The cross spectral coherence method developed by Simon Vaughan (Vaughan 2014) appeared promising. This method gives the spectral coherence of two time series. But, as with the subtraction method, very few frequencies were matched. However the Vaughan code sparked an idea on how to do frequency matching.

Within the Vaughn spectral coherence code was a feature that allowed frequency binning, in other words, create narrow bands of frequencies and look for coherence across bands. I had other issues with the Vaughn method, namely its overall complexity and not really being sure what the results meant. But, I used to idea of frequency binning to come up with a solution for subtracting known global oscillations from the tropical wave spectrums.

Periods are not discrete in these datasets. They tend to appear in clusters requiring operations to be performed on bands rather than single periods. To create a set of periodic bands, spectral binning was performed using a logarithmic series of bin locations. The same set of bins was used for tropical wave values and global oscillation values. The de-seasoned, noise free period values were put in bins. A logical test was used to perform the frequency subtraction as follows: Bins that have tropical wave periods but no global oscillation periods contain tropical wave periods for which no global oscillation period was found.

The first step was to create a series of bins that could be applied to all the spectrums used in the analysis. The range of periods in the spectrums was from days to thousands of days and one bin size across the entire spectrum would not work. As periods get longer in a spectrum they would require wider bins. A logarithmic series of bin widths was developed that began with a width of 1 day up to 4.6 days over the spectral range of 1 day to 4015 days, the number of days in the eleven year study period. This smoothly increasing set of bin widths was used to hold spectral components of each of the spectrums being analyzed. To place periods in their respective bins efficiently, the

IDL function MATCH_VALUES was used. The matching step was similar to the first step in creating a histogram, but without counting the number of elements within each bin.

Once the periods are assigned to bands, or bins, for all spectrums, logic was applied as follows to perform the subtraction: First, build an array of zeros with a size equal to the number of bins, in this new array mark bins with a 1 that correspond to bins that contain tropical wave periods. In a similar way, mark bins with a zero that correspond to any bins in the global oscillation spectrum. Over writing the tropical wave bins with zeros effectively subtracted known global oscillations from the measured tropical wave periods. What remained were periods that could not be matched with any known cycle in the Earth system that could have an impact on tropical wave cloudiness.

Table 12 shows the results of this analysis of periodic variability. Each AIRS product and the cloud fraction ratio have separate spectrums from which known oscillations were identified and removed.

Table 12: Unique periods

High Altitude CldFrcStd			Low Altitude CldFrcStd			Cloud Fraction Ratio		
Region	AOI (km)	Mean Period (days)	Region	AOI (km)	Mean Period (days)	Region	AOI (km)	Mean Period (days)
1	2000	691	2	500	9	2	500	98
1	2000	726	2	500	15	2	1000	9
1	2000	761	2	500	18	2	1000	180
1	2000	800	2	500	180	2	2000	11
2	1000	180	2	1000	11	2	2000	18
2	1000	1902	2	1000	13	2	2000	55
2	1000	2174	2	1000	78	2	2000	78
2	2000	7	2	1000	98	3	2000	7
2	2000	9	2	2000	55	4	1000	1085
2	2000	13	2	2000	216	5	2000	22
2	2000	22	2	2000	219	5	2000	75
2	2000	154	2	2000	953	5	2000	84
3	500	11	2	2000	1017			
3	500	15	3	500	7			
3	500	390	3	500	898			
3	500	400	3	1000	1089			
3	1000	18	4	500	1085			
3	1000	64	5	1000	562			
3	2000	1694	5	1000	585			
3	2000	3809	5	1000	1013			
4	500	213	5	1000	1166			
4	500	216	5	2000	75			
4	500	379	5	2000	543			
4	1000	329	5	2000	607			
4	1000	361	5	2000	949			
4	1000	525	6	1000	154			
4	1000	543	6	1000	157			
4	2000	157	6	1000	267			
4	2000	160	6	1000	270			
4	2000	219	6	1000	1065			
4	2000	354	6	2000	84			
4	2000	562						
4	2000	1898						
5	500	236						
5	500	239						
5	500	1013						
5	500	1085						
5	1000	75						
5	1000	267						
5	1000	270						
5	1000	585						
5	1000	949						
5	1000	1166						
5	2000	92						
5	2000	607						
5	2000	843						
6	1000	649						
6	1000	676						

Components of Variability

The Lomb periodogram is normalized to the variance of the input signal. Since both variance and power are squared values, the spectral power density of a Lomb periodogram is proportional to the variance of the input signal. As variances add, so too do components of spectral power. Therefore, each spectral component in the Lomb periodogram can explain a component of variability in the time domain. However, as with other methods of finding components of variability, such as Principal Components Analysis (PCA), there may not be any physical explanation of a component of variability found using a Lomb periodogram.

It is also important to state that the spectral components found in the Lomb periodogram of a tropical wave time series do not infer any cause and effect between a global oscillation or non-earth cycle and periodic variability in tropical wave cloudiness. As with correlation between two signals there is only an indication of a relationship. Further investigation needs to be done to determine if an actual cause and effect physical relationship exists between the two signals.

In determining the contribution of a known oscillation to the variability of tropical wave cloudiness, the energy spectral density was first found by integrating over the entire spectral range of the Lomb periodogram. This was denoted by E_{total} and includes both periodic and noise components of the periodogram. E_{total} was divided into periodic and noise components by using the 0.05 confidence limit. These two values are $E_{periodic}$ and E_{noise} respectively.

To find the contribution of variability due to known oscillations, frequency subtraction was used. The spectral components in the oscillation were removed from the tropical wave periodogram and a new value for E_{total} was calculated. The difference between the two values of E_{total} is equal to amount of energy contributed by the known oscillation and is denoted by E_{osc} . The fraction of variability explained by the known oscillation was found by taking the ratio of E_{osc} to E_{total}.

Equation 3: Fraction of variability

$$Fraction\ of\ variability = \frac{E_{osc}}{E_{total}}$$

Using this method, the spectral energy for each of the known oscillations was found and their fractional part of total variability was calculated. The results of the components of variability are shown in Table 13. Rows of the table are provided for all combinations of cloud layer, AOI size, and region. Columns in the table show the percent of variability that can be explained by the global oscillations. The last two columns show the total contribution of seasonality plus global oscillations and the total contribution of only global oscillations. At the bottom of the table the mean and standard deviation for each of the variability components are shown.

In all cases the total contribution of global oscillations is greatest in region 6. Variability in this region is dominated by the NAO. NAO tends to be the strongest contributor to variability in most cases explaining, on average, 20.9% of the total variability. In second place is the contribution of seasonality averaging 15.4% of total

variability and being strongest in regions 1 and 2 for the larger AOIs of 1000 and 2000 km.

Table 13: Components of periodic variability

subProduct	twExtent	region	seasonContrib	ensoContrib	mjoContrib	naoContrib	totalContrib	oscContrib	AOI mean
High Alt	500	1	0.086	0.01	0.012	0.171	0.279	0.194	
High Alt	500	2	0.115	0.009	0.008	0.101	0.234	0.118	
High Alt	500	3	0.002	0.018	0.008	0.115	0.143	0.141	0.153
High Alt	500	4	0.001	0.008	0.008	0.129	0.146	0.145	
High Alt	500	5	0.002	0.026	0.009	0.134	0.17	0.168	
High Alt	500	6	0.001	0.029	0.024	0.532	0.586	0.585	
High Alt	1000	1	0.232	0.006	0.012	0.177	0.427	0.195	
High Alt	1000	2	0.213	0.017	0.007	0.149	0.385	0.172	
High Alt	1000	3	0.002	0.02	0.008	0.127	0.156	0.154	0.170
High Alt	1000	4	0	0.007	0.008	0.129	0.144	0.144	
High Alt	1000	5	0.001	0.03	0.008	0.15	0.188	0.187	
High Alt	1000	6	0	0.038	0.023	0.52	0.582	0.582	
High Alt	2000	1	0.371	0.016	0.012	0.232	0.631	0.26	
High Alt	2000	2	0.407	0.018	0.006	0.203	0.635	0.228	
High Alt	2000	3	0.235	0.013	0.011	0.145	0.403	0.168	0.199
High Alt	2000	4	0	0.008	0.006	0.136	0.151	0.151	
High Alt	2000	5	0	0.032	0.005	0.153	0.189	0.189	
High Alt	2000	6	0	0.012	0.035	0.509	0.556	0.556	
Low Alt	500	1	0	0.006	0.006	0.16	0.172	0.172	
Low Alt	500	2	0.139	0.006	0.005	0.105	0.255	0.116	
Low Alt	500	3	0.286	0.019	0.011	0.177	0.492	0.206	0.179
Low Alt	500	4	0.646	0.017	0.012	0.207	0.881	0.236	
Low Alt	500	5	0.13	0.02	0.007	0.138	0.295	0.164	
Low Alt	500	6	0.004	0.089	0.03	0.461	0.584	0.58	
Low Alt	1000	1	0.174	0.005	0.009	0.165	0.353	0.179	
Low Alt	1000	2	0.107	0.004	0.004	0.109	0.225	0.118	
Low Alt	1000	3	0.354	0.019	0.015	0.194	0.581	0.227	0.193
Low Alt	1000	4	0.282	0.019	0.012	0.218	0.531	0.249	
Low Alt	1000	5	0.158	0.023	0.007	0.163	0.352	0.193	
Low Alt	1000	6	0.004	0.072	0.036	0.447	0.558	0.555	
Low Alt	2000	1	0.177	0.005	0.017	0.193	0.391	0.214	
Low Alt	2000	2	0.152	0.007	0.007	0.126	0.292	0.14	
Low Alt	2000	3	0.46	0.016	0.016	0.204	0.696	0.236	0.219
Low Alt	2000	4	0.279	0.024	0.008	0.223	0.534	0.255	
Low Alt	2000	5	0.247	0.032	0.006	0.214	0.499	0.252	
Low Alt	2000	6	0	0.034	0.031	0.376	0.442	0.442	
Ratio	500	1	0	0.009	0.01	0.186	0.205	0.205	
Ratio	500	2	0.13	0.007	0.004	0.097	0.238	0.108	
Ratio	500	3	0.142	0.006	0.012	0.11	0.271	0.129	0.147
Ratio	500	4	0.487	0.015	0.007	0.138	0.648	0.161	
Ratio	500	5	0	0.009	0.007	0.116	0.133	0.133	
Ratio	500	6	0.003	0.096	0.02	0.465	0.584	0.581	
Ratio	1000	1	0	0.003	0.009	0.136	0.148	0.148	
Ratio	1000	2	0.188	0.01	0.004	0.119	0.322	0.134	
Ratio	1000	3	0.219	0.009	0.012	0.137	0.377	0.158	0.159
Ratio	1000	4	0.334	0.019	0.01	0.187	0.55	0.216	
Ratio	1000	5	0.117	0.008	0.008	0.125	0.258	0.141	
Ratio	1000	6	0.007	0.096	0.026	0.513	0.641	0.635	
Ratio	2000	1	0.001	0.009	0.012	0.168	0.191	0.19	
Ratio	2000	2	0.452	0.014	0.004	0.164	0.634	0.182	
Ratio	2000	3	0.425	0.013	0.014	0.187	0.639	0.214	0.207
Ratio	2000	4	0.298	0.02	0.013	0.2	0.531	0.232	
Ratio	2000	5	0.257	0.02	0.009	0.187	0.473	0.216	
Ratio	2000	6	0	0.064	0.014	0.372	0.45	0.45	
Means			0.154	0.022	0.012	0.209	0.397	0.243	
Stdev			0.164	0.022	0.008	0.123	0.189	0.147	

The impact of ENSO on total variability was surprisingly small, but finding a maximum in region 6 except for the high altitude cloud fraction with a 2000 km extent. The contribution of MJO is smaller than that of ENSO, also with a maximum in region 6 except for the cloud fraction with a 2000 km extent where region 3 shares the same maximum value of 0.014.

On average, the contribution of periodic variability to total variability was 24.3%.

Of all the observations in this table perhaps the fact that region 6 has the strongest periodic variability is the most interesting. It includes the western half of the Gulf of Mexico and, to the south, includes a large section of the Pacific Ocean. This region includes more land mass than any of the other regions and is impacted by weather patterns occurring over the south central United States, primarily Texas, and almost all of Mexico. These weather patterns are combining with the diminishing tropical waves that have moved into region 6. So much of the influence on these weakened tropical waves is dominated by other weather systems. The high level of periodic variability in region 6 indicates that the non-tropical wave weather systems are more strongly dominated by periodic variability than the tropical waves entering the region.

Another observation of interest is the very strong contribution to total variability made by NAO. As shown in Figure 29, the periodogram for NAO includes a dense population of periodic components stretching from 5 days out to 3212 days. Also, it was previously shown that the NAO spectrum includes periods from the MJO and ENSO. In determining unique periods the MJO and ENSO components were removed. But in determining the contribution of the published NAO to total tropical wave variability it

was more appropriate to include the entire spectrum even though some might argue this is double counting MJO and ENSO. Probably the more important discussion is about the influence of MJO and ENSO on NAO.

The mean value of total periodic contribution for each AOI in Table 13 was calculated using only regions 1 through 5. Region 6 was not used in this calculation since it is comingled with non-tropical wave weather systems associated with land mass. The contribution for each AOI was calculated to verify the earlier premise that global oscillations have less of an effect on the tropical wave core, represented by the 500 km AOI, then on the larger AOIs. These values in Table 13 show a three step, positive trend for each product type.

CONCLUSIONS

Summary

The development of my dissertation topic of measuring tropical waves with an atmospheric sounder began with the launch of the CrIS instrument aboard the NPP satellite in October, 2011. The following year some of my coworkers were working with CrIS data and I became intrigued with the idea of being able to create a temperature profile of the atmosphere. At the same time I was studying the potential of using HDF-5 for LIDAR data, which is also the data format CrIS data is delivered in. The next year, during the spring semester of 2013, I took a course presented by Dr. Paul Houser that included a team project. As I worked with my team in planning our project I suggested we investigate, using CrIS data, to analyze whatever weather systems led up to the generation of Hurricane Sandy. One of my team mates, who was majoring in weather and climate, suggested tropical waves. So this became our goal: Find something to measure in the tropical wave associated with Hurricane Sandy. It was a successful project, we all got an A, and it formed the basis for my dissertation

The following summer of 2013 I spent time learning how to locate tropical waves and came across the NOAA TWD. I also learned during that time that there is no tropical wave database. If I wanted to collected locations of tropical waves I had to create my own archive. So I began parsing the text of the NOAA Tropical Weather Discussion for tropical wave locations.

The fall semester of 2013 included two project papers, one in a course presented by Dr. John Qu, and another led by Dr. Donglian Sun. In Dr. Qu's class I presented a paper on the cross section of tropical waves based on data collected from CrIS. In Dr. Sun's class I presented a paper on using text mining of the NHC Tropical Weather Discussion to create a tropical wave database. It was during Dr. Qu's class that he suggested I use data from the AIRS sensor which was launched in 2002, was the precursor atmospheric sounder to CrIS, and had long record of data.

In the spring semester of 2014 Dr. Mike Summers led a class on atmospheric physics. The paper I wrote for that that class was on finding the extent of a tropical wave. This was an important topic for me, because, since the spring 2013 class with Dr. Houser I did not know where within a tropical wave to make measurements. By the spring of 2014 I was determined to use atmospheric characteristics to provide a measurement region that was essentially the extent of a tropical wave. I presented some encouraging results in that paper but as mentioned earlier in this dissertation, determining the thresholds of the various atmospheric parameters had many of the same uncertainties as found in image analysis and I had to abandon that approach in favor of using fixed 500, 1000, and 2000 km square areas of interest centered on the core of a tropical wave.

The summer of 2014 was spent learning how to track tropical waves. Here the problem was: given a long list of tropical wave observations along with time and date, figure out which observations are of the same tropical wave and tie those observations into a track. My research into tracking algorithms led to an open source version of the multiple hypothesis algorithm which I modified and was able to create tracks of tropical

waves from the locations I text mined from the Tropical Weather Discussion. I documented this in a paper I wrote for another of Dr. Sun's class in fall of 2014.

Also in the fall of 2014 my curiosity about how a temperature profile of the atmosphere can be measured from an overhead sensor led to a paper and presentation on this in a class presented by Dr. Qu.

By the spring of 2015 I had everything needed to do my research except an in depth understanding of tropical waves themselves. At the same time I was forming my dissertation committee and writing my research proposal. By the end of that semester my goal was to have passed a candidacy examination. So my committee members challenged me and every single question I was asked involved the atmospheric aspects of tropical waves. This forced me to study the structure and dynamics of tropical waves. I was able to answer all of the committee's questions and write a research proposal based on all I had learned up to that point. This was the basis for my dissertation: to study the year to year variability of the tropical wave life cycle using data from an atmospheric sounder. The dissertation proposal was a mix of atmospheric physics and a remote sensing application. When asked by the committee which it was, I answered that it was a remote sensing application. But as the results of the research evolved it became more and more of a study in atmospheric physics, weather and climate. The technologies involved in this research not only make use of the Earth systems and geographic information science I have learned since starting this program but also reach back to my imaging science and electrical engineering background with regard to the signal processing in particular.

Optimizing the generation of tropical wave tracks was the main effort during the summer of 2015. Optimization efforts began with a manual review of tropical wave tracks leading to adjustments to the text mining and MHT code. A metric for track quality was developed and a series of experiments were run using the MHT algorithm. A few parameters needed to be added to the MHT code to optimize it for the tropical wave tracking application. By mid-September 2015 I had generated 345 tracks covering the 2003 to 2013 time period.

Fall of 2015 was spent using tropical wave locations from the track data to select AIRS data files. This included selecting the AIRS file that contains the tropical wave center but also adjacent files so that a 3 by 3 mosaic could be constructed. In addition, to cover gaps between imaging swaths, files from alternate orbital nodes where used to fill gaps between swaths. Each data file included all of the AIRS products. I made multiband mosaics and analyzed results for a number of the atmospheric profile products.

It wasn't until January, 2016 that I began working with the CldFrcStd product. CldFrcStd contains two levels of 15 km pixels each providing the fraction of the area covered by clouds. It was at this point that I decided to study the year to year changes in cloudiness during a tropical wave life cycle. One reason for this choice was my interest in cloud feedback, another was that clouds present the greatest uncertainty in climate prediction, and finally the multi-layer cloud product provided by AIRS culminates a tremendous amount fo the information collected by airs. It brings together atmospheric profiles of temperature, moisture and pressure and it is a combination of passive

microwave and optical sensor data. So cloud fraction standard seemed like it could provide some powerful insight on the tropical wave life cycle.

In February 2016 I finished building multiband mosaics for all CldFrcStd products from 2003 through 2013. It was also at this time I started looking at the ratio of cloud fraction in the high altitude band to the cloud fraction in the low level band. As it seemed plausible that this could provide some indication of the insulating quality of clouds I kept this parameter in the future analysis. This brought the parameters I would be analyzing to 3: High altitude (layer 0) cloud fraction, Low altitude (layer 1) cloud fraction, and cloud fraction ratio.

In March of 2016 I started working with frequency analysis of my data. I also brought in data sets for a couple of atmospheric cycles: ENSO and MJO. The idea was to see if frequency components in the known atmospheric cycles appeared in the tropical wave data. I initially used standard Fourier analysis, FFT, to do this. I ran into several problems trying to use FFT: uneven sampling, missing data, and insufficient low frequency resolution.

In April of 2016 I took a detour to write a paper for the Monthly Weather Review describing how I built a tropical wave data base. During this time I realized I needed to do validation of the positional data I had collected from the TWD. I contacted NOAA to get some information on how they identified tropical waves and determined their location. This led me to work done by Berry proposing an objective method to identify tropical waves based on wind vectors. I downloaded wind vector data from the NECP and displayed them with my tropical wave axis locations superimposed on top. I was able

to validate my positional data but felt that the analysis was subjective. Berry also proposed a number of other characteristics that could be used to identify tropical waves, and using the results of the MHT tracker was able to provide a more objective validation of my tropical wave data.

By mid-July of 2016 the validation was complete and the paper was submitted to Monthly Weather Review. I continued with analysis of the CldFrcStd product and the derived cloud fraction ratio. I used the Kendall test for trend and in the process created 6 regions across the Atlantic that would serve as the basis for a tropical wave life cycle. The Kendall test showed that year to year trends in cloudiness varied by cloud layer, extent of analysis (AOI) and stage in the tropical wave life cycle. I also performed the same test using the Spearman technique and the results were exactly the same.

In September of 2016 I learned about the LNP which performs spectral analysis similar to the FFT but does not require regularly spaced samples. The "normalized" part of this algorithm's name infers that the variance of the spectral output is equal to the variance of the time domain input. This characteristic allows significant spectral components to be extracted from spectral noise. I used the LNP to analyze tropical wave cloud fraction data and to find spectral components in atmospheric and non-earth cycles. I was also able to relate a LNP to a power spectrum and determine how much of the variance in tropical wave cloudiness could be explained by each of the periodic signals used in the analysis.

The results of the spectral analysis showed that many of the frequency components found in a multi-year sample of tropical wave cloudiness could be associated

with known atmospheric and non-earth cycles. This dissertation outlines those results in tables and example plots. But there were a number of periodic signals that could not be matched up with the known periodic signals I tested against. Most likely these are due to atmospheric oscillations I am not aware of, but there is the possibility that these unmatched signals are due to cyclical behavior that has not yet been identified.

Interpretation of Findings

Locating and Tracking of Tropical Waves

An automated process has been described in this dissertation to generate tropical wave tracks. The hypothesis was that tropical wave tracks can be generated from coordinates found in the NHC Tropical Weather Discussion and this was shown as possible to do. The track generation process consisted of two steps. The first step used text mining to extract tropical wave positions from archived bulletins issued by the NHC. The tropical wave positions appearing in the bulletins were manually derived by experts using satellite imagery and derived wind patterns. The second step was to turn the tropical wave positions and times into tracks. This was done using an implementation of the multiple hypothesis tracking algorithm.

As I worked through a validation process I determined that the reporting of significant weather systems associated with tropical waves is of interest to mariners while the more objective positioning of a tropical wave axis is of interest to the atmospheric scientist. The tropical wave positions I recorded do not necessarily state the location of trough axes, but they are close enough for a study of these synoptic systems assuming the region of interest is expanded well beyond the TWD coordinates.

In this work I made use of Ambient Geographic Information (AGI) (Stefanidis et al. 2013), a phrase used by geographic information scientists usually in association with social media. AGI, as opposed to Volunteered Geographic Information (VGI) (Jackson et al. 2013), is geographic information freely available in the public domain but is embedded in text or data that was not intended to be a geographic product such as a map. An example of AGI is the Tropical Weather Discussion, essentially a weather report. Extrapolating this idea, I believe there is other long term climate related information embedded in other archived, text based weather reports that could be harvested using text mining techniques.

The technique, when applied to multiple years of NHC bulletins, yields a track for each documented tropical wave. These tracks can be used to study the life cycle of individual tropical waves by supporting a satellite data selection process or to perform geospatial analysis of tropical wave movement.

Conclusions about tropical wave life cycle

A variety of secular and periodic trends were found indicating that variability in tropical wave life cycles from year to year is far from random. Consistent patterns of cloud growth and shrinkage were observed as tropical waves moved across the Atlantic Ocean. Short and long term periodic patterns were extracted in the otherwise chaotic quantities of clouds associated with tropical waves. A number of these periodic patterns could be associated with known atmospheric cycles, but many were not, leaving questions about their origins unanswered.

The AIRS cloud products used provided generic low and high altitude cloud fraction, so conclusions can be made with regard to relative cloud height. It is not surprising that life cycle patterns in low clouds compared to high clouds are different.

The high to low cloud fraction ratio exhibited a secular trend in the positive direction within some regions. If cloud fraction ratio is a reasonable metric for the insulating quality of clouds, then this trend over an eleven year period could prove to be of significance. However, in a climatologic and geographic sense this secular trend is rather insignificant due to the short, eleven year, time scale and the relatively small tropical Atlantic region of study. Because AIRS covers the entire planet, and multi-layer cloud products are available for the entire world, a broader analysis of this secular trend could prove interesting. As for time scale, this research does not cover other sources of cloud layer data that may have preceded AIRS. Continuing forward, the CrIS sensor is capable of producing the same set of cloud products. A crossover effort would need to take place in order to attach earlier and future cloud data to the AIRS data set. As a result of this research, most of the analysis has been automated. This includes the mosaicking of multi-layer cloud products. Although this research concentrated on clouds generated by tropical waves, other cloud producing systems could be examined. Furthermore, a global analysis of cloud fraction ratio could be done for all clouds over the time period of available data. Then, processes similar to the tropical wave locating and tracking described in this dissertation could be used to assign any secular trends found to specific weather system types. It is also possible that the reanalysis data created by the Climate Center may have cloud layer information available. Note also that this study of cloud

fraction ratio has implications for research on cloud feedback. This is a ripe field of study since the IPCC has determined that clouds present the greatest uncertainty in climate forecasting. It seems to me that a parameter such as cloud fraction would be fundamental in any modeling of a cloud feedback system.

Comparisons to numerical models

Through models, and comparison with actual data, Wheeler and Kiladis (Wheeler and Kiladis 1999) verified the existence of a number of equatorial waves. In particular, Kelvin waves were reported to have a broad periodic range of 4 to 10 days. This spans the salient 7.7 to 8 day range of periods observed region 4 low level cloud fraction and suggests that this unknown band of periods may be related to Kelvin waves.

In a two part series Kiladis (Kiladis et al. 2006) and Hall (Hall et al. 2006) develop African Easterly Wave (AEW) models and run them using reanalysis data covering the Sahel region of Africa. The results showed that once formed, the AEW core is stable and resistant to external influences such as global oscillations. Observations made with AIRS data in this research also found relatively stable cores in tropical waves. As tropical waves over the ocean develop from AEWs over land, the mechanisms that give robustness to tropical wave cores may be the same as those within AEWs.

The objective technique used by Berry (Berry et al. 2007) to identify African Easterly Waves is based on numerical model analysis and can potentially be used to identify tropical waves over the ocean. The research behind this dissertation used observations to locate tropical waves but the time period was limited to eleven years. To increase the time span of tropical wave research to one of significance to climate studies,

a time span of at least 30 years would be needed. This requires the use of reanalysis data but also requires numerical model analysis to identify tropical waves in the reanalysis data.

Comparisons to reanalysis data

This research spanned eleven years and is based on real data. Reanalysis on the other hand offers the potential for much longer time periods, but the data is based on models. However, reanalysis projects continue to improve. In particular, during the five year effort this research entailed, increased trust and usage of reanalysis was evidenced by work done by Bain (Bain et al. 2014) and Brammer and Thorncroft (Brammer and Thorncroft 2015). These projects made improvements in tracking of African Easterly Waves in reanalysis data and increased understanding of the evolution of AEWs as related to tropical cyclogenesis. Earlier work more closely related to this dissertation was done by others using reanalysis data.

Using outgoing long wave radiation measurements of the global tropics, Roundy (Roundy 2012) detected a variety of wave types in a study of tropical waves based on 29 years of reanalysis data. The dense spectral content Roundy found in wave centered sampling was also observed in this research using an observation based wave centered sampling technique. Using wavelet analysis Roundy observed Kelvin waves peaking in a band between 5 and 6.67 days for worldwide tropical data. This suggests the localized region 4 low altitude cloud fraction 7.7 to 8 day periods seen in this dissertation may fall within the confidence limits for Kelvin wave periodicity. Using the same technique,

Roundy found worldwide MJO signals to be centered on 48 days which is close to the 44 day period found in this research.

Theories

Cloud fraction ratio may be a useful measure of the insulating quality of clouds. A value greater than one indicates that there is a higher cloud fraction at higher altitudes compared to the cloud fraction at lower altitudes. A value greater than one implies that the atmosphere is transmitting radiation up into the bottom of the higher clouds and that there are more higher clouds than lower clouds reflecting that radiation back to the surface. The higher clouds, when they exist, are capturing a greater depth of the atmosphere than lower clouds, and thus more energy. This cloud fraction ratio in its simplest form is a rough estimate at best. One limitation is the creation of undefined or infinite values when the lower cloud fraction is zero. So a method of putting an upper limit on the cloud fraction ration needs to be developed. Another limitation is that the cloud fraction ratio, when based on sounder products such as from AIRS does not reveal actual cloud height, only a relative vertical position of the clouds. Values such as cloud layer height and cloud top temperature are available from AIRS, so these factors should be included in the ultimate parameter that represents cloud insulating factor. For conditions where the cloud fraction ratio is less than one, the lower clouds are reflecting more radiation back to the surface than the higher clouds are. But because clouds, at whatever level they are at, reflect radiation from the sun back into space, a ratio of less than one indicates that cloudiness is at or approaching a cooling effect. In other words, more radiation is being reflected back into space than is being reflected from a warm

atmosphere back to the surface. Again, this is dependent on the actual height of the lower clouds. The lower the cloud layer, the less atmosphere radiating energy up to the lower layer. An extreme situation would be if the lower clouds were actually fog sitting right on the surface and there are no clouds above. This would be the maximum case for radiation from the sun being reflected back into space. In this situation there is still some absorption of short wavelengths being absorbed by water vapor in the atmosphere as down welling and up welling short wave radiation passes through the atmosphere. But not all of that radiation is being absorbed. This presents an almost inverse situation in that with low clouds, more reflected radiation is being absorbed by greater atmosphere depth than with high clouds. So an investigation into that effect would also need to be done to prove that a cloud fraction ratio is a viable indication of a cloud insulating factor. The usage of cloud insulating factor would be a component in the development of a cloud feedback model. In this research I only investigated clouds associated with one type of weather system, tropical waves, and over a small area of the Earth's surface, the tropical North Atlantic Ocean. Investigation of cloud fraction ratio would need to be extended to other cloud producing systems such as tropical waves in the Pacific basin, subtropical weather systems, large areas covered by overcast conditions, and large fog systems. Ultimately a global cloud insulating factor could be calculated on an hourly basis and recorded. There is also the possibility of developing a cloud insulating factor archive based on climate reanalysis data. These long term cloud insulation data could be used to develop a model of cloud feedback and ultimately be used in weather, climate, and hydrologic predictions.

Another theory is that global oscillations that impact tropical wave life cycle, impact various stages of a tropical wave life cycle differently. This could be important in early prediction of tropical cyclone formation. If an additive confluence of oscillations are due to occur in a tropical wave region that is sensitive to the oscillations and is known to be a region where cyclone genesis occurs, than there is a higher probability of a tropical wave passing through that region at that time evolving into a tropical cyclone. The various oscillations I have studied here, ENSO, MJO, and NAO can be predicted with some reasonable certainty and an Oscillation Confluence Factor (OCF) can be applied to the tropical wave regions. So as a tropical wave forms and moves off of the coast of Africa, the timing of the OCF can be applied to each region in accordance with the predicted arrival time of the tropical wave. Uncertainty of the tropical wave speed is a factor here, but this can be tracked within a reasonable range allowing the OCF to be used as a predictor of tropical cyclone genesis.

Another theory concerns the robustness of a tropical wave core. Core robustness was documented earlier by Kiladis (Kiladis et al. 2006) and Hall (Hall et al. 2006) by using numerical models and reanalysis data. Through the use of observation data, this research verified the findings by Kiladis and Hall by showing that outside influences such as global oscillations have less of an effect on tropical wave cloudiness than on the surrounding areas. This is based on observations using the 500 km AOI showing greater independence than observations at the 1000 and 2000 km AOIs. It may be that global oscillations impact the formation of tropical waves over the Darfur highlands. But once the eddy forms and is ejected out over the Atlantic in the African Easterly Jet (AEJ), the

lifting of air and resulting precipitation and associated cloudiness are more dependent on the mechanisms within the tropical wave than the outside global oscillations that are impacting the non-tropical wave regions. A more detailed analysis of the tropical wave core and how it is impacted by global oscillations would help verify this conclusion. But the observations made in this research show the durable nature of the tropical wave and that evolution into a tropical cyclone may not be associated with global oscillations.

Assumptions and Limitations

The subjective methods used by the NHC to identify tropical waves are discussed elsewhere in this dissertation. In terms of accuracy and reliability the assumption is made that the time and tropical wave locations are adequate for the analysis performed in this study. This assumption was strengthened by validating a subsample of tropical wave observations with NECP wind streamfunctions.

Another assumption made in this study is that the clouds in a tropical wave location are generated by the tropical wave or as the tropical wave matures into the western Atlantic, the clouds in the tropical wave location are residual from earlier cloud generation.

In the generation of mosaics built from multiple AIRS granules, swaths, ascending and descending nodes, the assumption is made that the cloud features are moving slowly enough that a picture of the region around a tropical wave core can be constructed with enough accuracy for the analysis performed in this study.

When asked what methods are used to identify tropical waves, the NHC replied that it is a somewhat subjective process, but that work is being done to apply a more

objective process based on ideas presented by Berry (Berry et al. 2007). Subjectivity resides in the interpretation of data from overhead imagery, atmospheric soundings, and in situ measurements. The interpretation is based on meteorological knowledge and experience, which no doubt is in abundant supply at the NHC. So some may argue that the tropical wave locations used in this research were subjective, but they were the best that could be found at the time.

The scope of this study was limited to data collected by the AIRS sensor. This was a matter of interest in sounder data and seeing what kind of information could be derived from an instrument of this type. The study is further limited to the AIRS cloud products. Although, as discussed earlier, clouds are the product of a combination of temperature, moisture and pressure, AIRS has products that focus on these parameters specifically and a deeper understanding of the structure of tropical waves can be established by use of these more specific products.

The scope of this study was also limited by not using wind data. Tropical waves are the result of eddies in the African Easterly Jet. Because the study was limited to using only AIRS data no wind data was used in describing the year to year changes in tropical wave life cycle.

This study used tropical wave location rather than age to describe a tropical wave life cycle. The reason for this is that the actual birth of tropical waves observed in the Tropical Weather Discussion could not be determined. There is still a degree of uncertainty as to how tropical waves are formed, but the consensus seems to be leaning toward formation over the Darfur highlands. If this is the assumed birthplace, a tropical

wave could be traced back to a weather disturbance in this location, and the time and date of origination noted.

Suggestions for Future Research

The tropical wave database created in this study should be archived and made available through a university web site. The tropical wave data was compiled through 2013 so the years between then and the present should be added. In addition, the Tropical Weather Discussion and other sources of tropical wave observations should be utilized to add tropical waves for the years preceding 2003, the earliest year on-line versions of the Tropical Weather Discussion were available. The text mining and tracking software used in this research can be used to add the new data. Also, a process should be established to maintain the database so that when tropical waves are reported, tracks can be established and the information stored in the database.

With the tropical wave database available to other researchers, more detailed analyses of tropical waves can be made. These would include analysis of wind data, other sounder products, and tropical wave tracks. Of great benefit to society would be use of the tropical wave database to enhance tropical storm and hurricane prediction. Are there attributes of tropical waves that exist early in their formation that predict hurricane formation?

The MHT tracking software could be improved to produce more accurate and complete tracks. This study involved manual inspection of hundreds of tropical wave tracks to establish a quality rating. Tracking is a hard problem but the relatively few tropical waves being observed at any one time reduces the complexity.

Tropical waves are a significant producer of clouds. In climate studies, clouds are the largest single source of uncertainty in climate prediction. Studying clouds associated with tropical waves can be of benefit to the climate community. Of particular interest would be including tropical wave clouds in studying the concept of cloud feedback. The high to low cloud ratio concept should be explored as a component in a cloud feedback system.

The tropical north Atlantic is not the only region where tropical waves exist. A large number of studies in the literature report on tropical waves over the Pacific Ocean. Is there potential for creating a tropical wave database for the Pacific? Many of the concepts discussed in this study can be applied to tropical waves over the Pacific. This includes locating, tracking, cloud studies, and contribution to understanding global climate.

Objective identification of tropical waves continues to be a subject of research. In this study the fact that a weather system was tracked for several days added to the certainty that the weather system was in fact a tropical wave. Associating tracking with other objective techniques could enhance the accuracy of an objective identification method.

In the analysis of periodic variability a number of frequencies were not associated with known global oscillations or non-Earth periods. Where do these unassigned frequencies come from? Are they generated within the tropical wave? A research project that investigates this would need to first verify the unassigned periods found in this research and then work to find the source.

A future research project could include investigating the assimilation of the results of this research into reanalysis data. Another research effort could be directed at using the results of this research to test models and reanalysis data.

This research found in observation data the same robustness of the tropical wave core as documented earlier by Kilidas and Hall. One of the theories expressed in this dissertation is that because of resistance to external oscillations the tendency of a tropical wave core to develop into a cyclone is independent of periodic variability. A deeper exploration of this idea could be the topic of future research.

APPENDIX

Objective technique to identify tropical waves

Berry (Berry et al. 2007) described an objective method to identify tropical waves. It is based on the curvature of streamlines. This method was used to validate identification and location of tropical waves as found in the NHC Tropical Weather Discussion. In this section some examples of NCEP reanalysis streamfunctions are shown. To validate the NHC Tropical Weather Discussion tropical wave observations, 45 streamline maps were created for evenly sampled times across the full duration of the eleven year study. Three examples are shown here. In each figure the tropical wave axis positions are shown as derived from the NHC Tropical Weather Discussion with the tropical wave point designation "TWP".

Figure 33 summarizes the method to identify tropical waves as described by Berry. The thick black lines with the encircled numbers "1" and "3" are the positions tropical wave axes should be found. Position 3 is the location where wind pressure pushes warm moist air up causing an air parcel to expand, cool, and condensation occurs. An example of position 3 is shown in Figure 34 where the tropical wave observation TWP2013_97 has just moved off of the African coast. Because this axis is associated with a northward turning jet stream, the tropical wave location is probably correct. Figure 35 also provides a clear example of a tropical wave axis being well aligned with the rising edge of the jet stream.

Figure 36 shows several tropical waves at once. To the east, tropical wave axes are well connected to the rising edge of jet stream deviations. However, to the west the jet stream troughs have dissipated, yet the remnants of tropical waves are still being identified by the Tropical Weather discussion.

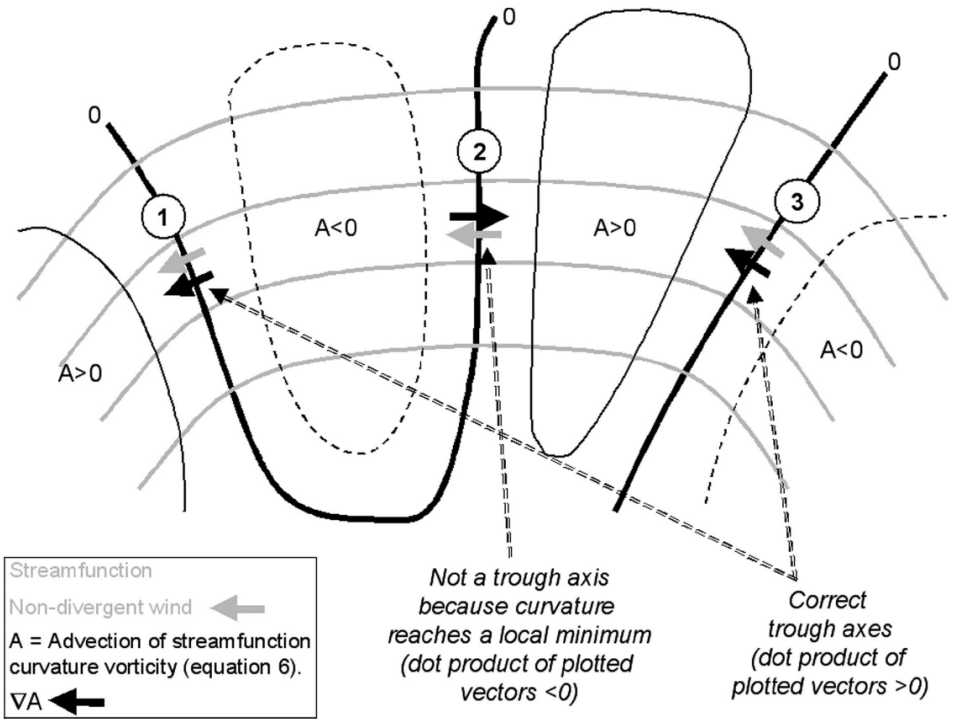

Figure 33: Placement of trough axes on streamfunction (Berry et al. 2007)

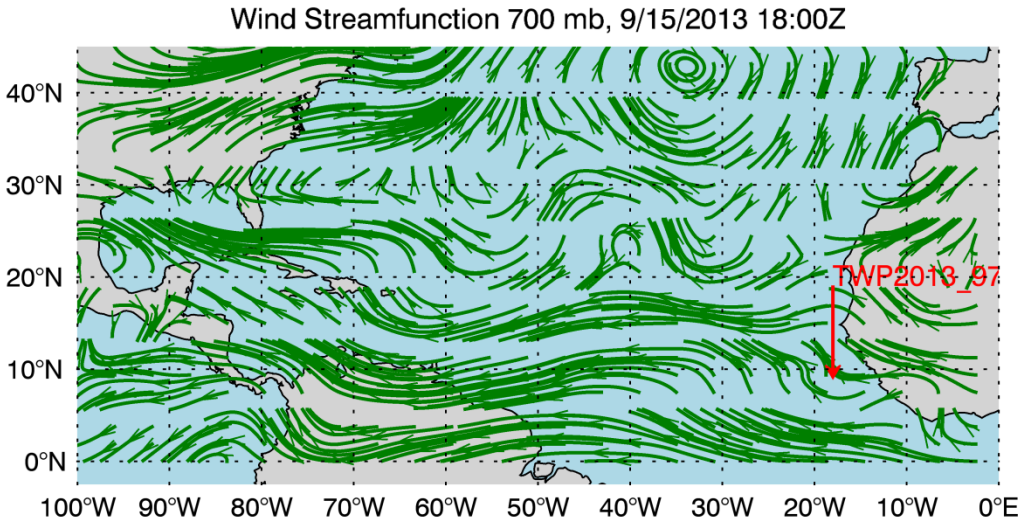

Figure 34: Wind streamfunction example 1

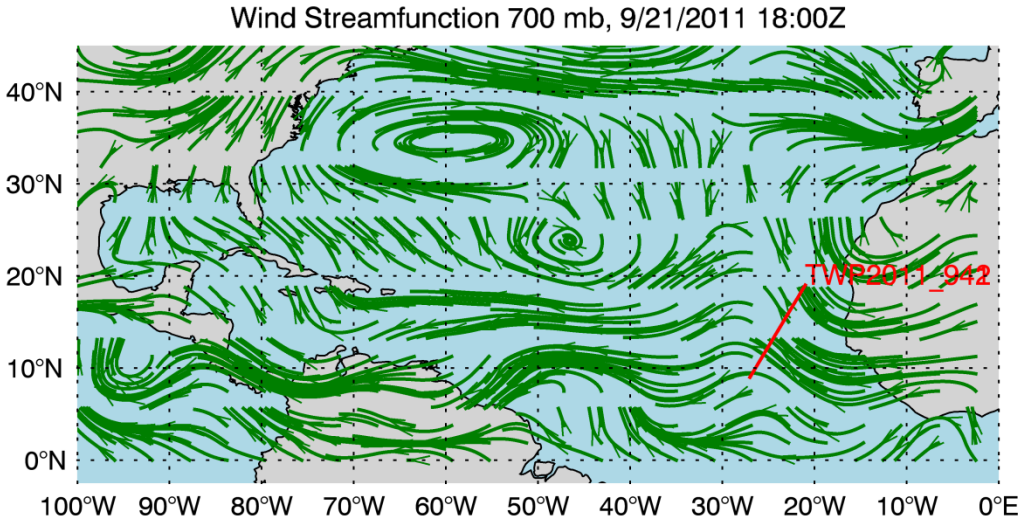

Figure 35: Wind streamfunction example 2

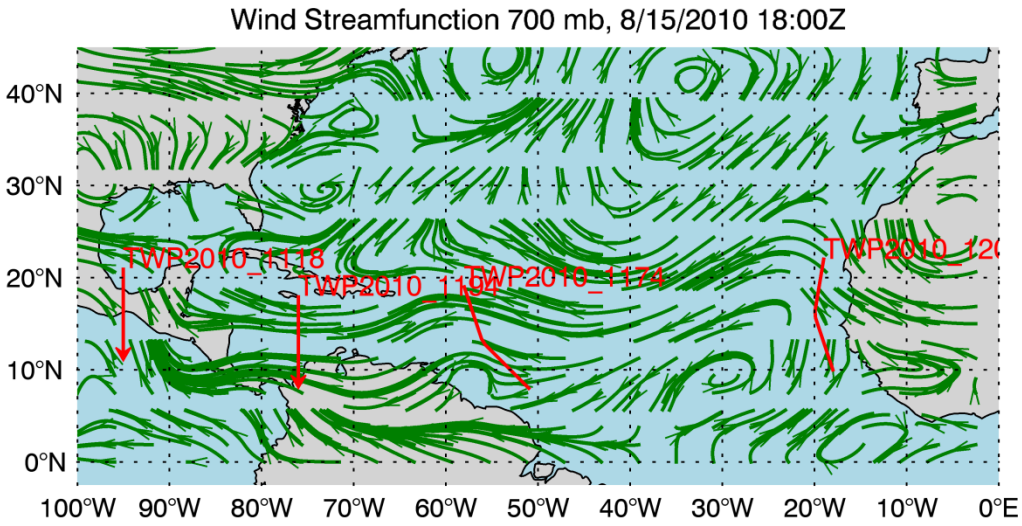

Figure 36: Wind streamfunction example 3

Frequency subtraction

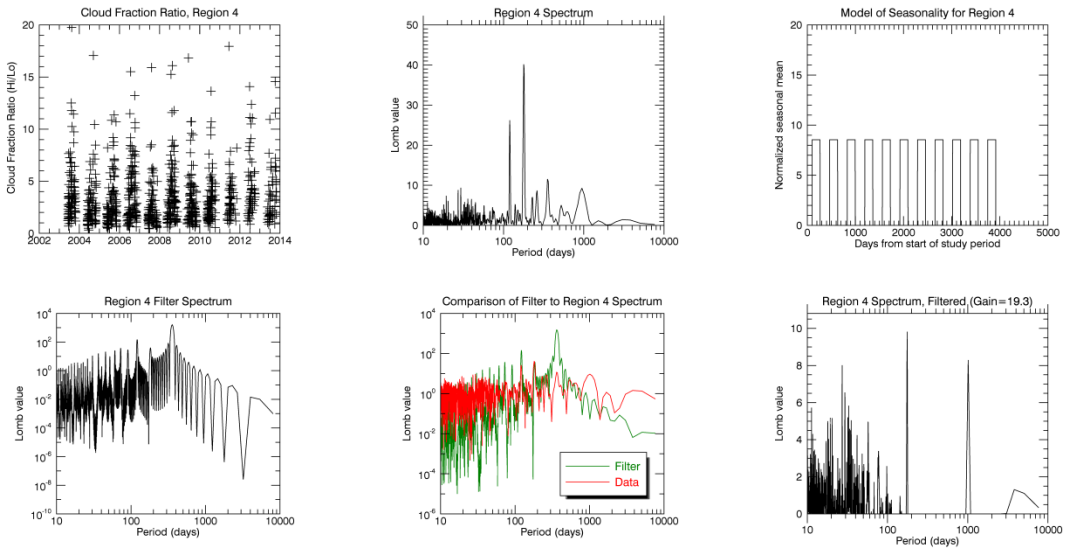

Figure 37: Frequency subtraction

Figure 37 shows the periodicity of cloud fraction ratio in region 4 using a 500 km AOI around tropical wave centers. This is an example of frequency subtraction. In this case we are trying to eliminate the frequency components associated with the seasonality of tropical wave cloud fraction ratio shown in the upper left chart. The next chart to the right shows the periodogram of the cloud fraction ratio. The dominate period is 180 days and is due to seasonality. The upper right chart shows the seasonality modeled as a square wave with a value of zero for off season times and above zero during in season. The spectrum for the seasonality model is shown in the bottom left chart. Three dominant periods can be seen: 365, 180, and 120 days. All of these periods are present in the cloud fraction spectrum but at different magnitudes. Since we are using the spectrum of seasonality as a filter it is labeled "Filter" in these charts. The filter and cloud fraction data spectrum are compared in the center plot of the bottom row. The filter is then subtracted from the data spectrum and the result is shown in the lower right. The 180 day

period is still present but reduced by a factor of 4. The 120 day and 365 day periods are completely extinguished.

REFERENCES

Agudelo, P. A., C. D. Hoyos, J. A. Curry, and P. J. Webster, 2011: Probabilistic discrimination between large-scale environments of intensifying and decaying African Easterly Waves. *Clim. Dyn.*, **36**, 1379–1401, doi:10.1007/s00382-010-0851-x.

Antunes, D. M., D. Figueira, D. M. Matos, A. Bernardino, and J. Gaspar, 2011a: Multiple Hypothesis Tracking in camera networks. *Computer Vision Workshops (ICCV Workshops), 2011 IEEE International Conference on*, IEEE, 367–374 http://ieeexplore.ieee.org/xpls/abs_all.jsp?arnumber=6130265 (Accessed February 13, 2015).

——, D. M. de Matos, and J. Gaspar, 2011b: A Library for Implementing the Multiple Hypothesis Tracking Algorithm. *ArXiv Prepr. ArXiv11062263*,. http://arxiv.org/abs/1106.2263 (Accessed February 13, 2015).

Bain, C. L., K. D. Williams, S. F. Milton, and J. T. Heming, 2014: Objective tracking of African Easterly Waves in Met Office models: Objective Tracking of African Easterly Waves. *Q. J. R. Meteorol. Soc.*, **140**, 47–57, doi:10.1002/qj.2110.

Berry, G., C. Thorncroft, and T. Hewson, 2007: African Easterly Waves during 2004—Analysis Using Objective Techniques. *Mon. Weather Rev.*, **135**, 1251–1267, doi:10.1175/MWR3343.1.

Blackman, S. S., 2004: Multiple hypothesis tracking for multiple target tracking. *Aerosp. Electron. Syst. Mag. IEEE*, **19**, 5–18.

Blake, E., T. Kimberlain, R. Berg, J. Cangialosi, and J. Beven, 2013: *Tropical Cyclone Report Hurricane Sandy*. National Hurricane Center, http://www.nhc.noaa.gov/data/tcr/AL182012_Sandy.pdf.

Boucher, O., and Coauthors, 2013: Clouds and aerosols. *Climate change 2013: The physical science basis. Contribution of working group I to the fifth assessment report of the intergovernmental panel on climate change*, Cambridge University Press, 571–657

http://pubman.mpdl.mpg.de/pubman/item/escidoc:2007900/component/escidoc:2007949/WG1AR5_Ch07SM_FINAL.pdf (Accessed December 24, 2016).

Brammer, A., and C. D. Thorncroft, 2015: Variability and Evolution of African Easterly Wave Structures and Their Relationship with Tropical Cyclogenesis over the Eastern Atlantic. *Mon. Weather Rev.*, **143**, 4975–4995, doi:10.1175/MWR-D-15-0106.1.

Burgwardt, C., T. Curtis, and C. Cameron, 2013: Analyzing the Tropical Wave Associated With Hurricane Sandy, October 2012.

Cecelski, S. F., and D.-L. Zhang, 2013: Genesis of Hurricane Julia (2010) within an African Easterly Wave: Low-Level Vortices and Upper-Level Warming. *J. Atmospheric Sci.*, **70**, 3799–3817, doi:10.1175/JAS-D-13-043.1.

Cox, I. J., and S. L. Hingorani, 1996: An efficient implementation of Reid's multiple hypothesis tracking algorithm and its evaluation for the purpose of visual tracking. *Pattern Anal. Mach. Intell. IEEE Trans. On*, **18**, 138–150.

Dee, D. P., and Coauthors, 2011: The ERA-Interim reanalysis: configuration and performance of the data assimilation system. *Q. J. R. Meteorol. Soc.*, **137**, 553–597, doi:10.1002/qj.828.

Diaz, M., and A. Aiyyer, 2013: The Genesis of African Easterly Waves by Upstream Development. *J. Atmospheric Sci.*, **70**, 3492–3512, doi:10.1175/JAS-D-12-0342.1.

Doyle, J. D., C. A. Reynolds, C. Amerault, and J. Moskaitis, 2012: Adjoint Sensitivity and Predictability of Tropical Cyclogenesis. *J. Atmospheric Sci.*, **69**, 3535–3557, doi:10.1175/JAS-D-12-0110.1.

Dunkerton, T. J., M. T. Montgomery, and Z. Wang, 2009: Tropical cyclogenesis in a tropical wave critical layer: Easterly waves. *Atmospheric Chem. Phys.*, **9**, 5587–5646.

Fayyad, U. M., and P. Smyth, 1999: Cataloging and Mining Massive Datasets for Science Data Analysis. *J. Comput. Graph. Stat.*, **8**, 589–610, doi:10.1080/10618600.1999.10474835.

FORMOSA, 2012: TROPICAL WEATHER DISCUSSION. http://www.nhc.noaa.gov/archive/text/TWDAT/2012/TWDAT.201210121151.txt.

Frank, N. L., 1969: The "'inverted V'"cloud pattern—An easterly wave. *Mon Wea Rev*, **97**, 130–140.

FRANK, N. L., 1970: ATLANTIC TROPICAL SYSTEMS OF 1969. *Mon. Weather Rev.*, **98**, 307–314, doi:10.1175/1520-0493(1970)098<0307:ATSO>2.3.CO;2.

Frank, W. M., and P. E. Roundy, 2006: The role of tropical waves in tropical cyclogenesis. *Mon. Weather Rev.*, **134**, 2397–2417.

Gaskill, J., 1978: *Linear Systems, Fourier Transforms, and Optics*. Wiley New York et al., 576 pp. http://www.wiley.com/WileyCDA/WileyTitle/productCd-0471292885.html (Accessed March 26, 2016).

Hall, N. M., G. N. Kiladis, and C. D. Thorncroft, 2006: Three-dimensional structure and dynamics of African easterly waves. Part II: Dynamical modes. *J. Atmospheric Sci.*, **63**, 2231–2245.

Helsel, D. R., and R. M. Hirsch, 2002: *Statistical Methods in Water Resources*. U.S. Geological Survey, 522 pp. https://pubs.usgs.gov/twri/twri4a3/pdf/chapter8.pdf.

Hirsch, R. M., and J. R. Slack, 1984: A Nonparametric Trend Test for Seasonal Data With Serial Dependence. *Water Resour. Res.*, **20**, 727–732, doi:10.1029/WR020i006p00727.

——, ——, and R. A. Smith, 1982: Techniques of trend analysis for monthly water quality data. *Water Resour. Res.*, **18**, 107–121, doi:10.1029/WR018i001p00107.

Hodges, K. I., B. J. Hoskins, J. Boyle, and C. Thorncroft, 2003: A comparison of recent reanalysis datasets using objective feature tracking: Storm tracks and tropical easterly waves. *Mon. Weather Rev.*, **131**, 2012–2037.

Holweg, E. J., and T. P. Center, 2000: *Mariner's guide for hurricane awareness in the North Atlantic Basin*. Tropical Analysis and Forecast Branch, Tropical Prediction Center, National Weather Service, National Oceanic and Atmospheric Administration, http://nasailor.com/wp-content/uploads/2010/09/marinersguide.pdf (Accessed February 1, 2015).

Iman, R., 1994: *A Data-based Approach to Statistics*. Duxbury Press,.

Kendall, M., 1938: A New Measure of Rank Correlation. *Biometrika*, **30**, 81–93, doi:10.2307/2332226.

Khouider, B., A. J. Majda, and S. N. Stechmann, 2013: Climate science in the tropics: waves, vortices and PDEs. *Nonlinearity*, **26**, R1–R68, doi:10.1088/0951-7715/26/1/R1.

Kiladis, G. N., C. D. Thorncroft, and N. M. Hall, 2006: Three-dimensional structure and dynamics of African easterly waves. Part I: Observations. *J. Atmospheric Sci.*, **63**, 2212–2230.

——, M. C. Wheeler, P. T. Haertel, K. H. Straub, and P. E. Roundy, 2009: Convectively coupled equatorial waves. *Rev. Geophys.*, **47**, doi:10.1029/2008RG000266. http://doi.wiley.com/10.1029/2008RG000266 (Accessed March 11, 2017).

Klotzbach, P. J., and E. C. J. Oliver, 2015: Modulation of Atlantic Basin Tropical Cyclone Activity by the Madden–Julian Oscillation (MJO) from 1905 to 2011. *J. Clim.*, **28**, 204–217, doi:10.1175/JCLI-D-14-00509.1.

Krishnamurti, T. N., L. Stefanova, and V. Misra, 2013: Tropical Waves and Tropical Depressions. *Tropical Meteorology*, Springer New York, New York, NY, 121–141 http://link.springer.com/10.1007/978-1-4614-7409-8_6 (Accessed February 1, 2015).

Kusiak, A., X. Wei, A. P. Verma, and E. Roz, 2013: Modeling and Prediction of Rainfall Using Radar Reflectivity Data: A Data-Mining Approach. *IEEE Trans. Geosci. Remote Sens.*, **51**, 2337–2342, doi:10.1109/TGRS.2012.2210429.

Lakshmanan, V., and T. Smith, 2010: An Objective Method of Evaluating and Devising Storm-Tracking Algorithms. *Weather Forecast.*, **25**, 701–709, doi:10.1175/2009WAF2222330.1.

Landsea, C. W., 2014: TCFAQ A4) What is an easterly wave ? *Freq. Asked Quest.*,. http://www.aoml.noaa.gov/hrd/tcfaq/A4.html (Accessed February 13, 2015).

——, and J. L. Franklin, 2013: Atlantic Hurricane Database Uncertainty and Presentation of a New Database Format. *Mon. Weather Rev.*, **141**, 3576–3592, doi:10.1175/MWR-D-12-00254.1.

Lin, J.-L., and Coauthors, 2006: Tropical intraseasonal variability in 14 IPCC AR4 climate models. Part I: Convective signals. *J. Clim.*, **19**, 2665–2690.

Lussier, L. L., B. Rutherford, M. T. Montgomery, M. A. Boothe, and T. J. Dunkerton, 2015: Examining the roles of the easterly wave critical layer and vorticity accretion during the tropical cyclogenesis of Hurricane Sandy. *Mon. Weather Rev.*, 150108110444005, doi:10.1175/MWR-D-14-00001.1.

Majda, A. J., 2000: Real World Turbulence and Modern Applied Mathematics. *Math. Front. Perspect. 2000*,.

Mapes, B. E., 2000: Convective inhibition, subgrid-scale triggering energy, and stratiform instability in a toy tropical wave model. *J. Atmospheric Sci.*, **57**, 1515–1535.

MATSUNO, T., 1966: Quasi-geostrophic motions in the equatorial area. *J Meteor Soc Jpn.*, **44**, 25–43.

Miller, M. L., V. Lakshmanan, and T. M. Smith, 2013: An Automated Method for Depicting Mesocyclone Paths and Intensities. *Weather Forecast.*, **28**, 570–585, doi:10.1175/WAF-D-12-00065.1.

Miller, R., A. J. Schrader, C. R. Sampson, and T. Tsui, 1990: The Automated Tropical Cyclone Forecasting System (ATCF). *Weather Forecast.*, **5**, 653.

Montgomery, M. T., and Coauthors, 2012: The Pre-Depression Investigation of Cloud-Systems in the Tropics (PREDICT) Experiment: Scientific Basis, New Analysis Tools, and Some First Results. *Bull. Am. Meteorol. Soc.*, **93**, 153–172.

Murakami, M., 1979: Large-Scale Aspects of Deep Convective Activity over the GATE Area. *Mon. Weather Rev.*, **107**, 994–1013, doi:10.1175/1520-0493(1979)107<0994:LSAODC>2.0.CO;2.

National Weather Service, NHC Marine Product Descriptions. http://www.nhc.noaa.gov/abouttafbprod.shtml#TWD (Accessed February 8, 2015).

Olaiya, F., and A. B. Adeyemo, 2012: Application of Data Mining Techniques in Weather Prediction and Climate Change Studies. *Int. J. Inf. Eng. Electron. Bus.*, **4**, 51–59, doi:10.5815/ijieeb.2012.01.07.

Park, M.-S., A. B. Penny, R. L. Elsberry, B. J. Billings, and J. D. Doyle, 2013: Latent Heating and Cooling Rates in Developing and Nondeveloping Tropical Disturbances during TCS-08: Radar-Equivalent Retrievals from Mesoscale Numerical Models and ELDORA*. *J. Atmospheric Sci.*, **70**, 37–55.

Pasch, R., and L. Avila, 1994: Atlantic tropical systems of 1992. *AMS J. Online*,. http://journals.ametsoc.org/doi/pdf/10.1175/1520-0493%281994%29122%3C0539%3AATSO%3E2.0.CO%3B2 (Accessed February 8, 2015).

Press, W. H., 2007: *Numerical recipes 3rd edition: The art of scientific computing*. 3rd ed. Cambridge University Press, Cambridge, U.K., 1235 pp. www.cambridge.org/numericalrecipes.

Provost, F., and T. Fawcett, 2013: Data science and its relationship to big data and data-driven decision making. *Big Data*, **1**, 51–59.

Root, B., M. Yeary, and T.-Y. Yu, 2011: Novel storm cell tracking with multiple hypothesis tracking. *Preprints, 27th Conf. on Interactive Information Processing Systems (IIPS), Seattle, WA, Amer. Meteor. Soc. B*, Vol. 8 of https://ams.confex.com/ams/91Annual/webprogram/Manuscript/Paper184250/AMSAnnual2011_MHTAbstract.pdf (Accessed February 13, 2015).

Roundy, P. E., 2012: The Spectrum of Convectively Coupled Kelvin Waves and the Madden–Julian Oscillation in Regions of Low-Level Easterly and Westerly Background Flow. *J. Atmospheric Sci.*, **69**, 2107–2111, doi:10.1175/JAS-D-12-060.1.

Saha, S., and Coauthors, 2010: The NCEP Climate Forecast System Reanalysis. *Bull. Am. Meteorol. Soc.*, **91**, 1015–1057, doi:10.1175/2010BAMS3001.1.

Sampson, C. R., and A. J. Schrader, 2000: The Automated Tropical Cyclone Forecasting System (Version 3.2). *Bull. Am. Meteorol. Soc.*, **81**, 1231.

Sieglaff, J. M., D. C. Hartung, W. F. Feltz, L. M. Cronce, and V. Lakshmanan, 2013: A Satellite-Based Convective Cloud Object Tracking and Multipurpose Data Fusion Tool with Application to Developing Convection. *J. Atmospheric Ocean. Technol.*, **30**, 510–525, doi:10.1175/JTECH-D-12-00114.1.

Straub, K. H., and G. N. Kiladis, 2003: Interactions between the boreal summer intraseasonal oscillation and higher-frequency tropical wave activity. *Mon. Weather Rev.*, **131**, 945–960.

Takayabu, Y., 1994: Large-scale cloud disturbances associated with equatorial waves. *J. Meteorol. Soc. Jpn.*, **72**, 451–465.

Vaughan, S., 2014: *Cross_Spectrum*. University of Leicester, Leicester, UK, http://www.star.le.ac.uk/~sav2/idl/cross_spectrum.pro.

Ventrice, M. J., and C. D. Thorncroft, 2013: The Role of Convectively Coupled Atmospheric Kelvin Waves on African Easterly Wave Activity. *Mon. Weather Rev.*, **141**, 1910–1924, doi:10.1175/MWR-D-12-00147.1.

Wang, Z., 2012: Thermodynamic Aspects of Tropical Cyclone Formation. *J. Atmospheric Sci.*, **69**, 2433–2451, doi:10.1175/JAS-D-11-0298.1.

Wheeler, M., and G. N. Kiladis, 1999: Convectively coupled equatorial waves: Analysis of clouds and temperature in the wavenumber-frequency domain. *J. Atmospheric Sci.*, **56**, 374–399.

Yang, Y., L. T. Wilson, and J. Wang, 2010: Development of an automated climatic data scraping, filtering and display system. *Comput. Electron. Agric.*, **71**, 77–87, doi:10.1016/j.compag.2009.12.006.

Yilmaz, A., O. Javed, and M. Shah, 2006: Object tracking: A survey. *ACM Comput. Surv.*, **38**, 13–es, doi:10.1145/1177352.1177355.

BIOGRAPHY

Lester Charles Burgwardt III received his Bachelor of Science in 1981 and his Master of Science in 1999, both from Rochester Institute of Technology. He has been employed in a number of research and development positions since 1981 and is currently with the Harris Corporation in Herndon, Virginia.